Re-Pt-Os Isotopic and Highly Siderophile Element Behavior in Oceanic and Continental Mantle Tectonites

Harry Becker
Institut für Geologische Wissenschaften
Freie Universität Berlin
Germany
e-mail: hbecker@zedat.fu-berlin.de

Christopher W. Dale
Department of Earth Sciences
Durham University
United Kingdom
e-mail: christopher.dale@durham.ac.uk

INTRODUCTION

Tectonically-emplaced mantle rocks, such as ophiolites, abyssal peridotites and orogenic peridotite massifs, provide a principle constraint on the composition of and processes in the Earth's upper mantle (Bodinier and Godard 2003). In the past, these 'mantle tectonites' have sometimes received different names because their history and origin has been unclear. Mantle tectonites are now understood to reflect a range of geologic environments regarding their emplacement and their origin (e.g., Dilek and Furnes 2013). The advantage of these rocks compared to mantle xenoliths is the large-scale exposure of textural and compositional relations between different rock types that can be used to identify processes such as melting, magma or fluid transport, chemical reactions, mixing or deformation at a range of spatial scales. A disadvantage of most mantle tectonites is that they commonly display substantial chemical modification of some elements, resulting from widespread serpentinization at low temperatures. In some cases, this may also affect abundances of several of the highly siderophile elements (HSE: Re, Au, PGE: Os, Ir, Ru, Rh, Pt, Pd), however, this can be tested by comparison with unaltered rocks of similar composition. As is discussed in Reisberg and Luguet (2015, this volume), Harvey et al. (2015, this volume) and Aulbach et al. (2015, this volume), peridotite xenoliths have their own alteration issues regarding sulfides and chalcophile elements.

Numerous studies have obtained Os isotope and/or highly siderophile element abundance data on many different types of mantle tectonites. Some of these studies have focused on large-scale chemical and isotopic variations, others on grain size-scale compositional variations to understand small-scale distribution processes. These studies have, together, significantly advanced the understanding of the processes that fractionate the HSE in the mantle at different spatial scales and have provided insights into the behavior of sulfide in the mantle – the phase that typically hosts the vast majority of the strongly chalcophile elements, including the HSE. Osmium isotopes and Re-Os model ages have provided tools to directly date melting of mantle tectonites and have changed views on the efficacy of mixing and melting processes in the mantle.

Here, we review these advances, which have mostly taken place in the past 15 years, aided by new developments in isotope dilution and ICP-MS based techniques and the application of in situ laser ablation ICP-MS. First, we provide a brief summary of the current views about geodynamic environments of different mantle tectonites. Work on Os isotopes and HSE abundances in mantle tectonites of different geodynamic settings will be reviewed subsequently. In the Discussion, we summarize the views on processes and chemical behavior of Os isotopes and the HSE in mantle tectonites.

BREVIA OF CONCEPTS, TERMINOLOGY AND ANALYTICAL CAVEATS

Re-Pt-Os parameters

In this chapter, we normalize isotopic abundance ratios to ^{188}Os following currently accepted conventions: $^{187}Os/^{188}Os$ = measured $^{187}Os/^{188}Os$, $^{186}Os/^{188}Os$ = measured $^{186}Os/^{188}Os$, $^{187}Os/^{188}Os_i$ = initial $^{187}Os/^{188}Os$ at age t. Up to the late 1990s some workers used the $^{187}Os/^{186}Os$ ratio to compare variations in ^{187}Os in natural materials. After it became clear that some minerals and rocks also display variations of radiogenic ^{186}Os from the decay of ^{190}Pt (Walker et al. 1997; Brandon et al. 1998, 1999), it was suggested to use ^{188}Os as the stable reference isotope (e.g., Shirey and Walker 1998). In the present work, conversion of early $^{187}Os/^{186}Os$ and $^{187}Re/^{186}Os$ data to $^{187}Os/^{188}Os$ and $^{187}Re/^{188}Os$, respectively, was performed by multiplication with a value of $^{186}Os/^{188}Os = 0.1203$. This value for $^{186}Os/^{188}Os$ was commonly obtained by early less precise and accurate isotopic ratio determinations. Later high-precision measurements of Os isotopic compositions of mantle-derived rocks using N-TIMS and faraday cup detection have yielded lower $^{186}Os/^{188}Os$ for the Earth's mantle and the bulk silicate Earth (0.119838 ± 0.000003, 2 s.d., Brandon et al. 2006). The measurement of Os isotopic ratios via OsO_3^- ions requires that the raw data is corrected for interferences produced by the minor isotopes of O. Fractionation of Os isotopes during mass spectrometric measurements is commonly corrected assuming $^{192}Os/^{188}Os = 3.0827$ (Luck and Allègre 1983, Shirey and Walker 1998). High-precision Os isotopic data require more elaborate measurement and correction protocols (e.g., Brandon et al. 2005a, 2006, Luguet et al. 2008a; Chatterjee and Lassiter, 2015).

The deviation of $^{187}Os/^{188}Os$ of a sample from an arbitrary 'average' chondritic composition (present $^{187}Os/^{188}Os = 0.12700$, $^{187}Re/^{188}Os = 0.40186$) at age t is given as γOs_t and was calculated using the equation and parameters given in Shirey and Walker (1998). The decay constant of ^{187}Re used for calculations is $1.666 * 10^{-11}$ year^{-1} (Smoliar et al. 1996; Selby et al. 2007). The average chondritic $^{187}Os/^{188}Os$ and $^{187}Re/^{188}Os$ have no specific meaning other than as a reference for comparing different materials. Initial $^{186}Os/^{188}Os$ of samples were calculated using $\lambda_{190Pt} = 1.48*10^{-12}$ year^{-1} (Brandon et al. 2006). Rhenium depletion model ages T_{RD} (Ch) and Re-Os model ages T_{MA} (Ch) have been defined previously relative to a chondritic evolution model (Ch) using the parameters mentioned above (Walker et al. 1989; Shirey and Walker 1998). Alternatively, these model ages may be calculated relative to the Re-Os evolution of the primitive mantle model composition, e.g., T_{MA} (PM). The primitive mantle has a slightly higher $^{187}Os/^{188}Os$ (0.1296) and $^{187}Re/^{188}Os$ (0.4346) than the 'average' chondrite reference values (Meisel et al. 2001).

Normalization of concentration data

In the literature, normalizations of HSE abundances in mantle rocks are sometimes performed relative to mean abundances in CI chondrites using data from compilations (e.g., Anders and Grevesse 1989; Lodders 2003; Horan et al. 2003). One disadvantage of this approach is that the HSE composition of the earth's mantle (and of the bulk Earth) likely does not match CI chondrites (Walker et al. 2002a, 2002b; Horan et al. 2003; Becker et al. 2006; Fischer-Gödde et al. 2010; Fischer-Gödde et al. 2011). However, it does have the advantage of using a measureable reference frame for normalization. An alternative approach to assess igneous fractionation of the HSE in mantle and crustal rocks is to normalize to a primitive mantle model composition (PM, sometimes also referred to as primitive upper mantle, PUM and bulk silicate earth, BSE), and to arrange elements according to their incompatibility as it is commonly performed for lithophile elements (e.g., Hofmann 1988). The HSE concentrations in PM used for normalization and the

sequence of HSE in normalized concentration diagrams are those given in Becker et al. (2006) and Fischer-Gödde et al. (2011). This theoretically has the advantage of providing comparison with the primitive mantle composition. Alternatively, a composition of 'average depleted spinel lherzolites' (based on mantle xenoliths and tectonites) has been defined in the literature for comparative purposes (Pearson et al. 2004). Here we use, in different situations to reflect different aims, both normalization to primitive mantle and to 'average' chondrite values calculated with equal weighting from ordinary, enstatite and carbonaceous chondrites, from data compiled in Walker (2009) and from Fischer-Gödde et al. (2010). We also use both logarithmic and linear scales to best display the variations present in each particular figure. The sequence of HSE in normalized concentration diagrams of terrestrial rocks commonly follows the sequence of increasing enrichment in basalts and komatiites (i.e. Os < Ir < Ru < Rh < Pt < Pd < Au < Re ≈ S), which is similar, but not always identical, to the depletion in many peridotites. Elemental patterns in some peridotites, that differ from this general depletion sequence, reflect re-enrichment in Re, Au, Pd and multi-stage histories.

Precision and accuracy of concentration data and analytical issues

Previous studies have indicated that some of the early analytical techniques used to determine HSE abundances or Re-Os systematics did not always produce complete recovery of Ir, Os and Ru, even at test portion masses of > 10 g (e.g., Shirey and Walker 1998; Meisel and Moser 2004; Becker et al. 2006, Lorand et al. 2008, Meisel and Horan 2015, this volume). In the discussion of processes that fractionate the HSE, we will primarily focus on more recent data that have been obtained either by Carius tube digestion at enhanced temperatures (T >230°C), by high-pressure asher (typically > 300°C), or by improved NiS fire assay techniques (Gros et al. 2002). If isotopic ratios were analyzed by ICP-MS or, in the case of Os, N-TIMS, these methods yield combined analytical uncertainties (1 s.d.) of concentrations that may range between better than a few % for Re and 15 % for Au for well-homogenized whole rock powders of lherzolites and test portion masses of about 2 grams or more (Meisel and Moser 2004; Pearson et al. 2004; Becker et al. 2006; Lorand et al. 2008; Fischer-Gödde et al. 2011). Heterogeneity of abundances of carrier phases of the HSE in powders of some peridotites is a well-known problem ('nugget effect'). In addition to the nugget effect, complete and reproducible digestion of refractory platinum group element minerals (PGM) in some harzburgites or dunites, may represent a challenge. Incomplete digestion of refractory alloy phases may bias ratios of Os, Ir and Ru. For further details, see Meisel and Horan (2015, this volume).

HIGHLY SIDEROPHILE ELEMENTS IN MANTLE TECTONITES FROM DIFFERENT GEODYNAMIC SETTINGS

Summary of mantle tectonites and their geodynamic settings

Mantle tectonites include peridotite sections of ophiolites, abyssal peridotites and orogenic peridotites that often, but not exclusively, occur in orogenic belts (also known as peridotite massifs, alpine or alpinotype peridotites). These different mantle tectonites can be distinguished by their geodynamic setting, and associated emplacement history and pressure-temperature (P, T) evolution, but also by their chemical composition. Most of the rocks concerned record a relatively simple cooling history from lithospheric mantle conditions (T of 1000-1300°C and P of the garnet, spinel or plagioclase lherzolite stability field) to some lower T and P equivalent to crustal conditions. Owing to their origin from in situ lithospheric or asthenospheric mantle conditions, these rocks are sometimes also referred to as 'high-temperature peridotites'. In contrast, 'low-temperature' orogenic peridotites are former high-temperature peridotites that have been subducted as part of a package of crustal rocks in collision zones (e.g., the Alpe Arami peridotite, Nimis and Trommsdorff 2001; peridotites of the Western Gneiss

region, Norway, Brueckner et al. 2010; Zermatt-Saas ophiolite, Barnicoat and Fry 1986). Low-temperature peridotites were partially re-equilibrated at high P/T conditions, but in some cases, this partial re-equilibration is hardly noticeable and chemical and textural features inherited from the high-temperature history of the peridotites predominate (e.g., at the Lanzo peridotite massif; Pelletier and Müntener 2006).

Improved understanding of the geodynamic evolution of passive continental margins (Dilek et al. 2000), the transition to ocean spreading and the role of ocean spreading rate in the lithological composition of the oceanic crust (Dick et al. 2006) have led to improved interpretations of the origin and geodynamic environments of mantle tectonites and ophiolites (Dilek et al. 2000; Dilek and Furnes 2013). It is now understood that high-temperature peridotite tectonites derived from continental lithospheric mantle may be exhumed during slow extension of continental lithosphere and the formation of sedimentary basins or small ocean basins. Well-known examples are the island of Zabargad in the Red Sea (Brueckner et al. 1988), the Pyrenean peridotite bodies in southern France (Vielzeuf and Kornprobst 1984; Bodinier et al. 1988), the peridotite bodies of NW Italy (Ivrea-Verbano Zone, Lanzo; Ernst 1978; Sinigoi et al. 1983; Shervais and Mukasa 1991; Mazzucchelli et al. 2009) and some of the mantle tectonites in the Alps and in Italy that sometimes have been referred to as 'ophiolites' (for instance the External Ligurian peridotites; Rampone et al. 1995). Some mantle tectonites were exhumed in oceanic environments as indicated by their alteration and association with ophicalcitic breccias, basalts, gabbros and cherts. Such rocks, for instance the Internal Ligurian peridotites of the Tethys ocean, do not show the classical Penrose-type ophiolite sequence and are most similar to exhumed mantle in modern ultraslow spreading environments, e.g., like parts of the SW Indian ridge or the Gakkel ridge (Dick et al. 2000, 2006; Michael et al. 2003). The classical Penrose-type ophiolite stratigraphy, which is believed to be representative of moderate to fast spreading ocean ridges, is represented by the Samail ophiolite in Oman and the Troodos ophiolite (Cyprus). However, it should be noted that these ophiolite complexes were at least partly affected by convergent plate margin processes (Dilek et al. 2000; Dilek and Furnes 2013).

Indeed, many ophiolites probably formed close to subduction zones and were later incorporated into the crust by collision of terranes or continental fragments. Evidence for the proximity of subduction zones is mostly derived from the composition of associated igneous rocks such as calcalkaline basalts or boninites. To what degree subduction processes affected the mantle tectonites is not always clear. For instance, mantle rocks in the northwestern segments of the ophiolites in Oman may have been influenced by supra-subduction zone melting processes or by migration of magmas that formed in subarc mantle, as is indicated by the abundance of podiform chromitite deposits in these rocks and the calcalkaline and boninitic affinities of the crustal rocks (Boudier et al. 2000; Ishikawa et al. 2002). In contrast, the southern massifs of the Samail ophiolite in Oman show little evidence for such rocks and the crust is predominantly MORB-like in composition (Koga et al. 2001; Pallister and Knight 1981). Some peridotite massifs contain abundant pyroxenite layers which sometimes carry chemical and isotopic evidence for the significant presence of recycled crust components (e.g., Beni Bousera, Ronda, Bohemian massif; Pearson et al., 1991a, 1991b, 1993; Becker, 1996a, 1996b). Such compositions only occur in mantle tectonites from areas that may have undergone lithospheric delamination and previous episodes of subduction. Some 'ophiolites', such as the Ligurian ophiolites (N Italy) and similar complexes in the Alps, were not affected by convergent processes and are more properly assigned to purely extensional environments (e.g., Piccardo and Guarnieri 2010; Rampone et al. 1995, 1996).

In the following sections, we will describe the HSE and Os isotopic characteristics of different types of mantle tectonites in the context of their formation environments, as far as these have been constrained. These sections contain basic information on the formation environment and evolution of the ultramafic bodies together with the Re-Pt-Os isotopic and HSE composition

213 of their various mantle lithologies. We will proceed from abyssal peridotites and other mantle
214 tectonites exhumed in extensional geodynamic environments to peridotite massifs and ophiolites
215 affected by magmatic processes at convergent plate margins. Interpretations of these
216 compositions will then follow in the Discussion. The geological settings covered, locations,
217 available HSE data and key references are summarized in Table 1.
218

Table 1. Locations, geological settings, available data and references for samples discussed in this chapter

Setting and location		HSE data	Key HSE references
Abyssal peridotites			
Atlantic - North	Kane Fracture Zone	^{187}Os, HSE	Snow & Schmidt, 1998; Rehkämper et al., 1999; Brandon et al., 2000; Luguet et al., 2001; Becker et al., 2006
	15° 20 N Fracture Zone	^{187}Os, HSE, Se-Te	Harvey et al., 2006; Marchesi et al., 2013
	Azores, North Atl Ridge	^{187}Os	Roy-Barman & Allègre, 1994
Atlantic - South	Shaka, 59° S, Bouvet, Dingaan, Islas Orcadas FZs	^{187}Os	Snow and Reisberg, 1995
Indian	SWIR	^{187}Os (WR, sulf), HSE	Roy-Barman & Allègre, 1994; Snow & Schmidt, 1998; Luguet et al., 2001; Alard et al. 2005; Warren & Shirey, 2012
Pacific	East Pacific Rise, Hess Deep	^{187}Os, HSE	Roy-Barman & Allègre, 1994; Snow & Schmidt, 1998; Rehkämper et al., 1999
Arctic	Gakkel Ridge	^{187}Os (WR, sulf), HSE	Liu et al., 2008; 2009; Warren & Shirey, 2012;
	Lena Trough	^{187}Os	Lassiter et al., 2014
Oceanic mantle tectonites			
Italy	Internal Ligurides	^{187}Os, HSE	Rampone et al., 1996; Snow et al., 2000; Luguet et al., 2004; Fischer-Gödde et al. 2011
Ophiolites – Little or no subduction influence			
Oman	Samail	^{187}Os, HSE	Hanghøj et al., 2010
Chile	Taitao	^{187}Os	Schulte et al., 2009
Ophiolites – Uncertain origin			
Tibet	Luobusa, Dongqiao	^{187}Os (WR, PGM), HSE	Zhou et al., 1996; Becker et al., 2006; Shi et al., 2007; Pearson et al., 2007
Finland	Jormua, Outokumpu	^{187}Os	Tsuru et al., 2000; Walker et al., 1996
Austria	Eastern Alps	^{187}Os	Meisel et al., 1997
Turkey, Tethyan	Marmaris, Tekirova, Koycegiz	^{187}Os, HSE	Aldanmaz et al., 2012
Cuba	Mayari-Cristal	^{187}Os (PGM)	González-Jiménez et al., 2009; Marchesi et al., 2011
Ophiolites – Convergent margin origin			
Cyprus	Troodos	^{187}Os, HSE	Büchl et al., 2002; 2004;
Scotland	Unst, Shetland	^{187}Os, HSE	Prichard and Lord, 1996; O'Driscoll et al., 2012
Philippines	Zambales	HSE	Zhou et al., 2000
Iraq	Qalander	HSE	Ismail et al., 2014
Egypt	Eastern Desert ophiolite	^{187}Os (PGM)	Ahmed et al., 2006
California	Feather River, Josephine, others	HSE, ^{187}Os (PGM)	Agranier et al., 2007; Meibom et al., 2002; Pearson et al. 2007

Convergent margin tectonites (High temperature)			
Spain	Ronda	^{187}Os, HSE	Reisberg et al., 1991; Reisberg and Lorand, 1995; Gueddari et al., 1996; Lorand et al., 2000; Fischer-Gödde et al., 2011; Marchesi et al., 2014
Morocco	Beni Bousera	^{187}Os, HSE	Gueddari et al., 1996; Roy-Barman et al., 1996; Pearson et al., 2004
Lower Austria, Czech Republic	Bohemian Massif	^{187}Os, HSE	Becker et al., 2001; 2004; 2006; Ackerman et al., 2013
Continental/Continent-ocean transitional tectonites			
France	Lherz	^{187}Os, HSE, Se-Te, PGM	Reisberg & Lorand, 1995; Becker et al., 2006; Luguet et al., 2007; Lorand et al., 2010; Riches & Rogers, 2011; König et al., 2014
France: other Pyrenees	e.g. Turon, Freychinede, Fontete Rouge	^{187}Os, HSE	Reisberg & Lorand, 1995; Lorand et al., 1999; Becker et al., 2006; Fischer-Gödde et al., 2011
Italy	Ivrea Zone: Baldissero, Balmuccia	^{187}Os, HSE, Se-Te	Wang et al., 2013; Wang and Becker, 2015
Italy	External Ligurides	^{187}Os, HSE	Rampone et al., 1995; Snow et al., 2000;
Swiss Alps	Totalp	^{187}Os, HSE	van Acken et al., 2008; 2010a; 2010b
Switzerland	Helvetic domain	^{187}Os	Meisel et al., 1996
Japan	Horoman	^{187}Os, HSE	Rehkamper et al., 1999; Saal et al., 2001
Italy	Lanzo	^{187}Os, HSE	Lorand et al., 2000; Becker et al., 2006; Fischer-Gödde et al., 2011

HSE in abyssal peridotites from spreading oceanic lithosphere

Rocks from slow spreading ridges share many characteristics with mantle tectonites exhumed in passive continental margin or transitional oceanic environments (see later sections). That is, a spectrum of peridotite compositions is often present, including lherzolites, harzburgites and replacive dunites. However, in some cases (e.g., 15° 20′ N fracture zone, Atlantic Ocean; Harvey et al. 2006), a greater degree of serpentinisation is present, sometimes with little primary mineralogy remaining, possibly due to the nature of emplacement and exposure of abyssal peridotites, either with little overlying crust (slow-ultra slow spreading) or bounded by transform faults. This can be important for the budgets of the HSE, as is discussed in the first section of the discussion.

Abyssal peridotites contain major and trace element evidence for significant melt depletion, and isotopic evidence for that melt extraction being ancient, with long-term depletion of incompatible elements. Early studies found Os isotope evidence for this depletion, with ^{187}Os/^{188}Os ratios between 0.1208 and 0.1304 in abyssal peridotite whole-rocks from several global localities (Martin, 1991; Roy-Barman and Allègre, 1994; Snow and Reisberg, 1995). These ratios range from close to the estimate for the primitive upper mantle (0.1296; Meisel et al., 2001) to values which equate to Re depletion at ~1.2 Ga (T_{RD}, see Fig. 4), assuming all Re was stripped from the residue during melting (Shirey and Walker, 1998). In reality, Re remains present in abyssal peridotites, although typically at much lower abundances than in the PM. This means that the actual age of depletion is older than calculated for a T_{RD} age, because evolution of ^{187}Os/^{188}Os didn't cease entirely after depletion. However, all abyssal peridotite sample suites display evidence for recent open system behavior, most probably in the form of Re addition (e.g., Harvey et al., 2006), but also sometimes Os loss and enrichment in ^{187}Os (Snow and Reisberg, 1995). This is apparent in the sub-horizontal trends within suites which show similar ^{187}Os/^{188}Os over a range of ^{187}Re/^{188}Os ratios (Fig. 1), and is consistent with the evidence for extensive

serpentinisation during fluid-rock interaction (e.g., Harvey et al., 2006). This seawater interaction can also be coupled with elevated and lowered $^{87}Sr/^{86}Sr$ and $^{143}Nd/^{144}Nd$ ratios, respectively (Snow and Reisberg, 1995). However, despite the extremely radiogenic isotopic composition of seawater ($^{187}Os/^{188}Os$ ~1.05; Levasseur et al., 1998), the modelled effects of seawater interaction on Os isotopes are small except at very high fluid/rock ratios (Fig. 17), due to the very low Os concentration in seawater (~11 fg/g; Levasseur et al., 1998) compared to mantle samples (~1-5 ng/g). Moreover, a comparison of the rims and cores of abyssal peridotites from Gakkel Ridge in the Arctic Ocean found no systematic difference in Os contents and only a very small increase in $^{187}Os/^{188}Os$ from core to rim (Liu et al., 2008). A possible alternative source of radiogenic Os is by reaction with percolating melts from enriched lithologies. There is, however, a much larger effect of seawater interaction on Re/Os ratios (cf. ~7.3 pg/g Re in seawater; Anbar et al., 1992), with examples of sample rims reset while sample cores display a co-variation between Re/Os and Al_2O_3 contents, which must be a primary melt depletion feature (Liu et al., 2008).

In general, the processes of alteration mean that the measured Re-Os elemental and isotopic values may not accurately represent the long-term history of abyssal peridotites, casting doubt on the accuracy of T_{RD} ages. Nonetheless, all abyssal peridotite suites consist primarily of samples with Os isotope ratios ranging from close to the PM estimate to sub-chondritic values (Fig. 1), reflecting long-term evolution in a low Re/Os environment following ancient melt depletion. Seawater interaction can only increase $^{187}Os/^{188}Os$, so both alteration and minor ingrowth of ^{187}Os since depletion would only serve to reduce the apparent age.

Snow and Reisberg (1995) proposed an 'uncontaminated' range for abyssal peridotites of 0.1221 to 0.1270, with a mean of 0.1246. Both Snow and Reisberg (1995) and Roy-Barman and Allègre (1994) identified that this range was less radiogenic than the range of early MORB analyses. Further analyses of samples from a forearc region and from slow or ultra-slow spreading ridges have significantly extended the known range of Os isotope compositions; whole-rock $^{187}Os/^{188}Os$ of 0.119, 0.117 and 0.114 were found, respectively, from the Izu-Bonin forearc (Parkinson et al., 1998), ODP Hole 1274a (15°20′ N transform, mid-Atlantic; Harvey et al., 2006) and Gakkel Ridge (Arctic; Liu et al., 2008). The unradiogenic samples of the forearc setting were first thought to indicate that subduction zones might be 'graveyards' for ancient depleted mantle (Parkinson et al., 1998). While mantle in subduction zones may be extremely depleted, the findings from the 15°20 N transform and Gakkel Ridge indicate that such portions of ancient depleted mantle are likely present throughout the upper mantle.

Sulfide compositions display greater Os isotopic variation than whole-rocks (some plotting at $^{187}Re/^{188}Os$ ratios up to ~12) and can be divided into two broad groups: rounded intragranular grains and more skeletal interstitial sulfides (Alard et al., 2005; Harvey et al., 2006). The latter typically have higher Re/Os and more radiogenic Os isotope signatures (see Discussion), and the rounded, included sulfides possess the least radiogenic $^{187}Os/^{188}Os$, lower than the host whole-rocks, reflecting depletion and isolation since an ancient melting episode.

Assuming that isochron information is typically compromised due to recent open-system behavior (see Fig. 1), then minimum Re depletion ages must be utilized; these are shown by the horizontal dashed lines in Fig. 1. The least radiogenic whole-rocks from Gakkel and sulfides from the 15°20 N transform equate to T_{RD} ages in excess of 2 Ga. The six rounded sulfides from one sample from Hole 1274a actually display a near-isochronous relationship. The age of this errorchron is ~2.05 Ga, consistent with the T_{RD} ages for these sulfides. Sulfides from South-West Indian ridge peridotites (Warren and Shirey, 2012) typically have more radiogenic compositions, closer to the PM value, and their sub-horizontal array suggests relatively recent resetting of their Re/Os ratios (Fig. 1). However, when combined with data from Alard et al. (2005) and with Pb

isotope data (Warren and Shirey, 2012), the broader array appears to give an age approaching 2 Ga.

As well as constraints on the ^{187}Os evolution of the convecting mantle, the combined ^{186}Os-^{187}Os systematics of abyssal peridotites from the Kane transform area of the Atlantic Ocean have been studied (Brandon et al., 2000). The average $^{186}Os/^{188}Os$ of these samples is 0.1198353 +/- 0.0000007, identical to the mean from alloys and chromitites (Walker et al., 1997; Brandon et al., 2006), indicating the general absence of significant fractionation of Pt and Os in the abyssal and ophiolite environments. The Kane samples display a co-variation of $^{187}Os/^{188}Os$ with Pt/Os ratio which would likely not have been preserved if recent melting had taken place (Brandon et al., 2000). No covariation of $^{187}Os/^{188}Os$ and Re/Os, due to seawater interaction, exists. The variability of $^{187}Os/^{188}Os$ could either be ascribed to differing ages of depletion or to variable degrees of depletion, perhaps with garnet present in which Re is thought to be compatible (Righter and Hauri, 1998). Brandon et al. (2000) proposed that Re is only depleted by about 40% in these rocks, therefore requiring very ancient melt depletion to produce the most unradiogenic samples. This ancient melting is not evident in $^{143}Nd/^{144}Nd$, indicating decoupling of the two isotope systems, perhaps due to the Nd budget being predominantly hosted by clinopyroxene which is continually involved in partial melting, whereas the Os budget is likely dominated by included sulfides which are isolated from moderate degrees of partial melting and thus retain an ancient signature (Brandon et al., 2000). The later work of Harvey et al. (2006), outlined above, supports the influence of shielded sulfides, which control much of the whole-rock Os signature.

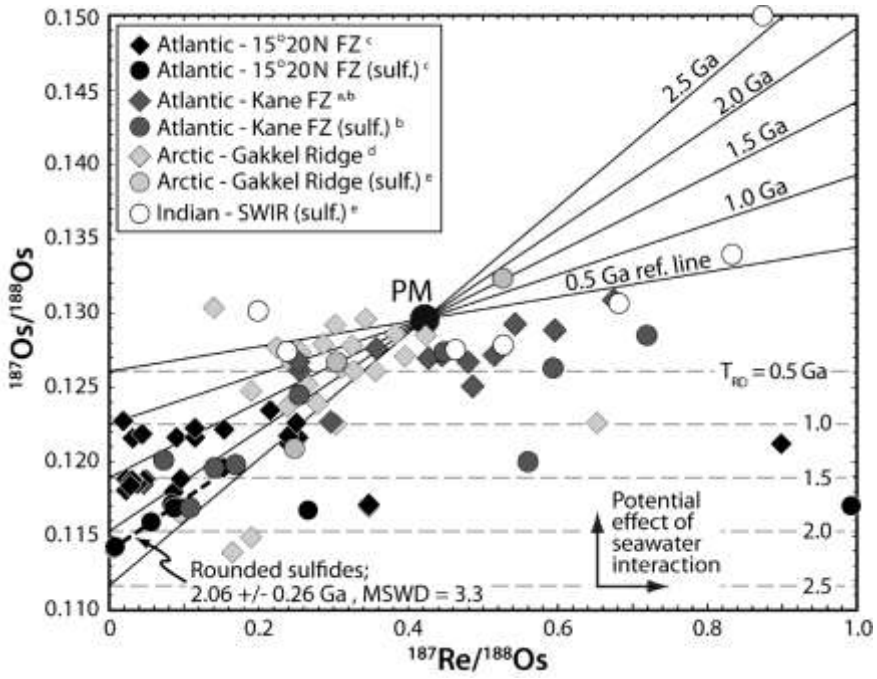

Figure 1. Re-Os isochron diagram for separated sulfides and whole-rock abyssal peridotites from the Atlantic, Arctic and Indian Oceans. Sub-horizontal trends within all sample suites indicate recent open system behavior (most probably Re addition) but sub-PM Os ratios strongly predominate in all suites, reflecting long-term evolution in a low Re/Os environment following ancient melt depletion. Sulfides display the greatest Os isotope variations, with the least radiogenic values and some radiogenic values ($^{187}Os/^{188}Os$: ~0.167) plotting with $^{187}Re/^{188}Os$ ratios up to ~12. Age reference lines are shown as solid lines; Re depletion (T_{RD}) ages are shown as horizontal dashed lines. The dashed line sub-parallel to the age reference lines is the best fit line for six rounded sulfides from a single Hole 1274a abyssal peridotite. Whole-rock data for Indian and Pacific peridotites are not shown due to the paucity of available data. Refs: [a] Brandon et al. (2000), Becker et al. (2006); [b] Alard et al. (2005); [c] Harvey et al. (2006); [d] Liu et al. (2008); [e] Warren and Shirey (2012).

The apparent disconnect between abyssal peridotites and their overlying crust found in the early Os isotope abyssal studies (also see Discussion) is clearly seen in refractory Macquarie Island peridotites (Southern Ocean) and their surprisingly enriched overlying crust (Dijkstra et al., 2010). Here, a slow spreading and low productivity ridge would not be expected to account for the 20-25% near fractional melting suggested by the very high Cr numbers for spinel (0.40-0.49) in the peridotites. Although many authors have suggested a minor or absent role for abyssal peridotites in the generation of oceanic crust (e.g., Liu et al., 2008; Dijkstra et al., 2010), a compilation of abyssal peridotite data by Lassiter et al. (2014), including new analyses of Lena Trough peridotites ($^{187}Os/^{188}Os$: 0.118-0.130, average 0.1244), is remarkably similar to the distribution of $^{187}Os/^{188}Os$ in xenoliths entrained in ocean island basalts (Fig. 2 and references in caption). The authors argue that this range of $^{187}Os/^{188}Os$ for both suites represents the composition of the convecting mantle, and is inconsistent with a refractory 'slag' hypothesis for abyssal peridotites (cf. Rampone and Hofmann, 2012). One issue with this interpretation, however, is that OIB xenoliths likely do not represent a deep source mantle for those melts, and instead might sample the lithospheric mantle which is plausibly genetically related to abyssal peridotites. Nonetheless, on an $^{187}Os/^{188}Os$-Al_2O_3 diagram (sometimes called an 'aluminachron', Fig. 2, where Al_2O_3 is used as a proxy for melt- and Re-depletion), abyssal peridotites and OIB xenoliths produce best-fit lines with similar 'initial' values, but differing slopes (the intersection of the correlation with the $^{187}Os/^{188}Os$ axis at $Al_2O_3 = 0$ yields the initial $^{187}Os/^{188}Os_i$ at the time of the partial melting event). The similarity of the most depleted 'initial' values suggests that the age of Re depletion is similar for the two suites. So rather than the different slopes reflecting different depletion ages, the steeper trend of the abyssal suite instead suggests additional recent depletion of Al during partial melting to form new oceanic crust (Lassiter et al., 2014). This argues for a role for abyssal peridotites in the formation of mid-ocean ridge basalts. It remains possible, however, that the trends instead represent mixing between melts and residues and that the differing slopes reflect different conditions (e.g. depth, fS_2 etc.) of such mixing.

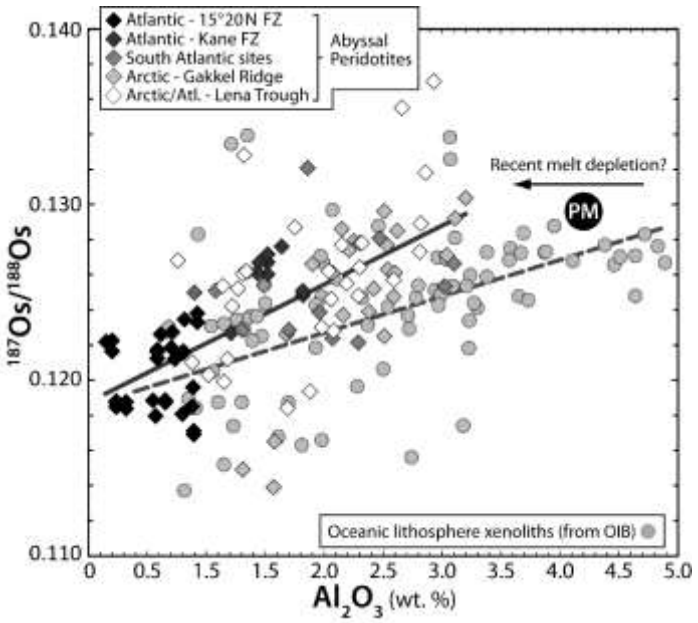

Figure 2. $^{187}Os/^{188}Os$-Al_2O_3 diagram (after Reisberg and Lorand, 1995, see also Fig. 4b) for whole-rock abyssal peridotites from the Atlantic and Arctic Oceans compared to xenoliths entrained by ocean island basalts (after Lassiter et al., 2014). There is considerable scatter in both the abyssal and OIB xenolith datasets, possibly reflecting variable ages of melt depletion, or recent resetting of $^{187}Os/^{188}Os$ by seawater or melt interaction. Overall, the best-fit lines for the two suites have similar 'initial' values, suggesting similar mean ages of depletion, but the abyssal peridotite trend is significantly steeper. Rather than representing an older age, this likely reflects depletion of Al during recent melting to form oceanic crust,

which would not therefore affect $^{187}Os/^{188}Os$. Data sources as in Fig. 1, except Lena Trough and South Atlantic abyssal peridotites from Lassiter et al. (2014) and Snow and Reisberg (1995), respectively. Circles represent peridotite xenoliths entrained in ocean island basalts (Hassler and Shimizu, 1998; Widom et al., 1999; Becker et al., 2006; Bizimis et al., 2007; Simon et al., 2008; Ishikawa et al., 2011).

Analyses of the range of HSE in abyssal peridotites showed that they are not present in strictly chondritic proportions (Snow and Schmidt, 1998), and thus may not be consistent with the theory that HSE in the silicate Earth were derived from a late veneer of primitive chondritic material, after core formation had ceased (Chou, 1978). Snow and Schmidt (1998) proposed that mantle HSE patterns instead reflected remixing of the outer core into the mantle. However, subsequent analyses using improved digestion techniques (Becker et al., 2006) cast doubt on the robustness of the Os, Ir and Ru data in that study (obtained by NiS fire assay), reducing the magnitude of the observed non-chondritic signature. Moreover, later work highlighted the importance of metasomatism and melt-rock reaction processes in producing non-chondritic HSE patterns in mantle rocks. Rehkämper et al. (1999) found that abyssal peridotites broadly contained HSE in chondritic proportions and that HSE ratios were inconsistent with an outer core input. Where non-chondritic ratios were identified in the Horoman peridotite, a petrogenetic model showed that these ratios were consistent with sulfide addition associated with melt percolation. Alard et al. (2000) then identified PPGE-rich (Pt-group) and IPGE poorer (Ir-group; Barnes et al. 1985) interstitial sulfides that were introduced during melt infiltration. These sulfides have the potential to produce non-chondritic HSE patterns in whole-rocks and also have suprachondritic Re/Os and $^{187}Os/^{188}Os$.

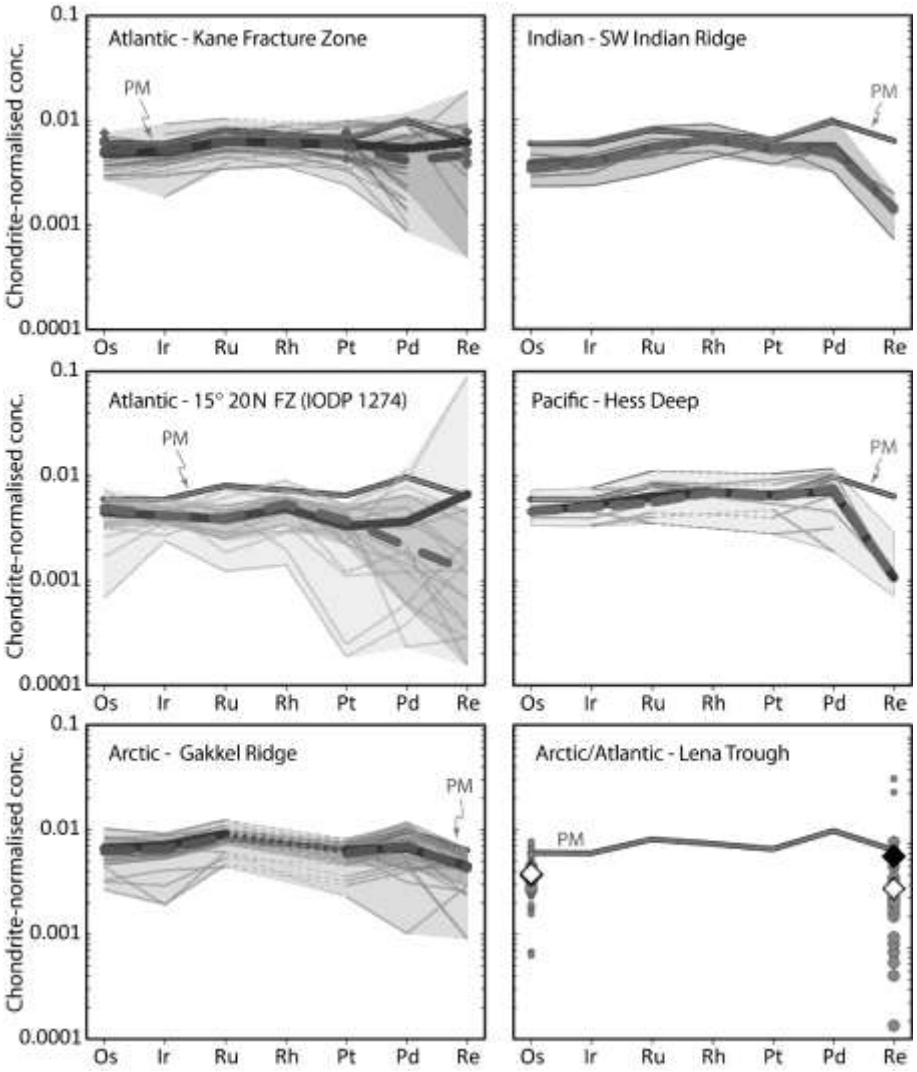

Figure 3. Chondrite-normalized concentration diagrams of the HSE in abyssal peridotites from the Atlantic, Indian, Pacific and Arctic Oceans. Average chondrite values were calculated with equal weighting from ordinary, enstatite and carbonaceous chondrites, from data compiled in Walker (2009) and from Fischer-Gödde et al. (2010). Thick solid lines denote mean compositions, thick broken lines are median values. The lightly shaded fields cover the whole range of compositions, while the darker shade represents only compositions within one standard deviation of the mean for that data set (not used for Indian and Pacific, where $n \leq 8$). For the Lena Trough (F), the black diamond denotes the mean and the white diamond is the median, smaller circles fall outside one standard deviation. References as for Figures 1 and 2, plus Kane FZ and Pacific – Rehkämper et al. (1999); Kane and Indian - Luguet et al. (2001; 2003); Kane, Indian, Pacific - Snow & Schmidt (1998); 15° 20 N FZ - Marchesi et al. (2013).

A study of Kane fracture zone peridotites (Atlantic Ocean) identified a range of HSE systematics in different lithologies (Luguet et al., 2003). Harzburgites have low Pd/Ir ratios and are sulfide-poor. Refertilised harzburgites often have higher concentrations of Pd, while lherzolites have approximately chondritic proportions of HSE and between 100 and 300 µg/g S, which encompasses the estimate for the PM (250 +/- 50 µg/g; Lorand, 1990; McDonough and Sun, 1995; Palme and O'Neill, 2014). Peridotites from the 15°20´ N fracture zone are typically more depleted (Marchesi et al., 2013) than those from Kane (Figure 3), and show complete consumption of sulfide in some cases, presumably with HSE (particularly the IPGE) then hosted by PGM. Both this study, and an earlier one looking at two sites with differing alteration from Gakkel Ridge (Liu et al., 2009), found there to be no significant mobilisation of the HSE during

serpentinisation, but S contents were reduced. The same is also true of weathering, except for Re and Pd in some cases. For the 15°20´ N fracture zone, there was also no observed mobilisation of HSE by sulfur- and Si-undersaturated melt, which is somewhat surprising given that S-undersaturated melt would be expected to dissolve sulfide. Presuming that sulfide was dissolved into the melt, the implication from the 15°20´ N samples is that all HSE are retained until sulfide is almost exhausted. However, this finding may be dependent on the phase relations in any given sulfide system, as fractionation of sulfide melt from solid sulfide would be expected to fractionate PPGE from IPGE (e.g., Mungall et al., 2005). In contrast to studies advocating melt percolation as a means to fractionate HSE (e.g., Alard et al., 2000), Liu et al. (2009) contend that supra-chondritic Ru/Ir and Pd/Ir in Gakkel peridotites cannot be reconciled with melt enrichment and therefore instead support an inherent primitive origin for such ratios.

HSE in mantle tectonites from continental extensional domains and continent-ocean transitions

Mantle tectonites exhumed in passive continental margin or transitional oceanic environments share many characteristics with similar rocks from ultraslow spreading ridges (see abyssal peridotite section). These environments often display the complete spectrum of peridotite compositions, including lherzolites, harzburgites and replacive dunites and because of their compositional variety, mantle rocks from these environments have been the focus of detailed petrological and geochemical studies of lithophile element behavior, HSE abundances and Re-Os isotopic studies. Many of these tectonites have been exhumed in the course of the development of small oceanic and sedimentary basins in the Alpine-Mediterranean realm (Piccardo and Guarnieri 2010).

Pyrenees. In the Pyrenees, numerous small, serpentinized peridotite bodies (typically km^2 size or less) occur as lenses in high-grade gneiss-granulite-sediment rock associations (e.g., at Lherz, Bestiac, Turon de Tecouere). The mantle and lower crustal rocks were presumably exhumed during extension and subsequent compressional movements between Iberia and the European plate in the Mesozoic to Cenozoic (Vielzeuf and Kornprobst 1984). The mantle rocks are predominantly variably serpentinized spinel lherzolites and harzburgites, with occasional spinel and garnet facies pyroxenitic banding (Bodinier et al. 1987, 1988). Melt infiltration affected incompatible trace elements, such as the light REE, in the mantle rocks to a variable extent (Vasseur et al. 1991). The small ultramafic body near the village of Lherz (Lers), the type locality of lherzolite, has been studied in detail and has yielded textural and geochemical evidence that the lherzolites in that body formed by reactive infiltration of incompatible element-depleted melt into older harzburgites (Le Roux et al. 2007). The peridotites at Lherz are a key example that shows how reactive transport of basic silicate melt may re-enrich depleted mantle rocks in incompatible major elements via precipitation of pyroxenes, a process called refertilization. The pyroxenites may represent leftover cumulates and reaction products from these processes. However, mechanical mixing of pyroxenite and harzburgite has also been proposed as a mechanism capable of producing the refertilisation at Lherz which is commonly attributed to melt reaction (Riches and Rogers, 2011).

Early Re-Os work on peridotites from Pyrenean ultramafic bodies by Reisberg and Lorand (1995) yielded positive correlations between measured $^{187}Os/^{188}Os$ and $^{187}Re/^{188}Os$ (the Re-Os isochron diagram, Fig. 4a), as well as Al_2O_3 contents (Fig. 4b), respectively. Al_2O_3 contents have been used as a preferred melt extraction index (see also Fig. 2) and proxy for the Re/Os ratio, because Re abundances are typically believed to have been partially affected by serpentinization, whereas Al is largely considered immobile during alteration processes (Reisberg and Lorand 1995, Shirey and Walker 1998). The positive correlation of $^{187}Os/^{188}Os$ with Al_2O_3 was interpreted to reflect past melt extraction, assuming the mantle rocks were cogenetic and

their different Al_2O_3, Re contents and Re/Os ratios reflected different degrees of partial melting. The intersection of the 'initial' $^{187}Os/^{188}Os$ and a chondritic evolution curve then gives a model age of 2.3 Ga (Reisberg and Lorand 1995). Figures 4b and 4c show this model age concept using the range of measured $^{187}Os/^{188}Os$ in bulk rocks of chondrites (Walker et al. 2002; Fischer-Gödde et al. 2010). The same approach was applied by Reisberg and Lorand (1995) to peridotites from the Ronda peridotite massif (see below). The ancient Re-Os model ages of these peridotite massifs, their coincidence with Sm-Nd model ages of overlying crustal rocks and their geodynamic position have been used to argue that these bodies represent fragments of exhumed subcontinental lithospheric mantle that have undergone Proterozoic melt extraction (Reisberg and Lorand 1995; Burnham et al. 1998). It is plausible to infer that the melt extraction processes may have occurred in an ocean ridge environment and consequently, the model ages would record the ancient formation of lithospheric mantle from asthenosphere.

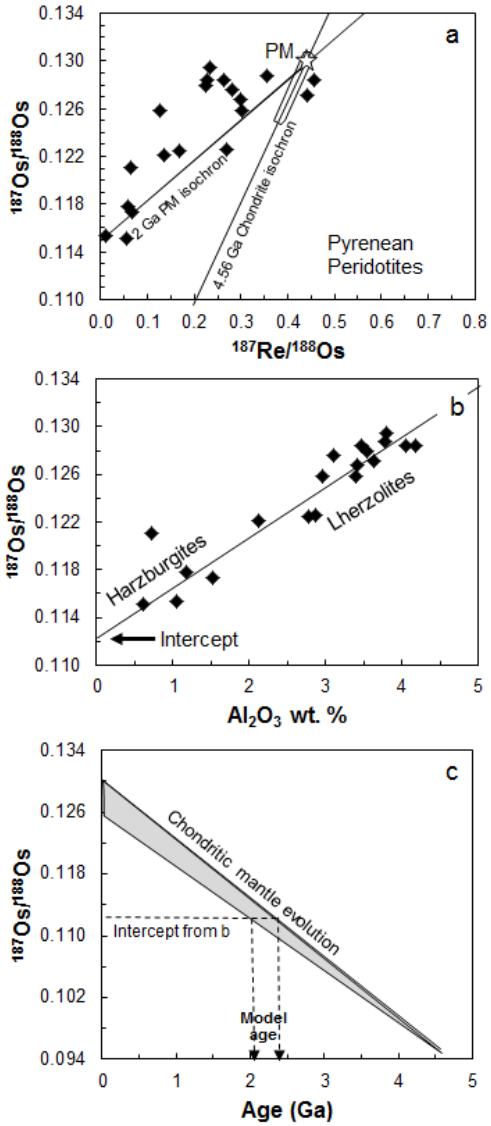

Figure 4. a) Re-Os isochron diagram showing measured $^{187}Os/^{188}Os$ and $^{187}Re/^{188}Os$ of peridotites from Pyrenean ultramafic bodies. Data sources: Reisberg and Lorand (1995); Burnham et al. (1998); Becker et al. (2006). Also shown is a 4.56 Ga chondritic reference isochron (Shirey and Walker 1998) and the primitive mantle model of Meisel et al. (2001) with an associated 2 Ga isochron. The field outlined on the isochron represents the spectrum (2 s.d.) of $^{187}Os/^{188}Os$ of bulk rocks of chondrites (Walker et al. 2002a; Brandon et al. 2005a, 2005b; Fischer-Gödde et al. 2010). b) $^{187}Os/^{188}Os$-Al_2O_3 diagram showing data from Pyrenean peridotites (from Reisberg and Lorand 1995). c) $^{187}Os/^{188}Os$ evolution diagram of the range of

chondritic compositions from a). Intersection of the $^{187}Os/^{188}Os$ of the correlation in b) at $Al_2O_3 = 0$ yields an initial $^{187}Os/^{188}Os_i$ that intersects the evolution curves in c) to yield Re-Os model ages of the inferred melt extraction that may have resulted in the development of the correlation in a) and b). The assumption behind this model age is that partial melting of the peridotites occurred approximately at the same time. If the assumption is incorrect, peridotites with the lowest $^{187}Os/^{188}Os$ may still yield a model age of melt extraction.

Subsequently published HSE concentration data for the same and additional samples show some features that are not only characteristic of peridotites from the Pyrenees, but also of mantle tectonites from many other locales. Here we will outline the differences between lherzolites and harzburgites, because these different lithologies have been well studied for their bulk rock compositions, as well as their sulfide and other accessory phase mineralogy and mineral compositions. The lherzolites (Fig. 5a) display limited abundance variations for Os, Ir, Ru and Rh, and variable abundances of Pt, Pd, Au, Re and the chalcogen elements S, Se and Te (Pattou et al. 1996; Lorand et al. 1999, 2008, 2010, 2013; Becker et al. 2006; Luguet et al. 2007; Fischer-Gödde et al. 2011; König et al. 2012, 2014; Wang and Becker 2013).

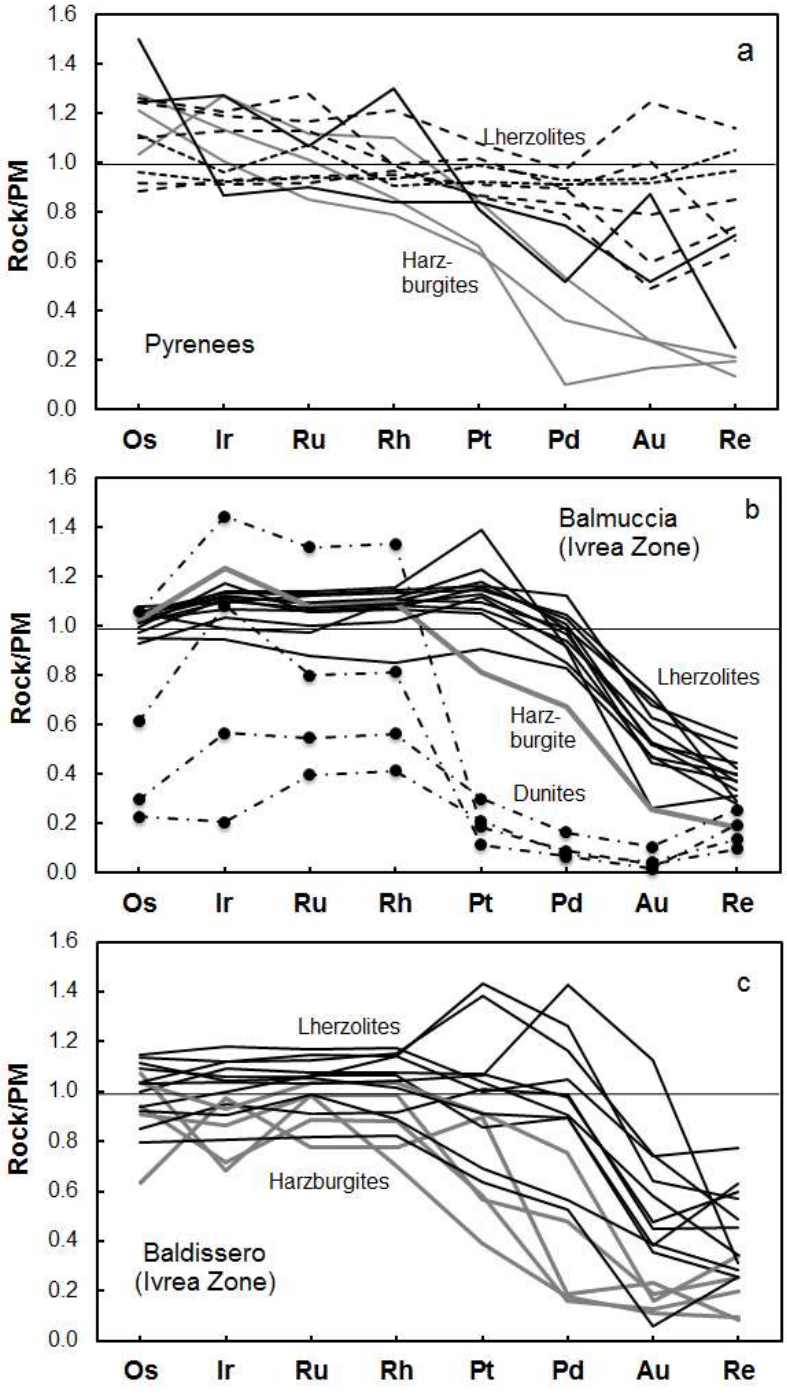

Figure 5. Primitive mantle normalized concentration diagrams of the HSE in representative peridotites from continental extensional and transitional oceanic environments. Note the linear concentration scale. a) Pyrenees (S France) - data from Fischer-Gödde et al. (2011). b) Balmuccia (N Italy) - Dash-dotted lines are tabular dunites, gray line harzburgite. c) Baldissero (N Italy) - Gray lines are harzburgites. Balmuccia and Baldissero samples from Wang et al. (2013). The primitive mantle values in this and subsequent diagrams are those given in Meisel et al. (2001); Becker et al. (2006) and Fischer-Gödde et al. (2011).

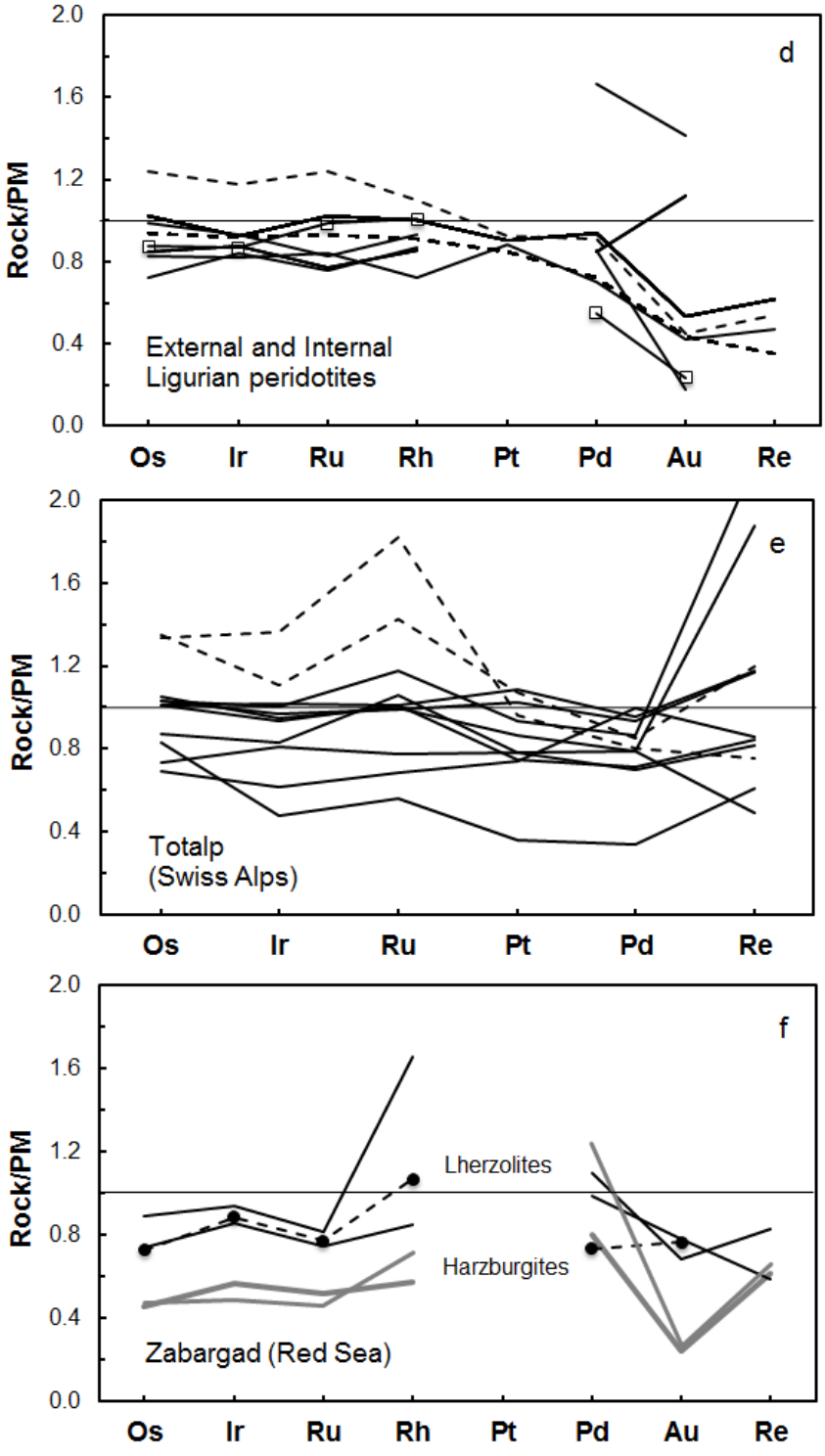

514

515 **Figure 5.** Continued. Note the different concentration scale compared to a-c. d) External and Internal
516 Ligurian peridotites (Luguet et al. 2004; Fischer-Gödde et al. 2011). e) Totalp (Swiss Alps) - No Au or Rh
517 data are available for these samples (van Acken et al. 2010a) and thus these elements were omitted from
518 the diagram. f) Zabargad Island (Red Sea) - Schmidt et al. (2000). Lherzolites are either solid or dashed
519 black lines in order to distinguish different patterns. Gray lines: harzburgites.

The highest abundances of Pt, Pd and Re in the Pyrenean lherzolites occur in samples that yield $^{187}Os/^{188}Os$ and major element compositions similar to estimates of the composition of the primitive mantle (Meisel et al. 2001; Becker et al. 2006). Ratios of the HSE in these samples suggest broadly chondritic proportions of the HSE, with the exception of Ru and Pd, which are suprachondritic compared to other HSE. In contrast, harzburgites (Fig. 5a) from the Lherz body are commonly strongly depleted in Rh, Pt, Pd, Re and chalcogens, whereas abundances of the Ir group PGE (IPGE; Os, Ir and Ru) were retained at similar to slightly higher levels than in lherzolites.

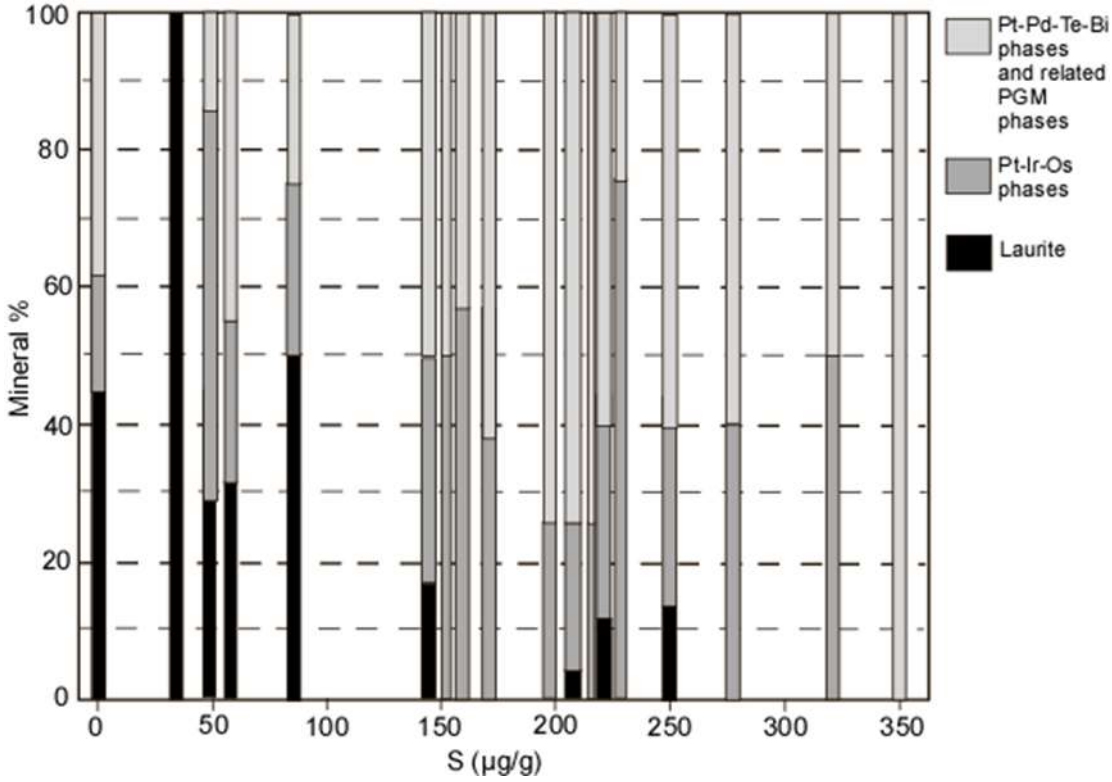

Figure 6. Proportions of different types of platinum group minerals in harzburgites and lherzolites from Lherz. The S content may be used as an indicator of the fertility of the rocks (modified from Lorand et al. 2010),

Study of the accessory phase mineralogy of peridotites from the Pyrenees has indicated the presence of variable proportions of different sulfide types (pentlandite, pyrrhotite, chalcopyrite, pyrite), alloy phases (Os-rich, Pt-rich, Au-rich) and other types of platinum-group metal phases such as Pt-bearing tellurides (Fig. 6) (Luguet et al. 2007; Lorand et al. 2008, 2010; Lorand and Luguet, 2015). The majority of these phases are likely low temperature exsolution products that formed during cooling of once homogeneous high-temperature phases such as sulfide liquids and monosulfide solid solution. The exsolution origin of such phases is reflected in strong chemical fractionations of some HSE (notably Pt, but sometimes also Pd and Au) and related elements (e.g., Bi, Te, Se and S) that are only observed on the grain scale, but not in corresponding bulk rocks. However, some alloy phases, for instance Pt-Ir- and IPGE-rich alloys may have been inherited from previous episodes of high degrees of melting (Lorand et al. 2010). The significance of these observations are discussed further below and by Lorand and Luguet (2015, this volume), and Luguet and Reisberg (2015, this volume).

Balmuccia, Baldissero and Lanzo peridotite bodies. In northern Italy, several peridotite bodies occur that also represent fragments of continental lithospheric mantle in an extensional continental margin setting. The peridotite bodies at Balmuccia, Baldissero and Lanzo were all derived from the southern European passive continental margin that had developed following the Variscan orogeny. Towards the end of the Variscan orogeny during the lower Carboniferous and upper Permian, the lower crust and presumably also existing continental lithospheric mantle were flooded with MORB like magma from the asthenosphere (Quick et al., 2009; Snoke et al., 1999; Voshage et al., 1990). The peridotite bodies of Balmuccia and Baldissero, mostly spinel lherzolites with subordinate harzburgites, discordant dunites and pyroxenites, show different distributions of their T_{RD} (Fig. 10 in Wang et al. 2013). In Balmuccia the model ages of the lherzolites show a single distribution peak of Paleozoic model ages, with a harzburgite yielding the only Proterozoic model age (Note: samples with $^{187}Os/^{188}Os < 0.1254$ yield Precambrian T_{RD}[PM] model ages, see Fig. 7). At Baldissero, a bimodal distribution of T_{RD} occurs with a Paleozoic and a Proterozoic peak (Fig. 10 in Wang et al. 2013). Lithophile element, Re-Os, Sm-Nd isotopic and HSE abundance data and textural relations can be interpreted such that depleted Proterozoic mantle (the harzburgites) were variably refertilized by MORB-like magma during the Paleozoic (Mazzucchelli et al. 2009, Mukasa and Shervais 1999, Obermiller 1994, Rivalenti et al. 1995, Wang et al. 2013). The greater compositional homogeneity of peridotites from Balmuccia compared to those from Baldissero (Fig. 5b, c) suggests that the former body was fluxed and re-equilibrated with melt more efficiently than the latter. IPGE concentrations in harzburgites in both bodies are lower than in lherzolites, which is opposite to observations from some other suites of peridotites (Pearson et al. 2004; Becker et al. 2006). Re-Os data suggests that some of the Cr-diopside-rich websterites at Balmuccia may have formed during these or earlier events of reactive melt infiltration. However, most Al-augite-rich clinopyroxenites yielded Jurassic model ages (Wang and Becker 2015c). Spinel and plagioclase bearing lherzolites from the Lanzo peridotite massif are similar to lherzolites from Baldissero in their HSE patterns (not shown in Fig. 5) and in their distribution of $^{187}Os/^{188}Os$ data (Fig. 7a, Becker et al. 2006, Fischer-Gödde et al. 2011).

External and Internal Ligurian peridotites. The External Ligurian peridotites are now recognized to represent mantle rocks of the subcontinental lithospheric mantle of the south European realm (but more distal than Lanzo, Balmuccia and Baldissero), presumably exhumed during the early- to mid-Mesozoic (Rampone et al. 1995; Piccardo and Guarnieri 2010). In contrast, the Internal Ligurian peridotites have been interpreted to derive from depleted mantle of ultraslow spreading ocean floor of the Jurassic Tethys Ocean (Rampone et al. 1996; 1998; Piccardo and Guarnieri 2010). In both cases, plagioclase-spinel lherzolites are the predominant rock type (with subordinate pyroxenites).

Detailed petrological and geochemical work in these and other studies has shown that the Ligurian peridotites have been variably affected by melt infiltration and refertilization (Rampone et al. 2004). In spite of the somewhat different tectonic setting, the Re-Os and HSE composition of External and Internal Ligurian peridotites is similar to other lherzolites (Figs. 5d and 7a; Snow et al. 2000; Luguet et al. 2004; Fischer-Gödde et al. 2011). Mantle lherzolites and pyroxenites with evidence for melt infiltration and chemical characteristics similar to lherzolite massifs from N Italy have been described from the suture zone in the Alps (e.g., Totalp, Swiss Alps; van Acken et al., 2008; 2010a; 2010b). The Totalp lherzolite body is notable for its Re-rich composition and slightly suprachondritic Re/Os of the lherzolites (Figs. 5e, 7c), which is different from most other peridotite tectonites. The Re-rich composition of the lherzolites and associated pyroxenites can be related to infiltration of melt with MORB-like isotopic compositions, presumably during the Mesozoic or late Paleozoic.

Zabargad peridotite. The peridotite body of Zabargad Island in the Red Sea represents a young example of subcontinental lithospheric mantle, exhumed during post-Miocene extension of the Red Sea (Bonatti et al. 1986, Piccardo et al. 1993).

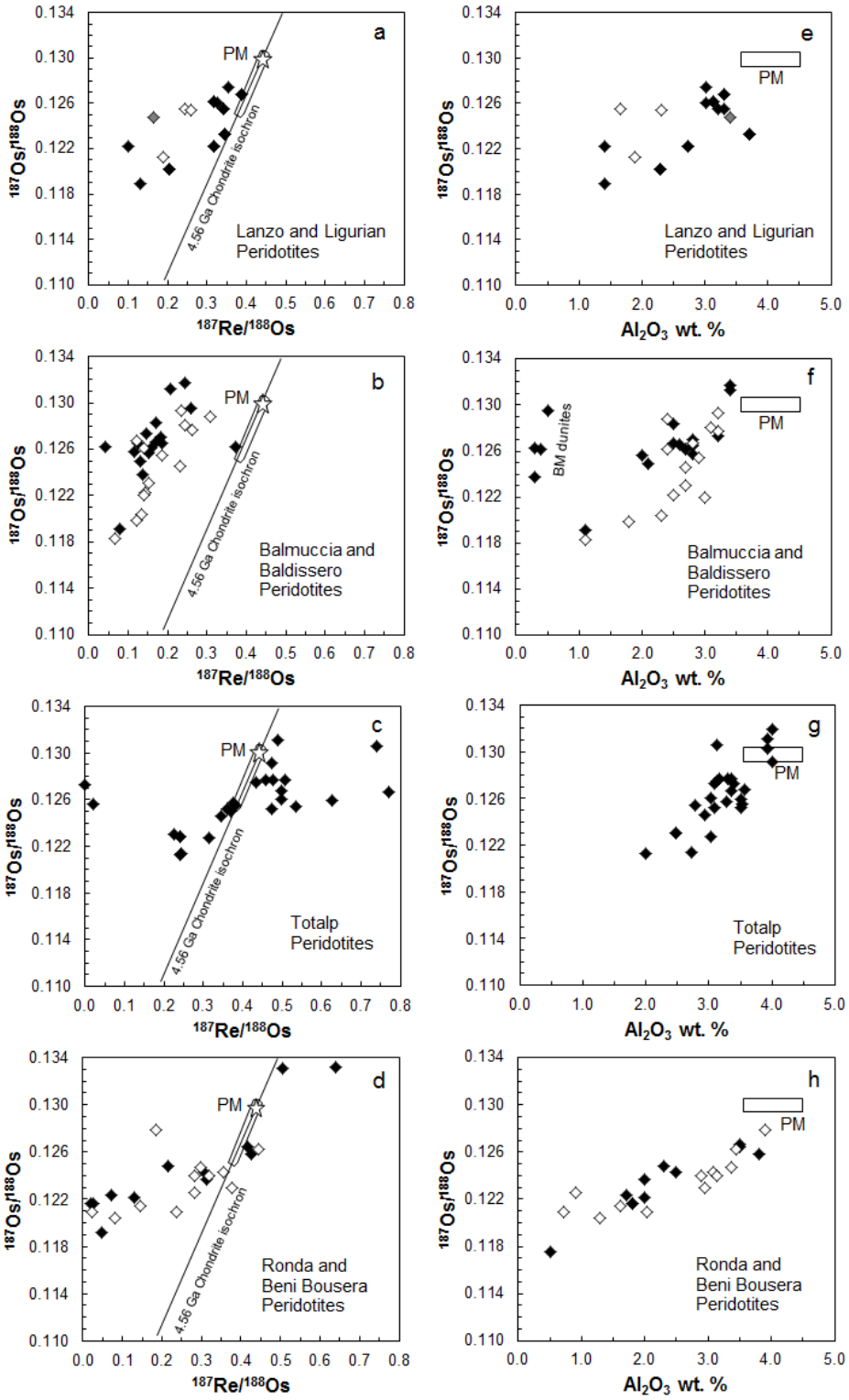

Figure 7. a-d) Re-Os isochron diagrams showing measured compositions of peridotites from different mantle tectonites. Peridotite data from Reisberg and Lorand (1995), Pearson et al. (2004), Becker et al. (2006), van Acken et al. (2010a), Fischer-Gödde et al. (2011), Wang et al. (2013). Further details see Fig. 4. e-h) $^{187}Os/^{188}Os$-Al_2O_3 diagrams. Estimates for the Al_2O_3 content of PM are given as a range from 3.5 to 4.5 wt. %, rather than a single value (McDonough and Sun 1995; Palme and O'Neill 2014 and references

therein). Solid diamonds: Lanzo (a, e), Balmuccia (b, f), Totalp (c, g), Ronda (d, h). Open diamonds: Internal Ligurides (a, e), Baldissero (b, f), Beni Bousera (d, h). Note that depleted peridotites tend to have low $^{187}Os/^{188}Os$, however, this is not the case for dunites from Balmuccia (BM).

Spinel-bearing lherzolites, amphibole harzburgites and dunites display evidence for metasomatism by fluids or hydrous melts which led to the formation of amphibole harzburgites (Piccardo et al. 1993). The HSE patterns and S abundances of the lherzolites are similar to comparable rocks elsewhere. However, Cu is notably depleted in these lherzolites (around 10 μg/g). Amphibole-bearing dunite and harzburgite have higher than expected abundances of Pd, Au, Re and S (Fig. 5f; Schmidt et al. 2000). An orthopyroxenite and a plagioclase wehrlite display high PGE and Au abundances, but low Re, S and Cu abundances (Schmidt et al. 2000).

Horoman peridotite. The Horoman peridotite body in Japan comprises outcrops of layered dunite, harzburgite and lherzolite that have been interpreted to be the result of variable degrees of melt-peridotite reaction that occurred during percolative melt transport in the mantle. Dunites, harzburgites and spinel- and plagioclase-bearing lherzolites at Horoman are believed to have undergone variable degrees of pyroxene dissolution into percolating olivine-saturated magma (Takahashi 1992; Takazawa et al. 1992, 1996, 1999). Despite the occurrence of highly unradiogenic Pb in the Horoman peridotite (Malaviarachchi et al. 2008), abundances of the HSE and $^{187}Os/^{188}Os$ data in lherzolites and harzburgites (Rehkämper et al. 1997; Saal et al. 2001) are similar to data from peridotites elsewhere. The correlation of Re abundances with MgO in the peridotites may be the result of refertilization processes (Saal et al. 2001).

HSE in ophiolites that formed at fast spreading ridges with little or no influence from subduction processes

Oman ophiolite, Wadi Tayin Section. The crustal and mantle section of Wadi Tayin in the SE part of the Samail ophiolite (Oman) represents one of the best exposed examples of fast-spreading oceanic crust and upper mantle on Earth (Pallister and Hopson, 1981; Hanghøj et al., 2010). Geochemical studies of the crustal rocks in the section indicate that the crust mostly comprises normal mid-ocean ridge-type basalts and gabbros (Koga et al. 2001, Pallister and Knight 1981). Part of the ophiolite likely formed at an ocean spreading center about 90-95 Ma ago, but must have been incorporated into an active subduction-collision zone that led to changes in magma compositions in the NW part of the ophiolite (Searle and Cox 1999, Tilton et al. 1981).

A study of PGE and Re abundances and $^{187}Os/^{188}Os$ in the lower crustal gabbros indicated low Re concentrations and systematically higher PGE concentrations compared to MORB (Peucker-Ehrenbrink et al. 2012). The Os isotopic compositions of some gabbros may have been affected by circulation of seawater. The HSE abundances and $^{187}Os/^{188}Os$ of parts of the exposed mantle section were studied across an 11 km transect from the exposed Moho into high- and then low-temperature peridotites underneath (Hanghøj et al. 2010). Platinum group element concentration data on harzburgites of similar composition have also been published by Lorand et al. (2009). The high-temperature peridotites likely represent textures and compositions of the mantle inherited from the ocean ridge stage, whereas the low temperature peridotites underneath may represent mantle modified by deformation, re-equilibration and fluid transport during obduction of the ophiolite. The mantle rocks at Wadi Tayin comprise serpentinized harzburgites and replacive dunites that are strongly enriched in fluid-mobile incompatible lithophile elements (e. g., Rb, Pb), which may reflect late alteration or, alternatively, retention of small quantities of melt during peridotite-melt interaction (Hanghøj et al. 2010). The strong fractionation of the REE in most of these samples is significantly greater than in abyssal peridotites and suggests that these rocks can be regarded as highly depleted melting residues in which the LREE were strongly depleted by fractional melting (Hanghøj et al. 2010). The dunites

are usually interpreted as forming by magmatic dissolution-precipitation processes that dissolve pyroxenes and increase the modal amount of olivine (Kelemen et al. 1995). Harzburgites typically show consistent HSE abundances with IPGE greater than most abyssal peridotites, slight depletion in Pt and enrichment in Pd. Dunites, however, show far greater variability, including their Os/Ir ratio, and range from moderately depleted abundances of Re, Pd and Pt to variable enrichments of Re, Pd and Pt, sometimes a factor of 2-3 times higher than values commonly observed in lherzolites (Fig. 8). The enrichments of Re, Pd and Pt in the harzburgites and dunites may have resulted from shallow precipitation of magmatic sulfide from S-saturated magmas, although S concentrations in the mantle rocks are low (typically a few tens of ug/g, Hanghøj et al. 2010) compared to Pd, Re and Cu abundances (Fig. 8). The initial $^{187}Os/^{188}Os_i$ (at 90 Ma) of the harzburgites and dunites are remarkable in that they display a large range from as low as 0.113 to suprachondritic values of 0.15 in dunites (Fig. 9). As in other mantle tectonites, most samples are in the chondritic to subchondritic range, however, some samples with suprachondritic $^{187}Os/^{188}Os$ either require interaction with magma with radiogenic $^{187}Os/^{188}Os$, or have lost a substantial amount of their original inventory of Re.

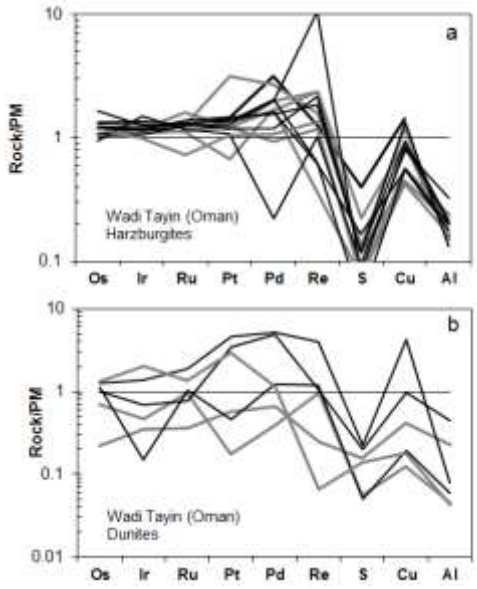

Figure 8. Primitive mantle-normalized logarithmic concentration diagrams of the HSE in a) harzburgites and b) dunites from Wadi Tayin, Samail ophiolite, Oman (Hanghøj et al. 2010). Black patterns are rocks with high-temperature fabrics, gray patterns are 'low-temperature' rocks from the lower part of the mantle section. Sulfur, Cu and Al are included for comparison with Re and Pd (see text).

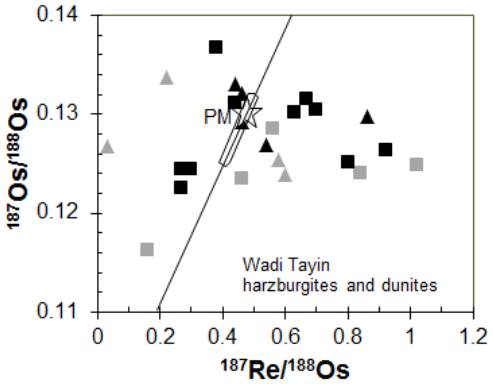

Figure 9. Re-Os isochron diagram for harzburgites (squares) and replacive dunites (triangles) from the Wadi Tayin section in the Samail ophiolite (Oman). The ophiolite formed part of a spreading center 95 Ma ago. Black symbols are rocks with high-temperature fabrics, gray symbols are 'low-temperature' rocks

from the lower part of the mantle section. Dunites with $^{187}Os/^{188}Os$ of up to 0.15 are not shown. Data from Hanghøj et al. (2010). Chondrite field, 4.56 Ga reference isochron and PM composition as in Fig. 4.

Taitao ophiolite (Chile). The Taitao ophiolite on the Taitao Peninsula in S. Chile is believed to represent part of the oceanic lithosphere formed about 6 Ma ago on the Chile Ridge, which is presently subducting under South America (Guivel et al. 1999). The ophiolite was obducted during or soon after its magmatic formation and was affected by hydrothermal alteration and a metamorphic overprint related to subduction, obduction and contact metamorphism imposed by young granitoid intrusions. The Taitao ophiolite displays a somewhat dismembered Penrose style sequence of serpentinized harzburgites, gabbros, basic dikes, pillow basalts and sediments (Schulte et al. 2009 and references therein). The chemistry of the basic rocks hints that at least some of these magmas may have been affected by subduction zone processes, similar to basalts from the active Chile Ridge (Klein and Karsten 1995). The serpentinized harzburgites display some variability in their HSE patterns ranging from samples that display variable depletions of Re and Pd, depletion of Pd but not Re, and samples showing positive or negative anomalies of Pt relative to Ru and Pd (Fig. 10; Schulte et al. 2009). Basic rocks tend to have very low abundances of IPGE, with variable positive Pt anomalies and strong enrichment of Re (Schulte et al. 2009). Measured $^{187}Os/^{188}Os$ range from 0.117 to 0.128, with many samples scattering around a 1.6 Ga reference line in an isochron diagram (Figs. 11). Because of the relatively large range in $^{187}Os/^{188}Os$ and the strongly depleted major element composition of the harzburgites, the slope in the $^{187}Os/^{188}Os$-Al_2O_3 diagram (Fig. 12) is different from other suites of peridotites (Figs. 2 and 7). Schulte et al. (2009), however, interpreted the HSE data of the mantle rocks to reflect a two-stage partial melting history at 1.6 Ga and 6 Ma ago. Textural evidence indicates that some harzburgites may have been affected by melt impregnation processes, which may have led to some of their chemical and isotopic variability. The initial $^{187}Os/^{188}Os_i$ (6 Ma) of the basic rocks ranges from chondritic to suprachondritic (γOs_i = -1 to +342). The suprachondritic composition may either reflect the presence of a rhenium-enriched component in the mantle source or the influence of seawater/altered crust during the emplacement of the magmas.

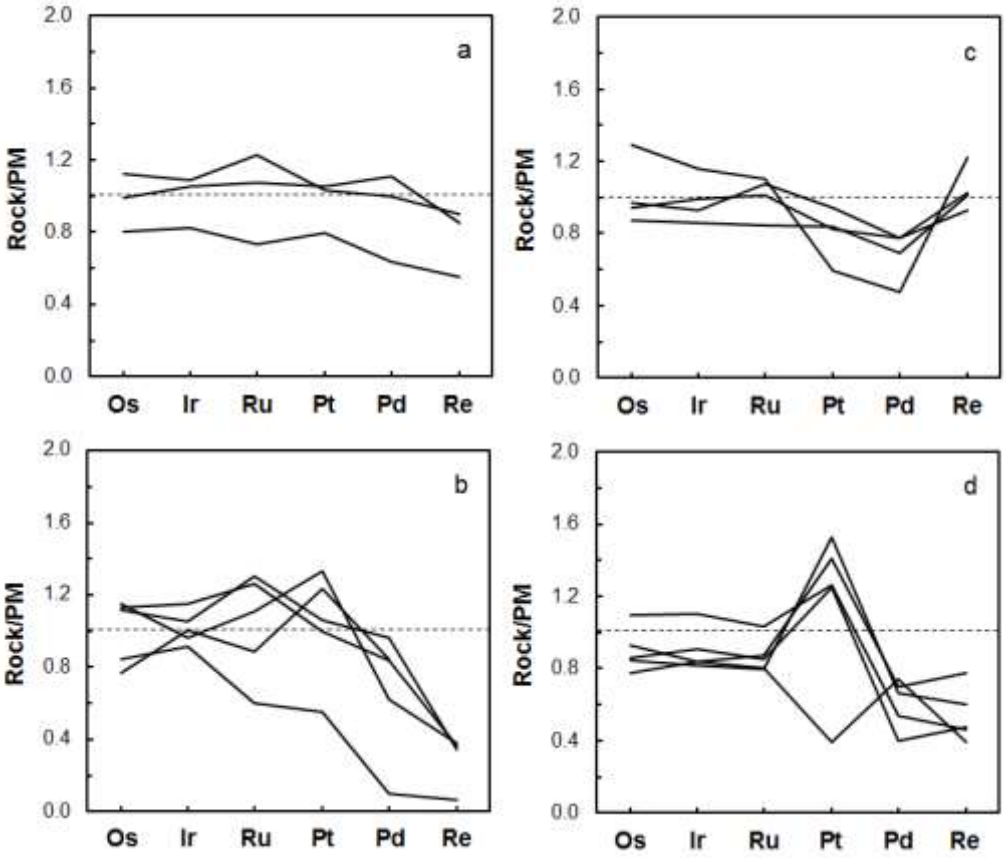

Figure 10. Primitive mantle-normalized concentration diagrams of the HSE in mantle rocks from the Taitao ophiolite. Four different types of patterns can be distinguished: a) relatively little fractionated peridotites; b) rocks with stronger depletions of Pd and Re (the sample with low abundances represents a pyroxenite); c) samples that display depleted Pd and re-enrichment of Re; d) rocks that display strong positive or negative anomalies of Pt. Data from Schulte et al. (2009).

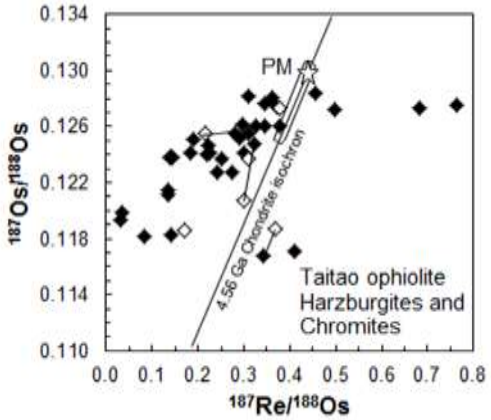

Figure 11. Re-Os isochron diagram for peridotites (solid symbols) and chromites (open symbols) in harzburgites from the Taitao ophiolite (6 Ma old). Tie lines connect chromites and corresponding bulk rocks, indicating small-scale Os isotopic disequilibrium in these mantle rocks. Data from Schulte et al. (2009),

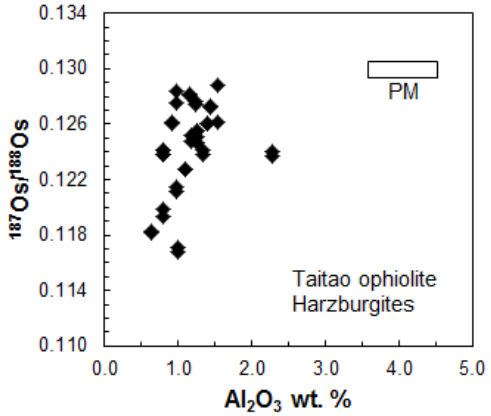

Figure 12. $^{187}Os/^{188}Os$-Al_2O_3 diagram for whole rock harzburgites from the Taitao ophiolite. Note the large range in $^{187}Os/^{188}Os$ in these depleted mantle rocks. Data from Schulte et al. (2009).

High-temperature orogenic peridotites from convergent plate margin settings

Many ophiolites have originally been emplaced near subduction zones and commonly even their mantle sections were affected by magmas that formed in supra-subduction zone environments (see below). Among high-temperature orogenic peridotites, evidence for the influence on mantle rocks by magmas that may have formed in convergent plate margin settings is not very common and, in fact, is somewhat ambiguous. Here, we discuss examples of mantle tectonites that were emplaced during or in the aftermath of subduction and collision processes. In the case of the Ronda and Beni Bousera ultramafic massifs these bodies represent mantle exhumed during the collapse of the Betic orogenic belt in the western Mediterranean during the Cenozoic (van der Wal and Vissers 1993; Blichert-Toft et al. 1999). In the southern Bohemian massif, similar processes occurred during collapse of the core zone of the Variscan belt during the Carboniferous (Medaris Jr et al. 2005). The principal evidence is mostly derived from geodynamic reconstructions in combination with the lithophile element and isotope geochemistry of peridotites and pyroxenites. Notably garnet bearing pyroxenite layers in these peridotite massifs show strong evidence that they formed from magmas with crustal geochemical and isotopic signatures (e.g., Eu anomalies, enrichments of LREE, graphite with $\delta^{13}C$ suggestive of organic protoliths, sediment-like Sr-Nd-Pb isotopic compositions; (Pearson et al. 1991a; 1991b; 1993; Becker 1996a).

Ronda (Southern Spain). The Ronda peridotite has been a classic study area of mantle processes (Frey et al. 1985, Reisberg and Zindler 1986, Reisberg et al. 1989). It shows a transition from garnet lherzolite to spinel lherzolite and plagioclase-bearing peridotites (Obata 1980). Initially the peridotites were regarded as residues of partial melting (Frey et al. 1985); however, later the significance of melt infiltration into continental lithospheric mantle was recognized and the latter process also may have caused partial re-equilibration of the peridotites at shallow pressure-temperature conditions (Bodinier et al. 2008). Re-Os model ages of depleted peridotites yield an average age of melt extraction in these rocks of 1.3 ± 0.4 Ga (Reisberg et al. 1991, Reisberg and Lorand, 1995; Becker et al. 2006). The HSE patterns (not shown) and $^{187}Os/^{188}Os$ (Fig. 7d, h) of the peridotites are similar to data on fertile to depleted peridotite tectonites exhumed in extensional tectonic settings (Lorand et al. 2000; Becker et al. 2006; Fischer-Gödde et al. 2011). Pyroxenite layers from Ronda have suprachondritic Re/Os and $^{187}Os/^{188}Os$, and Pd and Pt are enriched relative to IPGE (Marchesi et al. 2014; Reisberg et al. 1991). The depletion of Re in some pyroxenites relative to Pd (Fig. 21c) may reflect multi-stage melting processes (Marchesi et al. 2014).

Beni Bousera (Morocco). The Beni Bousera peridotite massif crops out on the Moroccan side of the Alboran Sea and shares a similar history with the Ronda body. Re-Os and HSE concentration data on peridotites are comparable with data from Ronda (Fig. 7d, h, Kumar et al. 1996; Pearson et al. 2004; Pearson and Nowell 2004; Luguet et al. 2008b; Fischer-Gödde et al. 2011). Studies of the Re-Os systematics in pyroxenite layers from Beni Bousera yielded highly variable Re/Os and $^{187}Os/^{188}Os$, the latter reflecting radiogenic ingrowth, but also partly incorporation of unradiogenic Os from reaction with the host peridotites (Kumar et al. 1996, Pearson and Nowell 2004). The Re-Os model ages cluster near 1.3 Ga, similar to results from some peridotites, and similar to Lu-Hf ages of some, but not all pyroxenites. The spectrum of Re-Os model ages and Lu-Hf isochron ages is consistent with other evidence that suggests a complex multi-phase history of both the Ronda and the Beni Bousera bodies (Loubet and Allègre 1982, Marchesi et al. 2014). Luguet et al. (2008b) and Marchesi et al. (2014) found variations of Pt/Os and Re/Os in some bulk rocks and sulfides from pyroxenites at Beni Bousera and Ronda, respectively. These rocks were interpreted to represent likely equivalents of the sources of mantle plume-derived picrite and komatiite lavas with elevated ^{186}Os signatures (Brandon and Walker 2005 and Discussion section).

Southern Bohemian Massif (Lower Austria, Czech Republic). In the Bohemian Massif, kilometer-sized bodies comprised of serpentinized high-temperature garnet lherzolites, spinel harzburgites and dunites occur enclosed in high-pressure granulites and amphibolite facies gneisses (e.g., Carswell and Jamtveit 1990; Becker 1996b; 1997; Medaris Jr et al. 2005). As in the peridotite massifs of the Betic cordillera, the garnet pyroxenite layers in the peridotites show chemical and isotopic compositions that suggest that they precipitated from basic magmas that formed in mantle contaminated by recycled sedimentary material (Becker 1996a). Detailed Re-Os work on layered peridotite-pyroxenite rocks indicates that peridotite-derived Os and Cr are mobilized during melt-rock reaction that led to the formation of layered pyroxenite-dunite rocks (Becker et al. 2001; 2004). The pyroxenites in these rocks show suprachondritic initial $^{187}Os/^{188}Os$ which may be inherited from subducted materials as indicated by initial Sr-Nd isotopic compositions. The variation of $^{187}Os/^{188}Os_i$ in modally layered lithologies indicates Os isotopic disequilibrium on the cm-scale resulting from magmatic infiltration processes. Another, yet different, example of metasomatic overprint that affected HSE abundances in peridotites in the Bohemian Massif are Mg-rich peridotites with relatively high IPGE contents (e.g., up to 10 ng/g Os), but not quite as high Pt, Pd and Re abundances (Ackerman et al. 2013). These rocks occur with pyroxenites and Fe-rich cumulate rocks with high Pt, Pd and Re abundances (Fig. 13).

In peridotites from Ronda, Beni Bousera and Lower Austria, measured $^{187}Os/^{188}Os$ are subchondritic or chondritic, similar to peridotites from extensional tectonic settings. Pyroxenites show high, but variable Re/Os and suprachondritic γOs_i. However, unlike some data on lithophile elements, these features are not necessarily indicative of the influence of subducted crust or subduction zone fluids. High Re/Os (and γOs_i) seem to be a hallmark of mantle pyroxenites and may be acquired by magmatic fractionation in the crust or during melting and transport of magmas in the mantle (e.g., Pearson and Nowell 2004; van Acken et al. 2010b; Marchesi et al. 2014; Wang and Becker 2015c). This topic will be discussed in later sections.

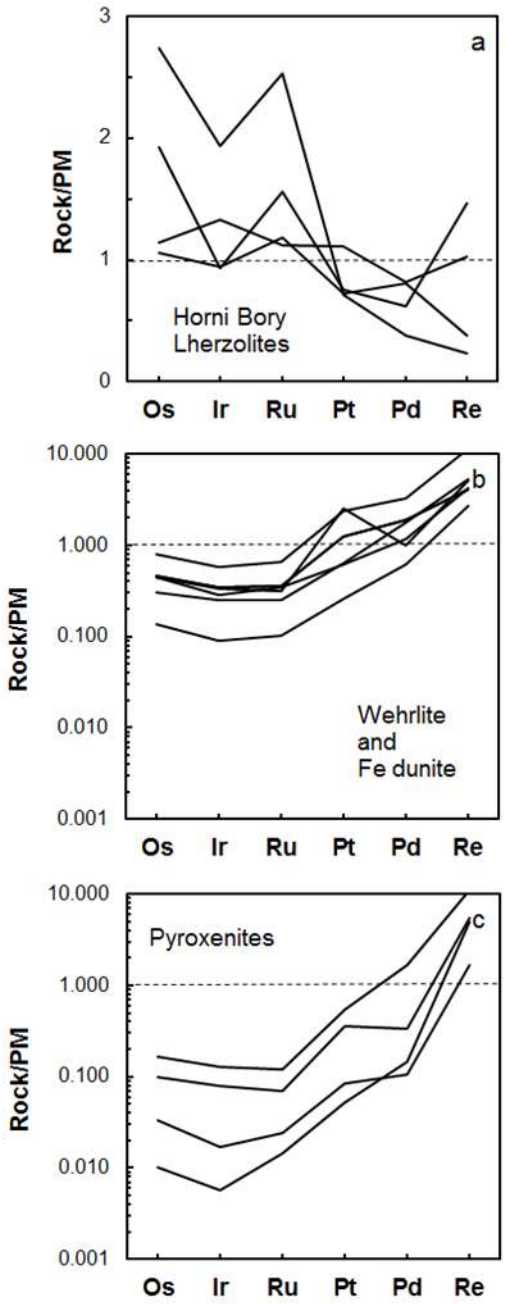

Fig. 13. Primitive mantle-normalized HSE concentration diagrams of a) mantle peridotites (lherzolite); b) metasomatic Fe-dunite-wehrlite rocks; c) pyroxenites from the Horni Bory peridotite massif (Bohemian Massif, Czech Republic). Note the linear scale in a). Data from Ackerman et al. (2013).

Highly siderophile elements in peridotites and melt-reacted lithologies of ophiolites influenced by convergent plate margin magmatism

In comparison to ophiolites with little subduction influence, convergent plate margin ophiolites typically comprise more depleted harzburgitic mantle sections and thicker ultramafic sequences in the lower crust. This is due to the greater degree of partial melting that usually occurs in the fluid-fluxed supra-subduction zone setting. However, the presence of hydrous

melts and fluids also promotes the formation of melt-reacted lithologies such as dunites, pyroxenites and, in particular, chromitites, in the mantle sections of ophiolites from convergent plate margins. Such melt-rock reaction, and the lithologies it produces, is diverse and depends principally on the melt/rock ratio and the degree of saturation of silica and sulfide in the melt. The variable impact on sulfide is, of course, critical to the behavior of the HSE, and melt-rock reaction is thus a major process by which HSE are fractionated and heterogeneity is generated. This fractionation of the HSE, including that which occurs during chromitite formation, likely plays an important role in defining the HSE characteristics of magmas at Earth's surface, particularly those of convergent margin ophiolites and in volcanic arc systems (e.g., Dale et al., 2012b).

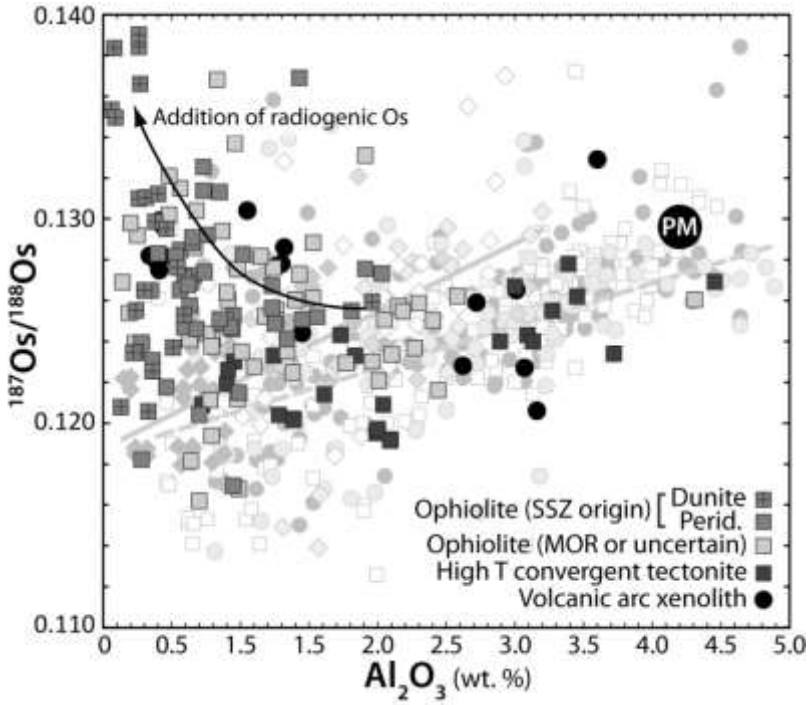

Figure 14. $^{187}Os/^{188}Os$-Al_2O_3 diagram for ophiolite ultramafic rocks (predominantly harzburgites, but also dunites), high-temperature convergent tectonites and sub-arc mantle xenoliths (see legend for symbols). Also shown for comparison are abyssal peridotites (diamonds), ocean island basalt mantle xenoliths (light grey circles), continent-ocean transitional tectonites (white squares) and sub-continental lithospheric xenoliths (mid-grey circles). There is considerable scatter in all datasets, partly reflecting variable ages of melt depletion, but also probably recent resetting of $^{187}Os/^{188}Os$ by seawater or melt interaction. The most Al-depleted ophiolitic samples (particularly those from convergent margin settings) and subduction zone-related ultramafics have more radiogenic ^{187}Os isotope compositions than peridotites from other settings. This presumably reflects a flux of radiogenic Os, or possibly a time-integrated addition of Re, related to the flux from the subducting slab, although greater melt-rock ratios in this environment may also play a part. Crustal contamination during emplacement is also possible. In part, the decoupling of $^{187}Os/^{188}Os$ from Al_2O_3 is due to the formation of dunitic rocks by melt-rock reaction, but many peridotites in convergent settings also possess more radiogenic Os than expected for a given Al content. Data sources for ophiolites: Snow et al. (2000); Kepezhinskas and Defant (2001); Büchl et al. (2004); Becker et al. (2006); Schulte et al. (2009); Hanghøj et al. (2010); Aldanmaz et al. (2012); O'Driscoll et al. (2012). High-T convergent margin tectonites: Reisberg et al. (1991); Roy-Barman et al. (1996); Becker et al. (2001, 2006); Pearson et al. (2004); Marchesi et al. (2014). Sub-arc xenoliths: Brandon et al. (1996); McInnes et al. (1999); Widom et al. (2003). Abyssal peridotites – see Figs. 1 & 2. Ocean island basalt mantle xenoliths – see Fig. 2. Continent/continent-ocean transition tectonite: Reisberg and Lorand (1995); Meisel et al. (1996); Roy-Barman et al. (1996); Rehkämper et al. (1999); Snow et al. (2000); Saal et al. (2001); Becker et al. (2006); Luguet et al. (2007); van Acken et al. (2008); Riches and Rogers (2011); Wang et al. (2013).

.

At the same time, there is the potential for sulfide to be exhausted during moderate to high degrees of mantle melting, particularly if sulfur solubility is increased (Jugo, 2009) due to an elevated oxygen fugacity of the sub- or back-arc mantle, relative to typical depleted MORB mantle (e.g., Carmichael, 1991; Kelley and Cottrell, 2009). Given the extremely chalcophile nature of the HSE (e.g., Mungall and Brenan, 2014; with the possible exception of Re; Brenan, 2008), sulfide exhaustion would cause HSE behavior to depart significantly from the typical mid-ocean ridge setting where sulfide is thought to remain in the residue.

Commonly, convergent margin ophiolites contain substantial units of podiform chromitite, enveloped in dunite, which require high degrees of melt depletion and are probably formed through a process of melt-rock reaction, particularly when a hydrous melt is present and the melt/rock ratio is high, or as cumulates from melts formed through high degrees of melting (Ballhaus, 1998; Zhou et al., 1998). Chromitites are known to contain variable but high concentrations of HSE (Prichard and Lord, 1996), particularly the IPGE, indicating their presence in high concentrations in the chromitite-forming melts. Further concentration of HSE occurs primarily because chromitites contain associated platinum-group mineral grains (PGM) which form due to a local oxygen fugacity-induced reduction in solubility of the HSE (Finnigan et al., 2008). This reduction in oxygen fugacity occurs locally around chromite crystals because of their preference for trivalent transition metal cations, particularly Cr^{3+} and Fe^{3+} ions. The IPGE have lower solubilities in silicate melts than PPGE, on the order of tens versus hundreds of ng/g (e.g., O'Neill et al., 1995; Borisov and Walker, 2000; Brenan et al., 2005; Ertel et al., 2006), and hence Os, Ir and Ru are particularly enriched in PGM from chromitites. Although chromitites and platinum-group minerals (PGM) are covered more comprehensively in O'Driscoll & González-Jiménez (2015, this volume), we include a brief Os isotope summary in the Discussion because ophiolitic chromitites are a major source of PGM, and they have a direct bearing on determining both the Os isotopic composition of the convecting mantle and the degree of mantle heterogeneity. Here we focus mainly on HSE behavior in the range of mantle lithologies present in ophiolites, rather than the specifics of PGM mineralogy and its role in HSE behavior (cf. O'Driscoll & González-Jiménez, 2015, this volume).

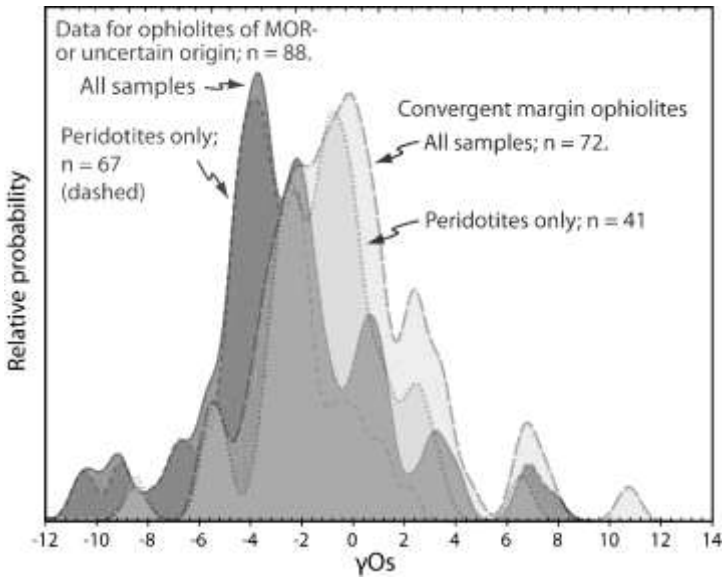

Figure 15. Probability density plot of $\gamma Os_{initial}$ in ophiolitic ultramafic rocks (peridotites, dunites and chromitites), grouped according to geological setting of formation. $\gamma Os_i = (^{187}Os/^{188}Os_{sample\ initial}/^{187}Os/^{188}Os_{chondrite\ initial} -1) \times 100$. The absolute values in this plot should be treated with caution as these include a correction for ingrowth based on the measured $^{187}Re/^{188}Os$, which, in some cases, may have been perturbed during/since emplacement. In addition, this plot is based on a limited number of different

ophiolites, with several ophiolites contributing a disproportionate number of data: Troodos (Cyprus), Samail (Oman), Shetland (UK), Taitao (Chile) and Jormua (Finland) ophiolites account for 129 of the 160 analyses. Given the different Os isotope records preserved by PGM grains from different ophiolites (Pearson et al., 2007), much of this difference could merely reflect large-scale mantle heterogeneity. Nonetheless, the overall offset between the two categories is two to four gamma units, which may represent a real difference generated by addition of radiogenic Os in the supra-subduction zone environment. Data sources given in Fig. 14, except Becker et al. (2006) and Dijkstra et al. (2010).

Troodos Ophiolite (Cyprus). Two complementary studies of melt percolation in the Troodos ophiolite found fractionated HSE abundances and variable $^{187}Os/^{188}Os$ in a range of residual and melt reaction products (Büchl et al., 2002, 2004). A sequence of spinel lherzolites, minor dunites and clinopyroxene-bearing harzburgites was found to have a large range of initial $^{187}Os/^{188}Os$ (at 90 Ma) from subchondritic (0.1168) to mildly suprachondritic (0.1361); a second unit, consisting of harzburgites, dunites and chromitites, has an even larger and more radiogenic range of 0.1234 to 0.1546. The subchondritic values can readily be explained by ancient melt depletion of Re (>800 Ma), as for abyssal peridotites and most other mantle rocks. The suprachondritic Os compositions, as with those from the Oman ophiolite described earlier (Hanghøj et al., 2010) and many other ophiolites (see Figs. 14 & 15), require the addition of a radiogenic melt component (unless samples have experienced significant recent Re loss), likely during the formation of the Troodos around 90 Ma ago. The ultimate source of this radiogenic Os is not known, and could relate to seawater contamination prior to concentration in chromitites (because a radiogenic signature is also evident in the most Os-rich chromitite samples) or to crustal contamination during emplacement, but the former at least is difficult to reconcile with the very low Os concentrations in seawater (Levasseur et al., 1998). Another possible mechanism, that would be applicable to both mid-ocean ridge and supra-subduction ophiolites, is the production of radiogenic melts due to preferential sampling of radiogenic interstitial sulfides (Alard et al., 2005; Harvey et al., 2011) or due to the presence of enriched domains in the mantle (cf. pyroxenites; Reisberg et al., 1991; Pearson and Nowell, 2003). However, melting of enriched domains is not consistent with the refractory boninitic melt that typically produces HSE- and Cr-rich chromitites. Given the apparent global distinction in Os isotopes between ophiolites of convergent and mid-ocean ridge origin (Fig. 15), the most plausible explanation for a significant part of the radiogenic signature is a flux from the subducting slab, with Os mobilized in oxidized chlorine-rich fluids (Brandon et al., 1996; Becker et al., 2004). In this scenario, despite the extreme fractionation of Re from Os in oceanic crust, the low Os contents and relatively young age of subducted mafic crust would suggest that a sedimentary input may be required to provide sufficient radiogenic Os to impart that signature on the Os-rich mantle.

The process(es) of dunite formation also induces significant HSE fractionation. Harzburgites, which could be simple residues of melting or, as Büchl et al. (2002) conclude, the product of melting during melt-percolation at low melt/rock ratios, have largely uniform IPGE patterns and concentrations that only range by roughly a factor of two (Fig. 16). Palladium and Re abundances do, however, vary over approximately an order of magnitude in harzburgites (Büchl et al., 2002). In contrast, a dunite rim and core, the product of high melt/rock ratios, together with a websterite and a boninite all display high and remarkably uniform concentrations of Pt (6.5 – 12.2 ng/g), moderately variable Pd and Re, and two or more orders of magnitude variation in Os content. Qualitatively, it seems that dunites and websterite could be produced by some sort of mixing process between harzburgite and boninitic melt, retaining high Pt but removing/diluting Os; requiring Os to be mobilised. This is supported by modelling of HSE ratios (dominated by mixing of harzburgitic and magmatic sulfides) and REE in clinopyroxene during open system melting (Büchl et al., 2002).

Shetland Ophiolite Complex (UK). Harzburgites from Unst, Shetland, have Os isotope compositions ranging from γOs of 2 to -6 (using an O-chondrite reference frame; $^{187}Re/^{188}Os$ = 0.422, $^{187}Os/^{188}Os$ = 0.1283). Most Os isotope ratios are consistent with an ambient convecting

mantle signature (see section on Os isotope heterogeneity in Discussion) but there is evidence of both melt depletion at ~1.2 Ga and also radiogenic Os addition for some samples (O'Driscoll et al., 2012).

Dunites have a wider range of $^{187}Os/^{188}Os$ than harzburgites (-22 to 12), reflecting the effects of melt-rock reaction involved in their formation (O'Driscoll et al., 2012). Chromitites have the narrowest range of $^{187}Os/^{188}Os$, from γOs +0 to +3.5. This relative homogeneity is perhaps surprising given the higher melt/rock ratios involved in producing chromitite, but this is set against the extremely high Os concentrations, and low Re abundances, that allow for accurate estimation of the initial Os isotope composition. In part, the range for dunites (and harzburgites) may reflect difficulties in age correcting over 492 Ma (as this is dependent on measured Re and Os concentrations – with the potential for recent disturbance). Overall, however, a radiogenic Os flux is required to explain the supra-chondritic γOs values. As discussed for the Troodos Ophiolite, there are various possible sources of the radiogenic Os, but a flux from the downgoing slab may be the most plausible mechanism.

Shetland Ophiolite samples display huge variations in HSE concentrations, with some chromitites containing up to ~100 µg/g Pt (Prichard and Lord, 1996; O'Driscoll et al., 2012) while some dunites contain less than 100 pg/g Pt. The most HSE-rich chromitites (from Cliff) have Ir and Ru contents that are roughly two orders of magnitude higher than the range of chromitites analysed from the Qalander, Luobusa and Zambales ophiolites (Fig. 16). Moreover, these chromitites have unusual HSE patterns with PPGE/IPGE ratios greater than unity and Pd concentrations up to 156 µg/g (O'Driscoll et al., 2012), compared with typical IPGE-rich chromitites which have Pd and Pt contents approximately four orders of magnitude lower (Zhou et al., 1996; Zhou et al., 2000; Ismail et al., 2014; Zhou et al., 2014). The range of HSE anundances between chromitites from different localities is, in itself, huge. The two other localities analysed have more typical HSE patterns, albeit in one case also enriched by one to two orders of magnitude. The degree of P-PGE enrichment has been linked to the thickness and sulfide content of the ultramafic dunite sequence and ultimately to the degree of melting, and, in the case of the extremely PPGE-enriched Cliff chromitites, also linked to hydrothermal redistribution from surrounding ultramafics (Prichard and Lord, 1996).

There are also large variations in the HSE concentrations and patterns of dunites, which show an overall depletion in Pt, relative to IPGE, and are enriched in Pd in many cases. Rhenium concentrations are low in almost all harzburgite, dunites and chromitites, although enrichment in Re does also occur in some dunites.

Zambales Ophiolite (Philippines). The Zambales Ophiolite contains two distinct blocks, which differ in the composition of their chromitites. The Acoje Block contains chromitites with high-Cr spinel, while the Coto Block is characterized by more Al-rich spinel (Zhou et al., 2000). A comparative study of these two blocks found variations and similarities in the HSE budget of the two chromitite types. As in other studies (e.g., Ahmed et al., 2006; Ismail et al., 2014) high-Cr chromitites are found to be richer in HSE than those with high-Al spinel. In this case, however, the IPGE contents vary significantly (e.g., Ru = 8-38 ng/g for Coto, and 62-70 ng/g for Acoje), while Pt and Pd contents and ratios are similar in the two types (Fig. 16) (Zhou et al., 2000). Dunites are also found to vary, particularly in Pt content, with the Acoje Block having more Pt-rich dunites. These spinel compositions and HSE contents are linked to the parental magmas of the chromitites. The Cr-rich Acoje chromitites were likely generated by interaction with a refractory boninitic melt, while the Coto chromitites probably had a more tholeiitic source. Boninitic melts are typically sulfide undersaturated, and thus may form with, and retain, high HSE abundances, compared to tholeiitic melts which are commonly saturated in sulfide thus inducing its precipitation and a reduction in HSE content of the remaining melt (Zhou et al., 2014).

Qalander Ophiolite (Iraq). The Qalander Ophiolite is a poorly preserved mélange-type complex, containing serpentinised dunites and harzburgites which surround two types of podiform chromitite; high-Al and high-Cr. The harzburgites and dunites analysed have comparable HSE patterns overall (Ismail et al., 2014), broadly similar to PM estimates (Becker et al., 2006), except offset to higher concentrations (Fig. 16) particularly for Os (4-9 ng/g Ir, 10-17 ng/g Os). As with other chromitite occurrences, Cr-rich and Al-rich types have differing relative proportions of HSE, although they almost all possess high IPGE/PPGE ratios (see Zhou et al., 2014; cf. Shetland, above). Cr-rich chromitites are the most strongly enriched in IPGE, and have the highest IPGE/PPGE ratios. Al-rich chromitites have significantly higher PPGE concentrations, above those of peridotite, while the Cr-rich type has PPGE at the low end of the peridotite range.

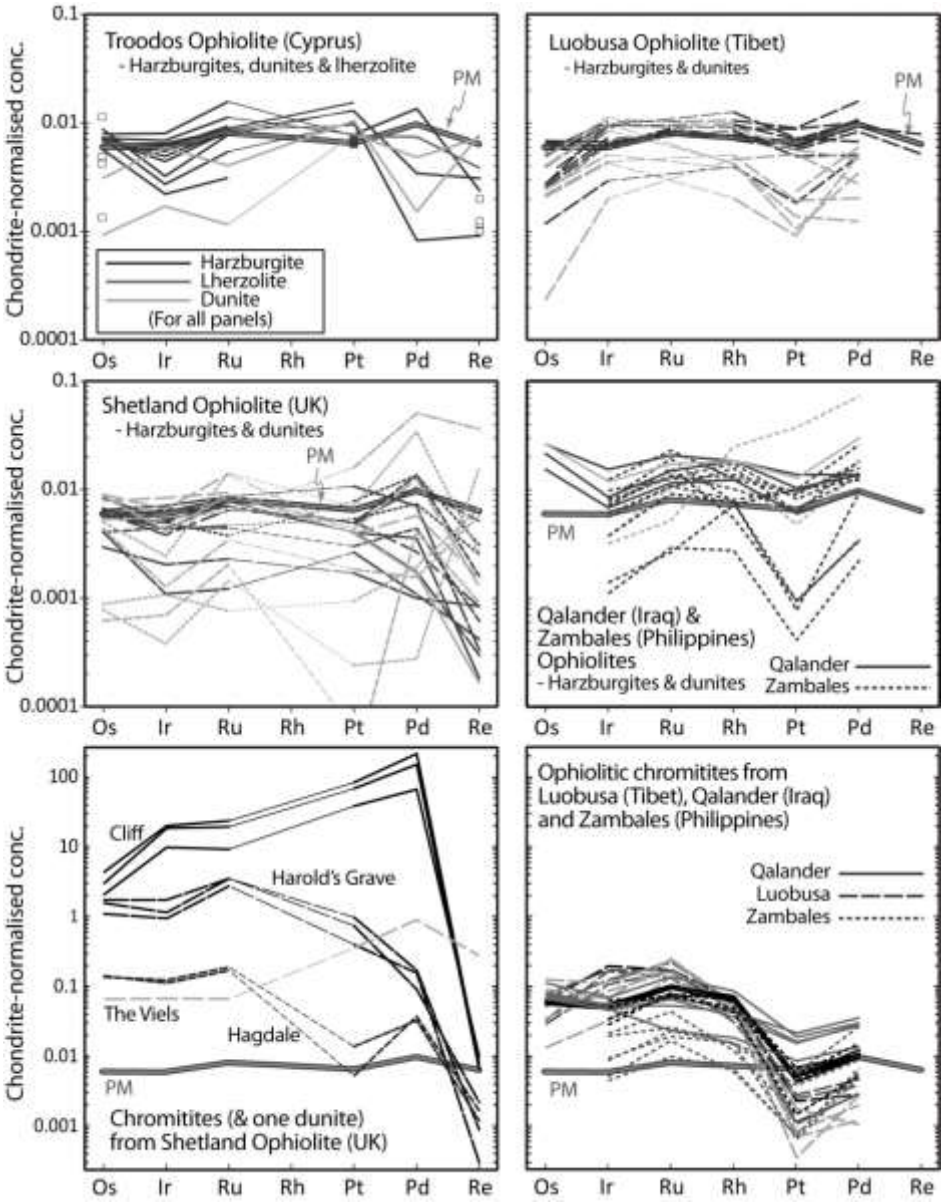

Figure 16. Chondrite-normalized concentration diagrams of the HSE in ophiolites of convergent margin (Troodos, Shetland, Zambales) or uncertain origin. PM estimate shown for comparison. See Fig. 1 for normalization values. White squares for Troodos denote Re-Os analyses of dunites. Qalander & Zambales

chromitites: black lines – Cr-rich, grey lines – Al-rich; Luobusa chromitites: black – massive, grey - disseminated. It is not clear why there is a discrepancy in the Os data for Luobusa, across two studies. Given that Becker et al. (2006) used high-temperature acid digestion and isotope dilution, these Os data should be used in the first instance; the other HSE data is broadly comparable between the two studies. (References: Zhou et al., 1996; Zhou et al., 2000; Büchl et al., 2002; Büchl et al., 2004; O'Driscoll et al., 2012; Ismail et al., 2014).

Egyptian ophiolites and podiform chromitites, Oman N massifs. The Os isotope composition of PGM from chromitites of the Proterozoic Eastern Desert ophiolite, Egypt and in the Phanerozoic Oman ophiolite were analysed by Ahmed et al. (2006). It was found that PGM from different regions of each ophiolite have distinct $^{187}Os/^{188}Os$ ratios, from sub- to broadly chondritic in some regions, to significantly suprachondritic in others (0.1293 for the Proterozoic Eastern Desert ophiolite and up to 0.1459 for the Oman ophiolite). At the same time, there are also distinct compositions of the chromitites themselves, with (i) concordant lensoid forms with intermediate-Cr spinel, which are relatively PGE-poor, and (ii) discordant, dyke-like chromitites, with high Cr spinel, which are PGE-rich. The authors conclude that the variety of chromitites, and the Os-HSE signatures that they contain, reflects the variety of formation processes. The radiogenic chromitites of the Eastern Desert are thought to be affected by crustal contamination, whereas the radiogenic, Cr- and HSE-rich chromitites from Oman reflect high degree melting and an input from a subducting slab, most likely in a supra-subduction zone setting (Ahmed et al., 2006), although here we note that some workers prefer a MOR origin and obducted emplacement method for the Oman ophiolite (see earlier section).

Feather River ophiolite (California). A suite of serpentinised peridotites from the Feather River ophiolite has been compared with serpentinised abyssal peridotites and used as a means of establishing the chemical impacts of serpentinisation at a range of water/rock ratios and depths in the mantle (Agranier et al., 2007). The serpentinites have elevated concentrations of seawater-derived fluid mobile elements, such as boron, although typically lower than abyssal peridotites. In contrast to many abyssal peridotites, however, Feather River serpentinites do not have corresponding seawater-affected supra-chondritic $^{187}Os/^{188}Os$ ratios (measured range: 0.1175 – 0.1279). Nonetheless, there is a probable covariation between Os abundance and Os isotope composition in Feather River rocks, albeit over this limited range of $^{187}Os/^{188}Os$ compared to abyssal rocks. Agranier et al. (2007) contend that the serpentinites formed at lower water/rock ratios (greater depth) than is typical for abyssal rocks, and are therefore more representative of bulk serpentinised lithosphere.

In summary, melt percolation in the supra-subduction zone environment generates substantial lithological heterogeneity, which is accompanied by significant Os isotope and HSE variability, both between lithological groups (harzburgites, dunites, chromitites, pyroxenites) and within groups. There is compelling evidence for addition of melt-derived radiogenic ^{187}Os to parts of the mantle sections of ophiolites (see above and Figs. 14 and 15), most probably due to a degree of Os fluxing from the downgoing slab, although other possibilities exist. However, the precise mechanism for such a transfer is not yet clear. The process of melt-rock reaction during melt percolation results in a decoupling of Al_2O_3 and $^{187}Os/^{188}Os$ (Fig. 14), which for other suites is considered a fairly robust method for determining the approximate ages of depletion for suites of peridotites, where measured Re contents are often unreliable (Meisel et al., 2001; Lassiter et al. 2014).

Highly siderophile elements in the mantle sections of ophiolites of uncertain origin

Luobusa ophiolite (Tibet). Chondrite-normalised HSE concentrations for harzburgites, dunites and chromitites from the Luobusa ophiolite are presented in Fig.16. The concentrations of Ir, Pt and Pd are broadly comparable between two different studies (Zhou et al., 1996; Becker et al., 2006), but the low Os/Ir ratios of the Ni-S fire assay data of Zhou et al. (1996) are not

supported by the high temperature (345°C) isotope dilution data of Becker et al. (2006), suggesting either different petrogenetic histories for the two sample sets or an unidentified analytical issue for Os in the Zhou et al. data. To err on the side of caution, we will assume the latter here and disregard the very low Os/Ir ratios in the harzburgites and chromitites.

The harzburgites appear to represent residua after MORB extraction (Zhou et al., 1996). The HSE abundances are similar to the PM mantle estimate (Becker et al., 2006), and do not indicate significant melt depletion, except perhaps for Pt (although data for Re – the most incompatible HSE – is only available for two samples). The Cr-numbers of Cr-spinel in melt-reacted dunitic rocks are higher than those in the harzburgites, suggesting interaction of a boninitic melt with the residual peridotite, which also removed pyroxene (Zhou et al., 1996). As a result, melts became more boninitic and saturated in Cr-spinel, which precipitated to form chromitite pods within the dunite zones. The inferred boninitic melts suggest a subduction-related origin for this ophiolite. Chromitites have distinct, strongly fractionated HSE patterns with high IPGE/PPGE ratios (e.g., normalized Ir/Pt ratios ~100). The concentrations of IPGE in the chromitites are an order of magnitude or more greater than those of the harzburgites, while Pt abundances are approximately five times lower in the chromitites than the harzburgites, and are comparable to the dunites (Fig. 16). These concentrations and patterns are similar to other Cr-rich chromitites from the Qalander and Zambales ophiolites (Zhou et al., 2000; Ismail et al., 2014). Dunites have similar PPGE contents to the chromitites, but without the enrichment in IPGE, due, presumably, to a lack of PGE saturation, and consequent PGM formation, during dunite formation.

Jormua ophiolite (Finland). Serpentinites, the oxides they contain, and podiform chromitites have all been analysed for Re-Os abundances and Os isotopes (Tsuru et al., 2000). As with most abyssal peridotites that have undergone serpentinisation, Os concentrations, although somewhat variable (1.5 to 11.7 ng/g) are broadly similar to those of the convecting upper mantle. Rhenium abundances are more variable; most samples are depleted in comparison with PM (Becker et al., 2006) but some experienced (probably recent) Re enrichment. Whole-rock samples have experienced open-system behavior, with respect to Re-Os isotopes, but chromite to Cr-rich magnetite separates have extremely low Re/Os and largely homogenous initial $^{187}Os/^{188}Os$ values, with a mean γOs of approximately -5, suggesting closed-system behavior. Other parts of the ophiolite contain chromitites with γOs between +1 and +3. The authors conclude that the positive values may indicate the presence of MORB-type and subcontinental lithospheric mantle sources. Addition of radiogenic Os by melt percolation may be another mechanism to explain the Os isotope data.

Outokumpu ophiolite (Finland). The Cr-rich nature of residual chromites and boninite-like volcanic rocks suggest a supra-subduction origin for this ophiolite, but an origin in a continental rift zone has also been proposed (Walker et al., 1996). The key conclusion of an Os isotope study (Walker et al., 1996), mainly of chromite, was that this mantle section displayed broadly chondritic $^{187}Os/^{188}Os$ ratios, and hence Re and Os abundances, which were used to support the 'late veneer' model (Chou, 1978). In detail, however, there were variations from a 'residual' sub-chondritic laurite (Ru (Os,Ir) S_2) to fluid addition with a composition of around 0.4 γOs. In this case, however, the radiogenic signature is thought to be derived either from seawater contamination or from a crustal input during emplacement, akin to that proposed for the Eastern Desert Ophiolite, Egypt (see previous section).

Tethyan ophiolites (Turkey). Harzburgites and dunites from Tethyan ophiolites at Koycegiz, Marmaris, Tekirova, Adrasan and Lake Salda in Turkey have been analysed by Aldanmaz et al. (2012). Both mid-ocean ridge and supra-subduction zone geochemical signatures have been identified in different parts of the ophiolites, and these have differing HSE systematics. The mid-ocean ridge harzburgites have broadly chondritic Os/Ir and supra-chondritic Pd/Ir and Rh/Ir,

similar to PM estimates (Becker et al., 2006), although some PPGE/IPGE enrichment is ascribed to sulfide addition. They also have a sub-chondritic range of $^{187}Os/^{188}Os$ of 0.1223 to 0.1254, and have corresponsingly depleted Re/Os ratios (Aldanmaz et al., 2012). In contrast, the peridotites of supra-subduction zone affinity have more variable HSE patterns and a wider range of $^{187}Os/^{188}Os$ from 0.1209 to 0.1318, which is -5.26 to 3.27 in γOs units, relative to O-chondrite evolution. The greater heterogeneity of supra-subduction zone peridotites, compared to those of mid-ocean ridge affinity, reflects a more complex evolution.

Eastern Alps ophiolites (Austria). Peridotitic units of Eastern Alps ophiolites (the Reckner, Hochgrossen, Kraubath, Steinbach and Bernstein peridotites; including two chromitites) have been found to have remarkably uniform $^{187}Os/^{188}Os$ ratios (~0.1266-0.1281), clustering around the chondritic evolution curve (Meisel et al., 1997), with the exception of one locality (Dorfertal) which has an Os isotope composition consistent with a minimum age of Re depletion of ~1.6 Ga. The authors considered the uniformity of Os composition to be somewhat surprising given the uncertain age and affinity of the samples. One important finding of that study was the robustness of Os isotopes, given a high degree of serpentinisation, compared with other geochemical data, and even petrographic and field methods.

Mayari-Cristal ophiolite (Cuba). The key finding of a study of PGM in the Mayari-Cristal ophiolite was the scale of Os isotope heterogeneity present within single hand specimens, thin sections and down to a scale of several millimeters that separated two PGM with contrasting Os isotope ratios ($^{187}Os/^{188}Os$: 0.1185 and 0.1232; Marchesi et al., 2011), which equate to Re depletion ages of 1370 and 720 Ma, respectively (O-chondrite reference). Given that the budget of Os for these PGM is thought to be sourced from several m^3 of mantle, this has intriguing implications for mixing (or the lack thereof) of distinct percolating melts in the mantle (Marchesi et al., 2011).

DISCUSSION

Influence of low-temperature alteration processes on the HSE in bulk rocks and minerals

Here we briefly discuss the influence of low-temperature (non-magmatic) processes on the bulk rock, sulfide and PGM composition of mantle tectonites. Ultrabasic rocks affected by oxidative weathering are usually not used for bulk rock chemical analyses to study high-temperature processes. Sulfides are at least partially oxidized by these processes, thus, it is expected that the abundances of chalcophile elements will be disturbed in non-systematc ways. Because areas of ultramafic rocks affected by oxidative weathering are easily identified by their brown color, stemming from ferric iron bearing secondary weathering products, such altered areas can be normally identified and removed.

The influence of serpentinization on HSE abundances and $^{187}Os/^{188}Os$. Serpentinization represents another common low temperature alteration process of ultrabasic rocks. Serpentinization reactions occur during the reaction of igneous and metamorphic ultrabasic rocks with seawater or freshwater under a range of geologic conditions and temperatures (e.g., Evans et al. 2013 and references therein). For instance, these processes occur today in oceanic mantle exposed on the seafloor and at greater depth where heated seawater moves within deep-reaching fractures. Similar processes occurred in ultramafic parts of ophiolites during their exhumation on or beneath past seafloors, during tectonic obduction or by reaction with fluids and meteoric water of variable origin during continental collision (Hirth and Guillot 2013). During serpentinization of peridotites, water reacts with olivine, pyroxenes, spinel (to a lesser extent) and sulfides that formed at high temperatures. Depending on temperature and progress of reaction, the new minerals formed include serpentine minerals (chrysotile, lizardite, at higher temperatures

antigorite), magnetite and other secondary minerals such as brucite (see for example Bach et al., 2004).

The influence of serpentinization on the abundances of HSE in mantle tectonites has not been studied in much detail. Early Re-Os studies of serpentinized peridotites (e.g., Snow and Reisberg 1995) have emphasized that serpentinization of peridotites in the oceanic lithosphere occurs under reducing conditions. Because of the low fO_2 environment caused by the local production of hydrogen and methane (Evans et al. 2013), secondary sulfides (heazlewoodite, millerite, godlevskite), Fe-Ni alloy phases (awaruite) and native metals (Au, Cu) may form (Klein and Bach, 2009) and thus, the HSE are able to retain a low valence. The extent to which the HSE are retained in these secondary phases compared to the original abundances in the unaltered bulk rocks and how much of the HSE may be lost into the fluids is poorly constrained. The similarities of abundances of Os, Ir, Ru, Rh, Pt and Pd in fresh and variably serpentinized peridotites with similar lithophile element composition have been used to argue that serpentinization at reducing conditions results in only minor changes in the abundances of these elements in serpentinized ultramafic bulk rocks that are difficult to resolve from analytical or intrinsic variations in such rocks (e.g., Becker et al. 2006; Fischer-Gödde et al. 2011; Foustoukos et al., 2015; Marchesi et al., 2013; van Acken et al. 2008). This contention is supported by abundances of these elements in serpentinized komatiites, which often preserve correlations between PGE and Mg or Ni, which were unequivocally produced by igneous fractionation processes (e.g., Brügmann et al. 1987; Puchtel et al. 2004, 2005).

The influence of serpentinization on Re and Au abundances is more difficult to predict, as no systematic studies exist and the applicability of experimental studies of Re behavior in specific hydrothermal fluids is difficult to evaluate (Pokrovski et al. 2014, Xiong and Wood 1999). Compared to Pd, Re is often depleted in serpentinized harzburgites, as expected for strongly depleted residues of partial melting; however, it may also be more enriched than Pd in normalized concentration diagrams (e.g., Figs. 3, 5, 9, 10, 16). It is difficult to judge if these abundances reflect secondary addition of Re from seawater (which has very low Re abundances) that has dissolved sulfides elsewhere, or, if re-enrichment of Re occurred before alteration (e.g., by precipitation of liquid sulfide from silicate melts, as may be plausible from observations of unaltered peridotites). Similar uncertainties arise in serpentinized lherzolites. Correlations of Re with indicators of melt extraction or refertilization such as Al, Ca or $Mg/(Mg + Fe^{2+})$ in peridotites have been interpreted as evidence for limited mobilization of Re by low-temperature alteration processes (e.g., Becker et al. 2006). In mantle pyroxenites that were affected by variable degrees of serpentinization, Re seems to be unaffected by alteration because it is typically systematically more enriched than Pd and Pt. Such a behavior is expected from crystal fractionation products of basic melts (van Acken et al. 2010b). The behavior of gold during serpentinization of mantle peridotites has not been studied systematically either. Although Au, in some cases, follows Pd and Re in its geochemical behavior in unaltered peridotites (Fischer-Gödde et al. 2011), it shows scattered distributions in element variation diagrams that are not well understood. Because of the known mobility of Au in hydrothermal systems in basic and ultrabasic rocks (Pokrovski et al. 2014) and the enrichment of Au in some serpentinite-hosted sulfide deposits (e.g., the Lost City hydrothermal field, Mid Atlantic Ridge), it is to be expected that Au may be rather mobile during serpentinization.

The question of whether or not the Os budget of serpentinized peridotites can be measurably affected by radiogenic ^{187}Os from seawater has been discussed in several publications (e.g., Alard et al. 2005, Brandon et al. 2000, Harvey et al. 2006, Martin 1991, Roy-Barman and Allègre 1994, Snow and Reisberg 1995, Standish et al. 2002). Cenozoic seawater has highly variable and mostly very radiogenic $^{187}Os/^{188}Os$ ranging between 0.5 and 1 (Peucker-Ehrenbrink and Ravizza 2000), however, the concentration of Os in seawater is extremely low (about 3.8 fg/g Os, (Sharma et al. 1997). These low abundances are in stark contrast to the ng/g levels of Os in

peridotites. Figure 17 illustrates the effects of simple peridotite-seawater mixing, assuming $^{187}Os/^{188}Os$ of 0.122 and 0.127 and 3.9 ng/g Os in unaltered peridotite and modern seawater with $^{187}Os/^{188}Os$ of 1 and 3.8 fg/g Os. Very high water-rock ratios of 10^3 to 10^4 are required in order to disturb the $^{187}Os/^{188}Os$ of peridotite bulk rocks at the % level or higher. Lower values of $^{187}Os/^{188}Os$ in seawater, such as 0.5, would not alter this conclusion. For comparison, water-rock ratios of significantly less than 100 have been calculated for rock units of the Oman ophiolite (McCulloch et al. 1981). Some workers have suspected that Mn hydroxide films in cracks and on surfaces may pose a problem because these phases tend to scavenge Os from seawater (Martin 1991, Roy-Barman and Allègre 1994). Although leaching studies of serpentinized peridotites have not yielded clear indications of contamination, it is preferable to remove such surfaces or avoid such rocks altogether. Most abyssal peridotites are strongly serpentinized, yet they are characterized by chondritic to subchondritic $^{187}Os/^{188}Os$, similar to unaltered or weakly serpentinized post-Archean peridotite xenoliths or other tectonites. Thus there appears to be no need to invoke late addition of radiogenic Os by serpentinization. Positive linear correlations of $^{187}Os/^{188}Os$ with Al_2O_3 contents in serpentinized peridotites provide the strongest argument against a significant influence of serpentinization on $^{187}Os/^{188}Os$ in such rocks (Reisberg and Lorand 1995). These correlations are a primary magmatic feature of mantle rocks (e.g., Handler et al. 1997; Peslier et al. 2000; Meisel et al. 2001; Gao et al. 2002).

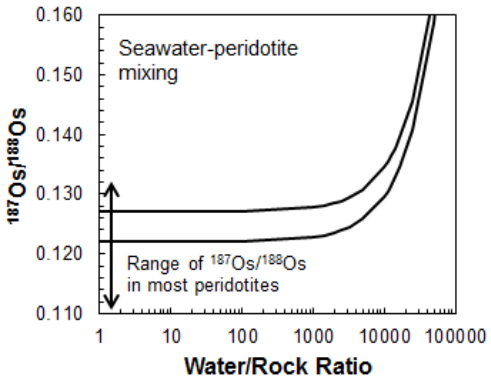

Fig. 17. The influence of contamination with seawater on $^{187}Os/^{188}Os$ values of peridotites. Typical water-rock ratios during alteration of ophiolites are < 100. Because of the large difference in the concentrations of ^{188}Os, even a small increase in $^{187}Os/^{188}Os$ of altered peridotites caused by addition of radiogenic Os from seawater ($^{187}Os/^{188}Os$ = 1) would require unrealistically high water/rock ratios. For details on end member compositions, see text.

Suprachondritic $^{187}Os/^{188}Os$ occasionally occur in bulk rocks of strongly serpentinized abyssal peridotites (Standish et al. 2002) and from serpentinized harzburgites and dunites of ophiolite sections and peridotite massifs (e.g., Becker et al. 2001, Büchl et al. 2002, Hanghøj et al. 2010). Standish et al. (2002) reported small-scale variations of $^{187}Os/^{188}Os$ in serpentinized harzburgites and dunites. In the latter study, isotopic differences in chromite ($^{187}Os/^{188}Os$ = 0.124-0.148) compared to bulk rocks ($^{187}Os/^{188}Os$ = 0.118-0.158) were interpreted to result from serpentinization and the addition of seawater-derived radiogenic Os in the altered portion of the rocks. Considering the Os concentration differences between seawater and peridotites, it is not clear how sufficient ^{187}Os can be added from seawater to raise the $^{187}Os/^{188}Os$ to values higher than 0.15. The Os isotopic data in Standish et al. (2002) cannot be reconciled with low-temperature alteration in a simple way, because Cr rich spinels sometimes have more radiogenic Os than their bulk rocks, and samples with the highest $^{187}Os/^{188}Os$ are characterized by unusually low Os concentrations (below 1 ng/g). Other workers have interpreted chondritic to slightly suprachondritic initial $^{187}Os/^{188}Os$ in serpentinized dunites and harzburgites to result from the interaction between magmas with suprachondritic $^{187}Os/^{188}Os$ and mantle rocks, which, because of magmatic dissolution of sulfide liquid or chromite, may also cause a decrease of Os

abundances in peridotites (Becker et al. 2001, Büchl et al. 2002, Hanghøj et al. 2010). Alard et al. (2005) and Harvey et al. (2006) have interpreted different generations of sulfides in serpentinized peridotites from the Atlantic Ocean to reflect magmatic impregnation from percolating magma with suprachondritic $^{187}Os/^{188}Os$, similar to observations from continental peridotites (Burton et al. 1999; Alard et al. 2002; Harvey et al. 2011; Reisberg and Luguet 2015, this volume). To conclude, the effects of serpentinization on the $^{187}Os/^{188}Os$ of serpentinized peridotite are likely minor and difficult to resolve from Os isotopic heterogeneities in mantle rocks inherited from high-temperature igneous processes.

Low-temperature decomposition of primary sulfides in peridotites. Work on sulfide compositions in peridotites and results of experimental data at typical mantle P-T conditions also noted that sulfides in peridotites, in particular sulfides on grain boundaries, display exsolution assemblages from a homogeneous sulfide phase, typically monosulfide solid solution (mss, (e.g., Lorand and Luguet, 2015, this volume). The result of these decomposition processes, which depends on the cooling history, is a heterogenous assemblage of intergrown sulfides (commonly pentlandite, pyrrhotite and chalcopyrite), and other minerals, notably platinum metal bearing alloys and Te-, Bi-, Se-rich phases (Alard et al. 2000; Lorand et al. 2010, 2013; Luguet et al. 2003, 2004, 2007). Because of these subsolidus processes, it is not uncommon that some elements (e.g., Pt, Te, Au) become strongly redistributed from sulfides into other trace phases in which they are a major element (e.g., Pt alloys, tellurides, selenides). As a consequence these elements may display negative anomalies in normalized concentration diagrams of exsolved sulfide phases (Alard et al. 2000, Lorand et al. 2010) that are not present on the bulk rock scale. A detailed discussion of phase assemblages and their composition will be given elsewhere in this volume (Harvey et al., 2015; Lorand and Luguet, 2015).

The influence of melt infiltration and partial melting on HSE abundances in mantle tectonites

Since the early 1980s, studies of lithophile element geochemistry and Sr-Nd-Pb isotope compositions have shown that mantle tectonites have undergone variable degrees of partial melting during past melting events. Typically this is indicated by their depletion in moderately and highly incompatible elements (e.g., Frey et al. 1985; Johnson et al. 1990) and unradiogenic Sr and radiogenic Nd isotopic compositions (e.g., Jacobsen and Wasserburg 1979; Polvé and Allègre 1980; Reisberg and Zindler 1986). The compositional pattern of major elements in mantle tectonites is such that most abyssal peridotites and ophiolites genetically related to convergent plate margins are harzburgites (and subordinate dunites), whereas lherzolites tend to occur more often in ultra-slow spreading environments, subcontinental settings or continent-ocean transitions. These compositional differences mirror different degrees of partial melting in these settings and are broadly consistent with the polybaric melting column model of upwelling upper mantle (Langmuir et al. 1992). The model predicts that below mid-ocean ridges or other regions of shallow mantle upwelling such as back arc basins, the highest degrees of melting and harzburgitic residues are expected at the top of the mantle, whereas lherzolites should occur at greater lithospheric depth where less melting occurs.

Subsequent work has established that many peridotites show petrologic and geochemical evidence for a multi-stage history of high-temperature processes (summarized by Bodinier and Godard 2003). These multi-stage processes include melt extraction and later melt infiltration and reaction with existing peridotite, which induces chemical changes in mantle rocks that range from kinetically controlled fractionation of incompatible trace elements (e.g., Vasseur et al. 1991) to significant modal mineralogical changes (Le Roux et al. 2007). The latter processes are capable of converting harzburgites into lherzolites ("refertilization") by stagnation of magma or repeated influx of magma saturated in a multiphase assemblage of pyroxene(s) ± Al phase (plagioclase, spinel or garnet) + sulfide in deeper parts of the lithospheric mantle. Melt-rock reaction in

shallow mantle tends to produce tabular dunite, rather than lherzolites (Kelemen et al. 1995, 1997) or plagioclase-pyroxene bearing impregnations, dikes and pockets in otherwise depleted harzburgite (Edwards and Malpas 1996, Seyler et al. 2004). As a consequence of these processes, the inventory of incompatible elements and their isotopic composition in these metasomatically modified rocks is mostly derived from the magma that produced these changes (for instance, the LREE-depleted compositions of lherzolites from Lherz in the Pyrenees and their isotopic compositions must have been inherited from the infiltrating magma, Le Roux et al. 2007). Melt infiltration and chemical reaction with peridotite has been recognized as an important process in many mantle tectonites from different tectonic settings (e.g., Pyrenees, Ronda, Ligurides, Ivrea Zone, Lanzo, Horoman, abyssal peridotites, ophiolites). It may be ubiquitous in melting columns, mantle diapirs and in the deep lithosphere and should be considered normal for open-system melting environments. In the following, we first discuss some general compositional constraints from peridotites that may be linked to melting processes. We then address the influence of reactive melt infiltration on sulfide-silicate equilibration and discuss partitioning of the HSE.

Behavior of the HSE during partial melting of harzburgites and lherzolites. A general observation is that harzburgites have similar abundances of Os, Ir and Ru (IPGE, Barnes et al. 1985) to lherzolites, whereas concentrations of other PGE, Re and Au are typically much lower in harzburgites than in lherzolites (Figs. 3, 5, 9, 10, 16). On the other hand, basalts and komatiites often have higher chondrite-normalized concentrations of Pt-group PGE (PPGE: Rh, Pt, Pd, Barnes et al. 1985), Au and Re than IPGE (Bezos et al. 2005; Brügmann et al. 1987; Hertogen et al. 1980; Puchtel et al. 2004; Rehkämper et al. 1999). These studies have pointed out that the main host phase of the HSE in lherzolites at high temperatures should be sulfide. Thus, the stronger depletion of Rh, Pt, Pd, Au, Re and sulfur in harzburgites compared to lherzolites likely reflects the consumption of sulfide in peridotite during high degrees of melting (e.g., Barnes et al. 1985; Keays 1995; Lorand 1988; Morgan 1986). The details of sulfide dissolution and HSE partitioning into basic magma have remained unclear, particularly for melting processes at P-T conditions that should yield lherzolite residues. Many workers have advocated sulfide-silicate partitioning (e.g., Brenan et al. 2015, this volume, and references therein). For chalcophile element partitioning, the assumption has been that during local partial melting in the mantle, a homogeneous sulfide liquid or solid should coexist in equilibrium with silicate melt, olivine, pyroxenes and an Al-rich phase (Keays 1995; Morgan 1986; Rehkämper et al. 1999). The amount of sulfide liquid dissolved into the silicate melt is controlled by ambient pressure, temperature and FeO content of the melt (Jugo et al. 2005; Mavrogenes and O'Neill 1999; O'Neill and Mavrogenes 2002). Another partitioning process, mss-liquid sulfide partitioning, that was also proposed to control HSE abundances (Bockrath et al. 2004) will be discussed below. During melting of upwelling asthenosphere or deep lithosphere, at temperatures >1250°C, it is expected that mantle rocks and coexisting magmas were chemically and isotopically equilibrated, as is commonly assumed for lithophile elements (Hofmann and Hart 1978).

At high degrees of melting, partitioning of Os, Ir, Ru, Rh and Pt may be controlled by the solubility of alloys of these elements in silicate melt (Pearson et al. 2004; Fonseca et al. 2011; 2012; Mungall and Brenan 2014; Brenan et al. 2015, this volume). The significance of this for the composition of harzburgites will be discussed later. Here, we specifically focus on processes during low and moderate degrees of melting in the deeper regions of the melting column where sulfide should be stable in the residue and sulfide-silicate partitioning has been proposed as the main control on the distribution of the HSE and other chalcophile elements (Barnes et al. 1985; Morgan 1986). However, it has been unclear if sulfide exists as a solid phase (mss), liquid sulfide, or both. Recent improvements in the accuracy and precision of liquid sulfide-silicate partition coefficients ($D^{sulf/sil}$) indicate values in the range of 10^5 to 10^6 and 10^4 for the PGE and Au, respectively (Li and Audétat 2013; Mungall and Brenan 2014; Brenan et al. 2015), whereas Re is much less chalcophile ($D^{sulf/sil} \approx$ 300-800, Brenan 2008; Fonseca et al. 2007). Assuming a

simple fractional melting process (batch melting yields similar results as long as the elements are not highly incompatible), element concentrations in the residues can be calculated according to the mass balance equation $C_r = C_o (1\text{-}F)^{((1/Db)-1)}$, with C_r = concentration of an element in the residue, C_o = total concentration of an element in the bulk system (residue + melt), D^b = bulk partition coefficient of an element between residue and melt, F = melt fraction. As long as sulfide is present in the mantle residue and it is equilibrated with silicates and silicate melt, the high $D^{sulf/sil}$ require nearly constant concentrations of all PGE in peridotites (Fig. 18a), because bulk partition coefficients of the PGE in lherzolites are >> 1: At 0.02 wt. % S in fertile lherzolite and 35 wt. % S in monosulfide solid solution, $D_{PGE}^b > 0.00057 \times 10^5 + 0.9994 \times 0.1 = 57$, assuming $D_{Pd}^{sil.min./sil.melt} < 0.1$ with other PGE likely having higher $D^{sil.min./sil.melt}$ (Mungall and Brenan 2014). Gold should also be retained in lherzolites that have lost a significant fraction of melt ($D_{Au}^b \geq 0.00057 \times 5 \times 10^3 = 3$, assuming $D_{Au}^{sil.min./sil.melt} < 0.01$ (Mungall and Brenan 2014), whereas Re should be moderately depleted at relevant fO_2 in normal upper mantle (FMQ-1), as its D^b is always below 1 in cases where no garnet occurs in the residue ($D_{Re}^b \leq 0.00057 \times 800 + 0.9997 \times 0.1 = 0.6$, assuming $D_{Re}^{sil.min./sil.melt} < 0.1$ (no garnet), Brenan 2008; Mallmann and O'Neill 2007).

The situation in mantle rocks, however, has been found to be more complicated; one indication being the difficulty in reproducing peridotite HSE patterns by sulfide-silicate equilibrium partitioning (Fig. 18a). In the following, we discuss evidence suggesting that many mantle peridotites are in chemical disequilibrium regarding chalcophile element partitioning at the scale of hand specimen to grain boundaries. An alternative partitioning scenario, such as mss-sulfide liquid-silicate liquid equilibrium, is also discussed below.

Melt infiltration at high temperatures induce chemical disequilibrium of chalcophile elements in mantle peridotites. Studies of chalcophile element abundances in sulfides of different textural position, in mantle xenoliths and in peridotite tectonites, have shown that significant compositional differences may exist between sulfides that occur as inclusions in olivine (and sometimes pyroxenes and spinel) and sulfides present at grain boundaries. The former are rich in Ir-group PGE and depleted in Pd, Au and Re, while the latter may or may not be depleted in IPGE and have higher Pd, Re and Cu (Alard et al. 2000; 2002; Luguet et al. 2001; 2003; 2004). Although these different assemblages are sometimes complicated by internal separation into multi-phase assemblages (pentlandite, pyrrhotite and other phases) that occurred late during slow cooling, it is clear from their different compositions that included and grain boundary sulfides were not chemically equilibrated during their formation. The sulfide assemblages on grain boundaries are sometimes associated with pyroxene-spinel assemblages that have been interpreted to have formed during melt infiltration and refertilization. From this observation, it follows that reactive melt infiltration likely led to sulfur saturation in these magmas and precipitation of the sulfides located on grain boundaries (e.g., Alard et al. 2000). The reaction of silicate melts and sulfide segregation processes are not only indicated by the different sulfide assemblages in the peridotites, but also by the HSE abundances in mineralogically zoned boundaries between pyroxenites and host peridotites and disequilibrium sulfide assemblages in mantle pyroxenites (see section on mantle pyroxenites below).

Some authors have proposed that sulfide melts may be mobile in mantle rocks, and thus may change the Re-Os and PGE systematics of mantle rocks (Gaetani and Grove 1999). The existing data on peridotites, however, do not support pervasive or wide-spread sulfide melt mobility, as linear correlations between $^{187}Os/^{188}Os$, Re and S abundances and lithophile elements such as Al, Ca or Mg in peridotites would not be maintained over long periods of time in the mantle (Fig. 4, 7; e.g., Becker et al. 2006; Meisel et al. 2001; Reisberg and Lorand, 1995; Wang and Becke,r 2013), although minor mobility is not precluded due to scatter in the datasets. The role of fluids as metasomatic agents in the redistribution of HSE and other chalcophile elements has been invoked in some cases (e.g., Lorand and Alard, 2010). One possibility is that such fluids are the end products left after crystallization of mantle-derived melts or, if they are of

external origin, may have been derived from crustal sources at lower temperatures during the exhumation history of mantle tectonites. Regardless of the origin of the fluids, what is not yet clear is the effect of these small-scale observations on the mass balance of bulk rocks. In summary, silicate melts are the main metasomatic agents that, by way of coupled precipitation of sulfide melt, pyroxenes and an Al phase, clearly produce significant modifications of HSE abundances and $^{187}Os/^{188}Os$ at magmatic temperatures in the mantle.

Detailed surveys of the accessory mineral inventory of peridotites (e.g., Fig. 6) have revealed the occurrence of Pt-Ir alloys, Ru-Os-bearing sulfides and Os-Ir-Ru alloy phases (Luguet et al. 2007; Lorand et al. 2010; O'Driscoll and González-Jiménez, 2015, this volume). These phases are expected to become stabilized by decreasing fS_2 shortly before or during the exhaustion of liquid sulfide in harzburgite residues at moderate to high degrees of melting (e.g., Fonseca et al. 2012; Mungall and Brenan 2014; Brenan et al., 2015, this volume). Thus, their occurrence in harzburgites (e.g., at Lherz; Luguet et al. 2007) is not unexpected.

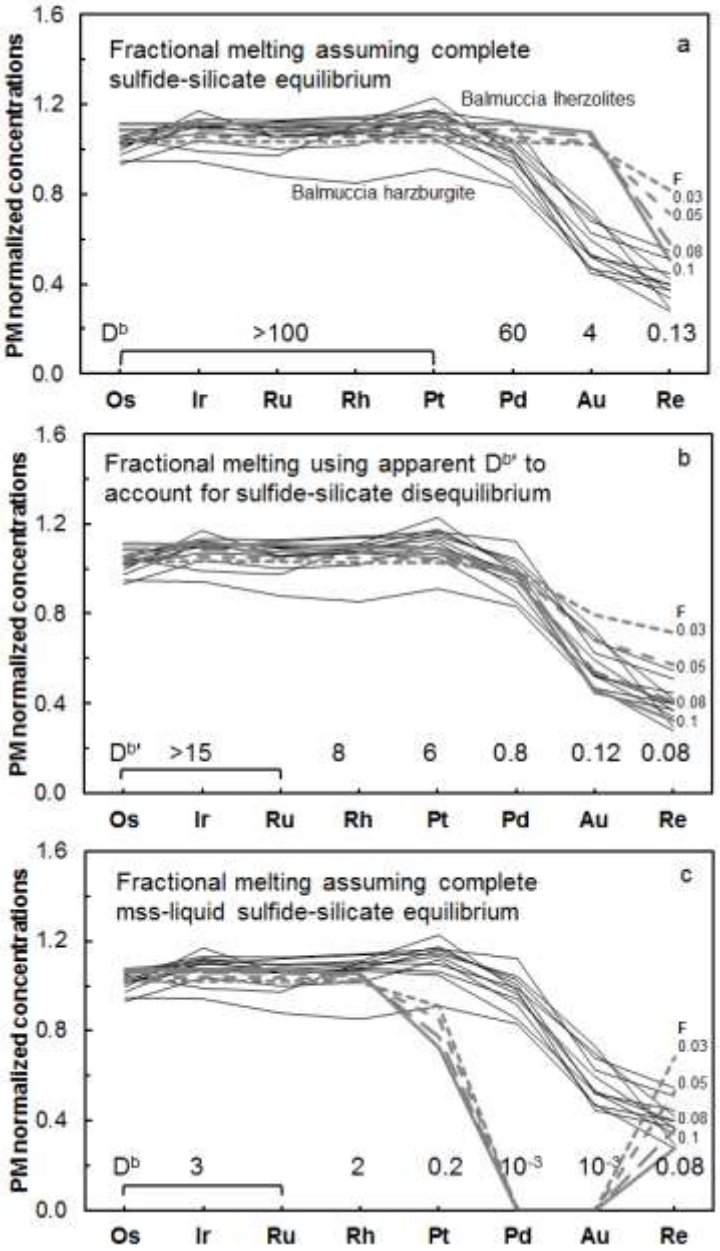

Figure 18. Primitive mantle-normalized concentration diagrams of the HSE in residues of fractional melting of fertile peridotite in comparison to lherzolites and a harzburgite from the Balmuccia peridotite massif (data from Wang et al. 2013). The latter are shown here as an example, because concentration data of HSE and lithophile elements in lherzolites are relatively homogeneous and lithophile incompatible element data suggest that these rocks are residues of fractional melting (see text). The linear concentration scale was used to show details of the fractionation between Pt, Pd, Au and Re. Shown are the effects of equilibrium and disequilibrium distribution of the HSE between rock and coexisting melt and different melt fractions F. a) Ideal sulfide-silicate equilibrium partitioning. Bulk partition coefficients D^b were calculated based on sulfide-silicate and mineral-silicate melt partition coefficients at fO_2 near FMQ-1 (Brenan 2008; Fonseca et al. 2007; Mallmann and O'Neill 2007; Mungall and Brenan 2014). b) Apparent bulk partition coefficients $D^{b'}$ were estimated to account for mixing and the disequilibrium distribution between sulfides and silicates during open system melting (see text). c) The effects of monosulfide solid solution (mss)-liquid sulfide-silicate partitioning, assuming equilibrium among all phases. Mss-sulfide melt partition coefficients from Ballhaus et al. (2006), Brenan (2002), Li et al. (1996), Mungall et al. (2005). Note that for the PGE, some silicate mineral-silicate melt partition coefficients (e.g., pyroxenes) are not well-constrained. In such cases partition coefficients for olivine were used. Thus D^b for Pd and Au in c) may be higher if these elements are more compatible in pyroxenes and in the Al phase.

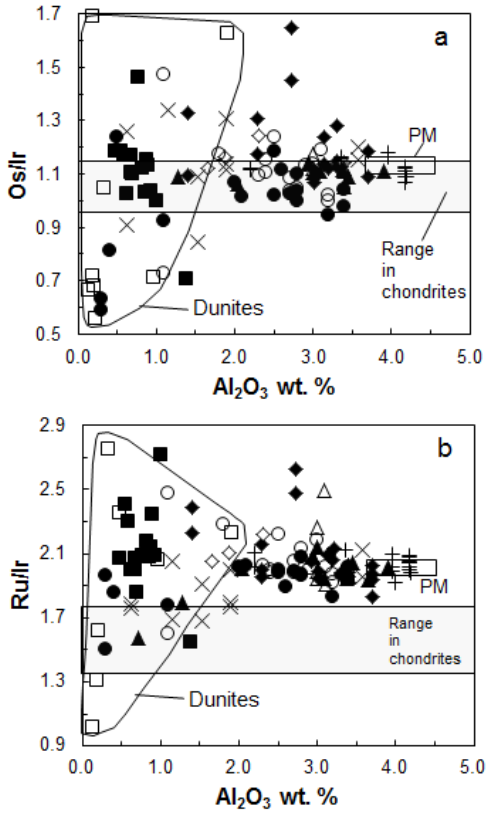

Figure 19. a) Os/Ir-Al_2O_3 and b) Ru/Ir- Al_2O_3 in peridotite tectonites. Representative lherzolites and harzburgites from continental extensional and transitional oceanic environments (Balmuccia: solid circles, Baldissero: open circles, Lherz: x, Turon de la Tecuere: +, Lanzo: solid diamond, Internal Ligurides: open diamond). Also shown are harzburgites (solid squares) and dunites (open squares) from the Wadi Tayin section of the Oman ophiolite, dunites from Balmuccia (solid circles within the Dunite fields, see also Figs. 5, 8b) and lherzolites from Ronda (open trangle) and Beni Bousera (solid tringle). For data sources of peridotites see Fig. 5 and text. Chondritic range from Horan et al. (2003) and Fischer-Gödde et al. (2010). Primitive mantle model from Becker et al. (2006). The data show relatively homogeneous ratios in lherzolites and larger variations in harzburgites and in replacive dunites (see text for details).

However, such phases have also been detected in lherzolites from Lherz that formed by refertilization, albeit they occur in smaller proportions than in harzburgites (Lorand et al. 2010).

If the alloy phases were indeed inherited from more depleted parent rocks, their presence in some lherzolites may also reflect chemical disequilibrium between these phases and the more abundant sulfide minerals that were precipitated as sulfide liquid from silicate melt. The impact of such inherited and presumably 'residual' alloy phases on bulk rock budgets of lherzolites that formed by refertilization appears rather limited. For instance, the bulk rock Os/Ir ratios of lherzolite tectonites is rather homogeneous and overlaps chondritic values (Fig. 19a, Becker et al. 2006; Fischer-Gödde et al. 2011; Liu et al. 2009; Pearson et al. 2004; Wang et al. 2013). Because of the different solubilities of Os and Ir metal in silicate melt (e.g., Mungall and Brenan 2014), chondritic Os/Ir are not a priori maintained in residual peridotites at higher degrees of melting (as witnessed by the larger scatter of this ratio in harzburgites). Pt/Ir and Pt/Os in lherzolites range from chondritic to mildly subchondritic. Only rarely do lherzolites display enrichments of Pt that are decoupled from Pd, Au and Re (e.g., Fig. 5b, c) and might be ascribed to the excess presence of Pt minerals. In this context, it is noteworthy that ratios of Ir, Os and Ru in mantle tectonites tend to be more scattered in harzburgites than in lherzolites (Fig. 19). The difference in homogeneity of the different rock types may either reflect digestion problems in the laboratory, i. e. the difficulty of complete dissolution of refractory platinum group metal alloys in harzburgites (Meisel and Horan, 2015, this volume, and references therein), or it may be due to dissolution of refractory alloy phases in coexisting sulfur-undersaturated melt at high temperatures.

Osmium isotopic disequilibrium within mantle peridotites. Evidence for small-scale chemical disequilibrium regarding chalcophile elements is provided by Re-Os data that suggest that grain- to hand specimen-scale Os isotopic disequilibrium is common in the mantle. Burton et al. (1999) found that different mineral separate fractions from mantle xenoliths showed differing $^{187}Os/^{188}Os$ that were not related by isochronous behavior. Leaching experiments of powders of refertilized mantle xenoliths and tectonites show that $^{187}Os/^{188}Os$ frozen in during the Archean or Proterozoic survived Phanerozoic refertilization, most likely because of the preservation of ancient chromite or olivine that contained inclusions of HSE carrier phases (Chesley et al. 1999; Becker et al. 2006; Wang et al. 2013). Alard et al. (2002; 2005) showed that the sulfide populations with different PGE compositions also display systematic differences in Re/Os and $^{187}Os/^{188}Os$. In peridotite xenoliths and abyssal peridotites, sulfides on grain boundaries tend to have chondritic to suprachondritic Re/Os and $^{187}Os/^{188}Os$, whereas sulfides in inclusions also display subchondritic values (Harvey et al., 2006; Harvey et al., 2011; Warren and Shirey, 2012). The heterogeneous $^{187}Os/^{188}Os$ in different bulk rocks of essentially all suites of peridotites, xenoliths or tectonites from different geodynamic environments (e.g., Figs. 1, 2, 4, 7, 9, 11; and Reisberg and Luguet 2015, this volume) also represents a manifestation of disequilibrium on the scale of hand specimen and outcrops. In principle, such variation may have been caused by differences in the age of partial melting and melt infiltration. However, evidence for grain-scale initial Os isotopic heterogeneity at times of melt infiltration (in cases where the timing can be constrained) suggest that mixing of residues and melts with different $^{187}Os/^{188}Os$ during reactive melt infiltration did not result in full Os isotopic equilibrium. A good example are the ultramafic tectonites in the Pyrenees and in the Italian and Swiss Alps (Baldissero, Balmuccia, Lanzo, Totalp), where episodic melt infiltration into Proterozoic continental lithospheric mantle during Paleozoic and Mesozoic extension only partially re-equilibrated $^{187}Os/^{188}Os$ values. All these data and observations suggest that disequilibrium must have been maintained even at high temperatures in the upper mantle and in the presence of silicate melt. The widespread heterogeneity of initial $^{187}Os/^{188}Os$ at the grain boundary- to centimeter-scale in mantle rocks also suggests that sulfide liquids are efficiently trapped even during recrystallization processes.

Alongside evidence from textures and lithophile elements (e.g., Le Roux et al. 2007; Mazzucchelli et al. 2009; Müntener et al. 2005; Rivalenti et al. 1995), the extent of re-equilibration is manifested in the scatter of HSE abundances displayed by different suites of peridotites, in the abundance of harzburgite rocks in outcrops and in the distribution of Re-Os model ages in these bodies. At Lherz, Lanzo and Baldissero Re depletion ages of peridotites

display bimodal distributions of Proterozoic and Phanerozoic ages, with harzburgites or depleted lherzolites typically showing older model ages (i. e., lower measured $^{187}Os/^{188}Os$) than lherzolites (Reisberg and Lorand 1995; Burnham et al. 1998; Becker et al. 2006; Fischer-Gödde et al. 2011; Wang et al. 2013). In contrast, at Balmuccia and Totalp, depleted lherzolites and harzburgites are rare and display Proterozoic Re depletion ages. Model ages of fertile lherzolites at these locales range from Phanerozoic to future ages (van Acken et al. 2008, 2010; Wang et al., 2013). Of note is that the scatter of the concentrations of Os, Ir and Ru in fertile peridotites at these localities is more limited than in other lherzolite bearing tectonites (compare Fig. 5b with 5a and 5c).

Osmium isotopic heterogeneity is also prevalent in abyssal peridotites, which are commonly presumed to represent melting residues of MORB-type magmas. Harvey et al. (2006) have shown that sulfides in harzburgites from the 15°20' N fracture zone (Atlantic Ocean) preserve small-scale isochronous relationships that date back to the Paleo-Proterozoic. Such preservation of early- to mid-Proterozoic $^{187}Os/^{188}Os$ values in bulk rocks and sulfides has also been reported in other abyssal peridotites (Parkinson et al. 1998; Alard et al. 2005; Liu et al. 2008; Warren and Shirey 2012). Further evidence of small-scale disequilibrium is apparent in studies of platinum-group minerals from ophiolites. Platinum group minerals from the Mayari-Cristal Ophiolite, Cuba, have been found to have diverse $^{187}Os/^{188}Os$ ratios even on the scale of a single thin section (Marchesi et al., 2011). The most extreme example found was the presence of two PGM only a few millimeters apart, with $^{187}Os/^{188}Os$ ratios of 0.1185 and 0.1232 (Marchesi et al., 2011), which give T_{RD} ages of 1370 and 720 Ma, respectively (ordinary chondrite reference evolution line; Walker et al. 2002). The mechanism of formation for such PGM is not well known, but given that the budget of Os for these PGM is thought to be sourced from at least several m^3 of mantle (total Os equivalent to ~$1m^3$ mantle), this would imply little if any mixing of percolating melts, or a lack of equilibration between mineral grains and subsequent percolating melts.

The influence of disequilibrium between mantle and magmas on HSE distributions. The predicted behavior of the HSE can be compared with HSE patterns of peridotites. Relatively 'constant' concentrations have been noted for the Ir group PGE in many studies of lherzolite tectonites. However, Rh and Pt display a tendency towards higher concentrations in lherzolites (e.g., Fischer-Gödde et al. 2011). In some (but not all) suites of peridotites, Pd correlates with fertility indicators such as Al_2O_3 abundances (e.g., Becker et al. 2006). Some workers (e.g., Lorand et al. 1999, Pearson et al., 2004) have noted that the variable depletion of Pd in lherzolites is difficult to reconcile with partial melting and very high sulfide-silicate partition coefficients (> 10^4 to 10^5). The smooth depletion of Pd, Au and Re relative to other HSE in lherzolites from Balmuccia and elsewhere (e.g., Fig. 18) is inconsistent with equilibrium partitioning and the liquid sulfide-liquid silicate partitioning data. It is also difficult to explain by other equilibrium partitioning processes involving sulfides, e.g., mss-liquid sulfide (see below). Furthermore, concentrations of Os, Ir and Ru in peridotite tectonites of similar lithophile element composition display considerable scatter (e.g., Fig. 5), as do Os isotopic compositions. For lherzolites, at least, the different concentrations cannot entirely be an artifact of heterogeneous distribution of sulfide grains within sample powders or the rock (Meisel and Moser 2004; Meisel and Horan 2015, this volume). Instead, these concentration variations may reflect the compositional variability of sulfide grains in the rock; as indicated by variable Ir and Ru concentrations in peridotitic sulfides (e.g., Alard et al. 2000). As there is indisputable evidence for widespread, or even ubiquitous, chemical and isotopic disequilibrium of the HSE in peridotites, it is plausible that the distribution of chalcophile elements between peridotite and magma is partly controlled by the composition of sulfide liquids from infiltrating primitive magmas and partly by mixing processes between such liquids and sulfide liquids already present in the rocks (e.g., Lorand et al. 1999; Alard et al. 2000; Pearson et al. 2004; Lorand et al. 2010).

In the melting model shown in Fig. 18b apparent sulfide-silicate partition coefficients were used to match the patterns of peridotites from the Balmuccia peridotite massif. Apparent partition coefficients take into account the extent to which the HSE composition of peridotites displays the effects of mixing, and thus the influence of the original infiltrating melt compositions, rather than just sulfide melt-silicate melt equilibrium. It is clear that the fractionations inherited from the melt contribute to the lowering of D^b, compared to the equilibrium case. The differences will be particularly notable for Pd and Au. As Pd in depleted lherzolites is commonly slightly depleted, the apparent bulk distribution coefficient for this element should be < 1 and apparent sulfide-silicate distribution coefficients in the model in Fig. 18b would be about 1300; far lower than the 10^5 to 10^6 range for sulfide-silicate equilibrium (Mungall and Brenan 2014). For Pt and Rh apparent partition coefficients may also be lower. Gold abundances in depleted lherzolites are lower than in fertile lherzolites and this, coupled with the slight enrichment of Au in primitive basaltic magmas, suggests that Au also has an apparent bulk distribution coefficient < 1. Consequently, apparent sulfide-silicate distribution coefficients for Au are significantly lower (about 200 in the case of Fig. 18b) than equilibrium values (4000-10000; Mungall and Brenan 2014). Rhenium and other moderately chalcophile elements with equilibrium sulfide-silicate partition coefficients < 1500 are not sensitive enough to identify chemical disequilibrium, as the influence of the silicate mineral-silicate melt partition coefficients is substantial. Combined sulfide-silicate and silicate mineral-silicate melt partition coefficients of these elements yield bulk partition coefficients < 1, whether or not equilibrium is assumed.

Figure 20 displays the variation of Re concentrations versus Pd concentrations in various suites of mantle tectonites (note that in more strongly serpentinized peridotites, such as from the Oman ophiolite, Re may also be affected by late-stage alteration). Both elements tend to correlate in harzburgites and in depleted lherzolites, however, in more fertile rocks, Re displays larger variations (0.07 to 0.4 ng/g) at relatively constant Pd (5 to 9 ng/g). The most likely explanation for this observation is that sulfide and other HSE carrier populations in harzburgites and depleted lherzolites reflect mixing and full disequilibrium, whereas pre-existing phases in fertile lherzolites may have partially reacted and equilibrated with a larger fraction of silicate melt and sulfide liquid. The data also suggest that HSE carriers in fertile peridotites of some suites (e.g., Balmuccia and Baldissero) must be more depleted in Re than other suites, which may be a property of the melts that precipitated sulfides during reactive infiltration. The curved trend defined by some data in Fig. 20 may be related to the quantity of melt that reacted and precipitated sulfide liquid in the rock. The systematic behavior of Pd, Au, Re and of other chalcophile elements such as S, Se, Te, Cu and Ag in most peridotites and in MORB (Wang and Becker 2015b) indicates that the relative depletion and enrichments of these elements in peridotites and in MORB may be described by apparent bulk partition coefficients. Melt compositions calculated by this approach may yield similar concentrations of Pd, Au and Re as in primitive MORB, although the latter almost certainly require a more complicated fractionation history (e.g., Langmuir et al. 1992; Rehkämper et al. 1999; Bezos et al. 2005; Mungall and Brenan 2014; Wang and Becker 2015c).

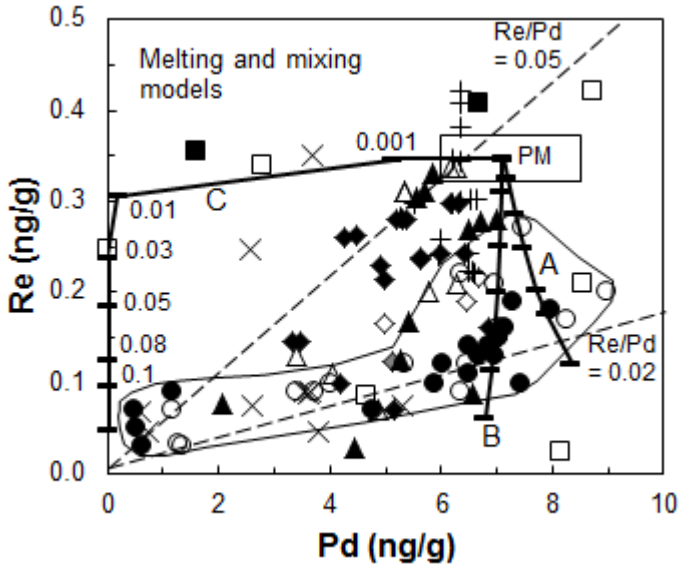

Figure 20. Concentrations of Re and Pd in peridotite tectonites and evolution of the composition of residues in different melting models. Symbols as in Fig. 19, melting curves A to C calculated using parameters from Fig. 18 and the text. A: equilibrium liquid sulfide-silicate partitioning (Fig. 18a), B: disequilibrium distribution, taking into account the effect of mixing of different types of sulfide with different partitioning histories (Fig. 18b), C: mss-liquid sulfide-silicate partitioning (Fig. 18c). Different Re/Pd ratios in lherzolites are indicated by dashed lines. None of the melting models yields a satisfactory match for the data distribution of different peridotite suites. In this diagram, ideal binary mixing processes without chemical reaction should result in linear correlations; e.g., mixing of 'residual' Re- and Pd-depleted sulfide liquid with Re-Pd-rich sulfide liquid precipitated from percolating magma. Most peridotites from Lanzo display such a trend along a Re/Pd of 0.05. Depleted lherzolites and harzburgites from Baldissero and Balmuccia also display a linear trend albeit at a lower Re/Pd, presumably because the infiltrating magma was more depleted in Re and other incompatible elements. In fertile lherzolites the data is scattered, likely because of the predominance of sulfides derived from infiltrating magma and partial chemical equilibration. Chemical equilibration tends to decouple variations of Re and Pd because of their very different partitioning behavior at low to moderate degrees of melting (Brenan et al. 2015, this volume).
Symbol key: Balmuccia: solid circle (dunites at low Re and Pd concentrations), Baldissero: open circle, Lherz: x, Turon de la Tecuere: +, Lanzo: solid diamond, Internal Ligurides: open diamond, External Ligurides: gray diamond, Ronda: open triangle, Beni Bousera: solid triangle. Also shown are harzburgites (solid square) and dunites (open square) from the Wadi Tayin section of the Oman ophiolite, For data sources of peridotites see Fig. 5 and text.

An alternative model of HSE partitioning during mantle melting was presented by Bockrath et al. (2004) and Ballhaus et al. (2006). These authors proposed that residual mss may coexist with liquid sulfide over a significant pressure-temperature range in the mantle. Partitioning between these phases may control the HSE abundances in residues and silicate melts. However, because of uncertainties in the position of the sulfide liquidus in different experimental studies, the stability of mss in the asthenosphere or deeper lithosphere is debated (see Fonseca et al., 2012; Mungall and Brenan 2014). The relevance of mss-liquid sulfide partitioning in the upper mantle can be evaluated on the basis of existing partitioning data for chalcophile elements and the composition of mantle rocks, basalts and their sulfides. Melting models of bulk rock compositions of lherzolites that employ mss-liquid sulfide partition coefficients (Fig. 18c) display a poor match for Pt, Pd and Au. However, it must be acknowledged that bulk partition coefficients are strongly influenced by the silicate mineral-silicate melt partition coefficients. Only for olivine-silicate melt partitioning does sufficient data exist for Pt, Pd and Au (see equations 11-13 in Mungall and Brenan, 2014, which yield low $D^{olivine/silicate}$ melt for these elements at fO_2 of 10^{-9} to 10^{-10} bar). Pyroxene-silicate melt partition coefficients for these

elements are poorly constrained, and thus D^b may be higher. As for sulfide liquid-silicate partition models, Re fits well because its D^b is strongly controlled by the large mass fraction of silicates and the well-determined mineral-silicate melt partition coefficients.

In principle, mss-liquid sulfide partitioning may account for the different patterns of Ir group and Pt group PGE in sulfide inclusions and sulfides on grain boundaries in peridotites (e.g., Ballhaus et al. 2006). However, the behavior of Re concentrations in sulfide inclusions versus grain boundary sulfides argues against this process. Equilibrium mss-liquid sulfide partitioning would predict higher Re and Os concentrations in residual sulfides compared to coexisting sulfide liquids, because both elements are compatible in mss ($D_{Os}^{mss/sul\ liq}$ = 3-7, $D_{Re}^{mss/sul\ liq}$ = 3, Brenan 2002; Ballhaus et al. 2006). Although sulfide inclusions in silicates of peridotites may have higher Ir and Os than sulfides on grain boundaries (e.g., Alard et al. 2000, Alard et al. 2002), Re is depleted in the former and enriched in the latter, commonly accompanied by correlated Re/Os (Alard et al. 2005). Recently, it has been proposed that some harzburgites contain sulfides with high Se/Te ratios similar to what is expected from mss-liquid sulfide partitioning (König et al. 2014; 2015). However, because of the low concentrations of these elements, the mass balance of such phases in strongly depleted peridotites is difficult to constrain, and they may also reflect precipitation of sulfide from somewhat more fractionated magma with high Se/Te and Re/Os (Wang and Becker, 2015a). Work on Cu and Ag abundances in peridotites has shown that the relative behavior of these elements in bulk rock lherzolites is consistent with the systematics predicted by sulfide liquid-silicate partitioning but not with mss-liquid sulfide partitioning (Wang and Becker 2015b).

The differing $^{187}Os/^{188}Os$ of the two sulfide populations suggests that sulfides precipitated on grain boundaries during melt infiltration did not equilibrate with included sulfides, which is a basic requirement for equilibrium mss-sulfide liquid-silicate melt partitioning models. Thus, as shown before in the discussion of sulfide liquid-silicate melt partitioning, none of the proposed partitioning processes that are potentially relevant during partial melting yields a satisfactory quantitative description of the HSE composition of many mantle peridotites. Sulfide melt-silicate melt partitioning seems to be the best match for the observed HSE pattern in lherzolite bulk rocks. However, at least for Pd, Au, Re and S, their ratios in lherzolites may be mostly inherited from the melts that infiltrated depleted precursor rocks (e.g., harzburgites; Fig. 20). The origin of the HSE fractionation in the infiltrating melts and their sulfide liquids will be discussed below.

HSE fractionation during the formation of mantle pyroxenites. Mantle pyroxenites are important because they represent products of magmatic fractionation in the mantle and thus yield information on the composition of relatively 'primitive' magmas (Bodinier and Godard 2003). Pyroxenites are cumulates that formed by reactive infiltration and fractional crystallization of primitive to more evolved basic magmas. Websterites ('Cr diopside suite') and orthopyroxenites sometimes display mineralogically zoned reaction domains with peridotites, which have formed due to melt infiltration into the surrounding peridotite (e.g., Becker et al., 2004; Bodinier et al., 1987, 2008). Quite often, clinopyroxenites ('Al augite suite') appear to have formed from more evolved compositions and the absence of reaction zones may indicate their formation at shallower levels (e.g., Sinigoi et al., 1983; Suen and Frey, 1987).

Only limited data are available for HSE abundances and Os isotopic compositions in mantle pyroxenites from tectonites, including pyroxenites from Ronda (Reisberg et al. 1991, Reisberg and Lorand, 1995; Marchesi et al. 2014), Beni Bousera (Kumar et al. 1996, Pearson and Nowell 2004; Luguet et al. 2008b), Lower Austria (Becker et al. 2001, 2004), Troodos (Büchl et al. 2002), Totalp (van Acken et al. 2008, van Acken et al. 2010b), Hori Bory (Ackerman et al. 2013) and Balmuccia (Wang and Becker 2015c). The HSE patterns of pyroxenites in mantle tectonites are broadly similar to data from sulfides in pyroxenite xenoliths. In general, the relative fractionation of the HSE is similar to that in basalts, but with higher concentrations of Os, Ir, Ru,

Rh, Pt and Pd than in MORB. Websterites and orthopyroxenites often display HSE patterns that are less strongly fractionated than clinopyroxenites (Fig. 21).

Concentrations of S and Re in pyroxenites are similar or lower than in MORB, but often higher than in lherzolites. Abundances of other HSE in pyroxenites are similar or lower than in lherzolites (Fig. 21). Some pyroxenites display a depletion of Re relative to Pd, which may have been caused by multi-stage melting (Marchesi et al. 2014). The occurrence of

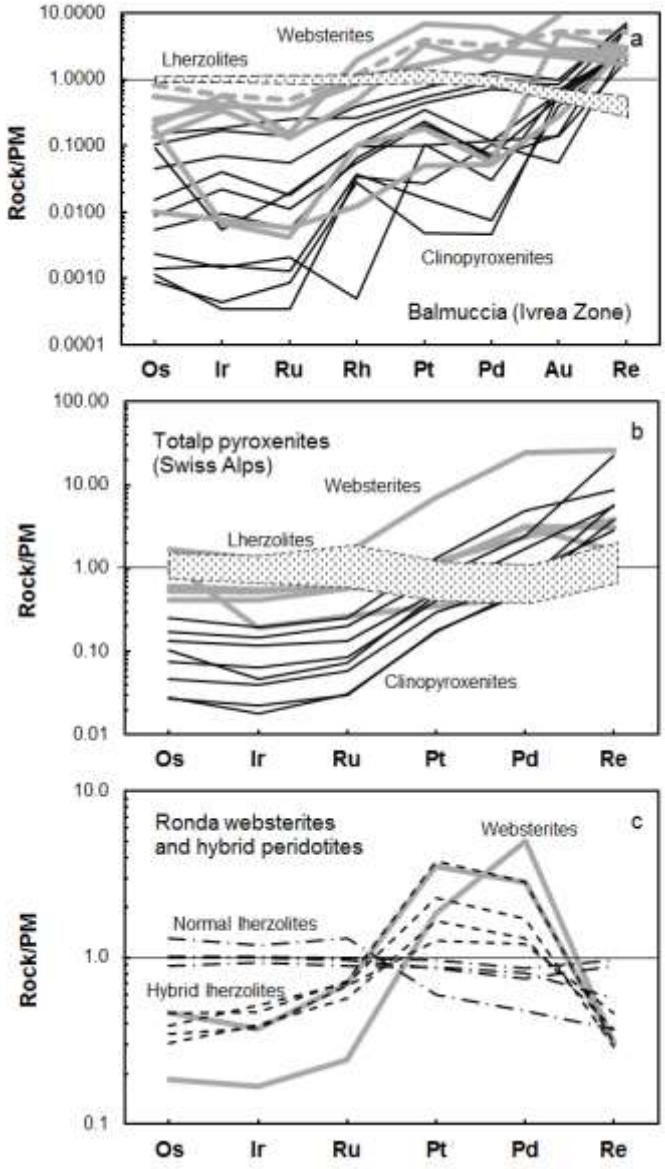

Figure 21. Primitive mantle-normalized concentration diagrams of mantle pyroxenites from peridotite massifs. Websterites: gray lines, clinopyroxenites: black lines. a) Balmuccia (Wang and Becker 2015c) Balmuccia lherzolites from Wang et al. (2013). b) Totalp (van Acken et al. 2010b) Totalp lherzolites from van Acken et al. (2010a). c) Ronda (Marchesi et al. 2014): Hybrid lherzolites (dashed lines) were also affected by reactive infiltration of magma, but differ in composition from the pyroxenites and normal lherzolites. Typical Ronda lherzolites (dash-dotted lines) from Fischer-Gödde et al. (2011).

centimeter-scale Os isotopic heterogeneity between alternating pyroxenite-peridotite layers (Becker et al. 2001, 2004; Büchl et al. 2002; van Acken et al. 2008) is another indication of the

difficulty of small-scale Os isotopic equilibration between silicate melt and existing sulfide populations. A study of a zoned clinopyroxenite-websterite-orthopyroxenite rock from Lower Austria that represents a former reaction zone between high-temperature silicate melt and peridotite has shown that Sr and Nd isotopic compositions were equilibrated across a 10 cm distance of the rock at the time of its formation (Becker et al. 2004). In contrast, both γOs_i and Os concentrations display strong gradients over the same distance, indicating disequilibrium. HSE compositions of sulfides in single thin sections of Totalp pyroxenites vary from those with Ru/Ir, Pd/Ir and Re/Ir similar to peridotitic sulfides, to those with high ratios of these elements, typical of melt compositions (van Acken et al. 2010b). The detailed processes that resulted in the close association of these different sulfide populations are not yet clear, but they suggest that disequilibrium among sulfides may be common in mantle pyroxenites as well as peridotites.

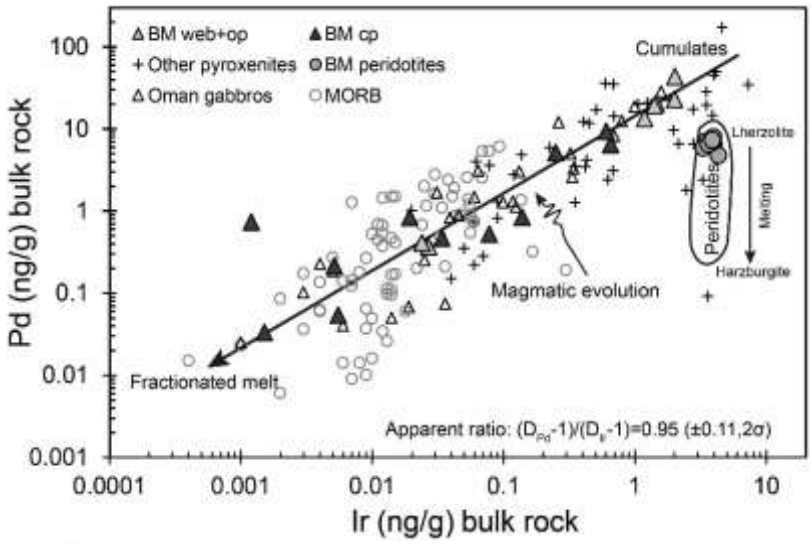

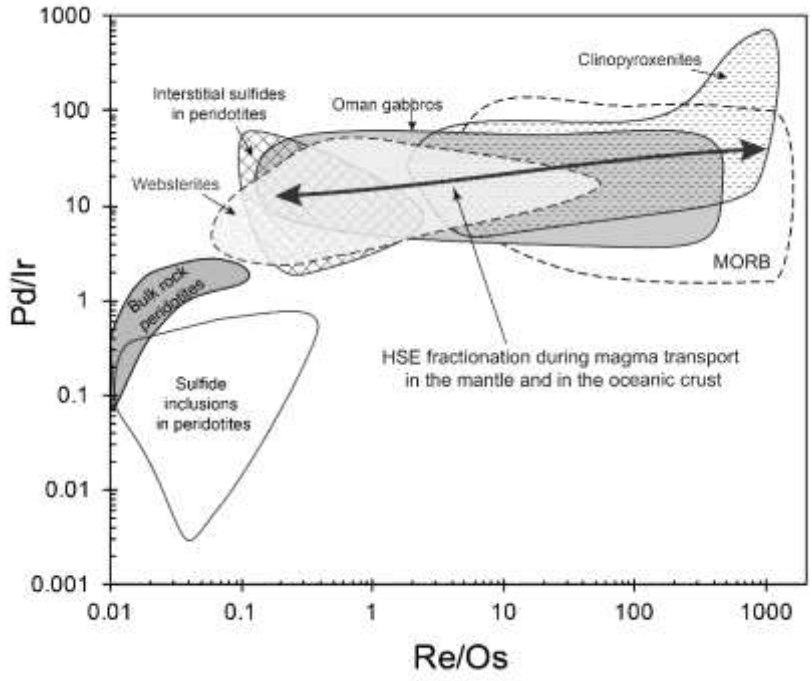

Figure 22. a) Pd-Ir diagram of bulk rock concentrations in mantle peridotites, pyroxenites (BM = Balmuccia, Ivrea Zone), MORB and gabbros of the oceanic crust. Web: websterite, op: orthopyroxenite, cp: clinopyroxenite. The correlation suggests that, with the exception of a few gabbros and MORB, mantle-derived magmatic rocks define a continuum between melt compositions and pyroxenites ('cumulates'). Most magmatic products are offset from the peridotite data, indicative of disequilibrium between magmas and bulk peridotite. b) Pd/Ir-Re/Os diagram showing the limited range of fractionation of Pd/Ir in magmatic products compared to Re/Os. The Pd/Ir data are consistent with similar bulk distribution coefficients of these elements during magmatic processing in mantle and crust (see a). Most magmatic rocks shown in (b) define fields that overlap with or lie along the extension of grain boundary sulfides from peridotites, indicating a common origin of grain boundary sulfides and mantle-derived igneous rocks. Both diagrams are modified from Wang and Becker (2015c). Data sources: Oman gabbros, Peucker-Ehrenbrink et al. (2012); MORB: Hertogen et al. (1980), Rehkämper et al. (1999b), Bezos et al. (2005), Lissner et al. (2014); BM pyroxenites and peridotites, Wang et al. (2013, 2015c); other pyroxenites are from Totalp, van Acken et al. (2008, 2010b); Beni Bousera, Luguet et al. (2008); Ronda, Marchesi et al (2014); Horní Bory (Ackerman et al. 2013); Dramala massif, Pindos ophiolite (Sergeev et al., 2014); interstitial sulfides and sulfide inclusions in peridotites, Alard et al. (2005), Harvey et al. (2006).

A comparison of Re/Os and Pd/Ir in pyroxenites with data on ocean ridge basalts and gabbros from the lower oceanic crust indicates considerable overlap (Fig. 22). This observation suggests that significant fractionation of HSE ratios in magmas already occurs by precipitation of sulfide liquid during magmatic transport and reaction in the mantle (Wang and Becker 2015c). In contrast to Re/Os, which shows large variations in magmatic products over several orders of magnitude, the variation of Pd/Ir in the latter is much more limited and Pd and Ir show similar bulk partitioning behavior. Because of the segregation of sulfide liquid from magmas during magmatic transport in the mantle, the HSE compositions of basaltic magmas may preserve little direct information on HSE concentrations of deeper parts of the melting region. Figure 22a also shows that the data fields defined by most magmatic products, particularly the basalts, are offset from the bulk compositions of peridotites, but overlap with ratios in grain boundary sulfides from peridotites. A similar observation was made for variations of Se/Te (Wang and Becker 2015c). This observation may provide the best indication so far that most magmas that contribute to the oceanic crust did not fully equilibrate with the bulk rock of mantle peridotite residues.

HSE fractionation during the formation of harzburgites and replacive dunites. Data on HSE and other chalcophile elements in harzburgites show that many of these rocks have high abundances of IPGE and lower abundances of Rh, Pt and Pd (e.g., Pearson et al. 2004; Becker et al. 2006; Luguet et al. 2007). These IPGE-PPGE fractionations are generally consistent with fractionation of melting residues at moderate to high (15 to 30 %) degrees of partial melting (Mungall and Brenan 2014; Brenan et al., 2015, this volume, and references therein). The incongruent breakdown of liquid or solid sulfide occurs at advanced degrees of melting at low fS_2 and may play an important role in the stabilization of Os-Ir-Ru and Pt-Ir alloy phases that have been found in such rocks (Lorand et al. 1999; Luguet et al. 2007; Lorand et al. 2010; Fonseca et al. 2012; Mungall and Brenan 2014; Brenan et al. 2015). With progressive melting in the absence of a Fe-Ni-rich sulfide phase, all Re, Au and Pd should be dissolved in coexisting melts, provided that residues and melts were equilibrated. The abundances of Os, Ir, Ru, Rh and Pt, and their fractionation in harzburgite residues (e.g., Fig. 20) should be controlled by the solubility of these elements in sulfur-bearing silicate melts and the stability of Os-Ir, Ru-Os and Pt-Ir phases (Mungall and Brenan 2014).

However, harzburgites may show variations in HSE abundances that are not entirely consistent with a simple melting history as envisioned before. Normalized abundances of Re and S in harzburgites are sometimes higher than normalized abundances of Pd (Figs. 5, 10). These patterns have been interpreted either in terms of precipitation of secondary sulfides from infiltrating melts with high Re/Os and fractionated HSE patterns (Chesley et al. 1999, Pearson et al. 2004, Becker et al. 2006; Wang and Becker 2015a). Alternatively, enrichments of Re and S

compared to Pd and Pt (and of Se relative to Te) in some harzburgites have been interpreted to reflect the presence of mss of residual origin (König et al. 2014). The former explanation is consistent with magmatic re-enrichment processes of incompatible elements (e.g., light rare earth elements) in some of these rocks. Some harzburgites display lower abundances of IPGE than expected for depleted mantle peridotite, e.g., < 3 ng/g Ir, instead of 4 to 5 ng/g expected for residues of moderate to high degrees of melting (Figs. 5, 10). In order to understand this behavior, it is useful to recall that even at high temperatures most peridotites likely contain unequilibrated sulfide melt (maybe also mss), with a range of HSE concentrations. Complete dissolution of some of these sulfide droplets (but not others) into sulfur-undersaturated melt, without concurrent precipitation of IPGE alloy phases, will result in a net decrease of the abundances of all HSE. This process almost certainly plays an important role in the formation of some replacive dunites and associated harzburgite-lherzolite-pyroxenite rock assemblages (Becker et al. 2001, 2004, Büchl et al. 2002, 2004, Hanghøj et al. 2010, Wang et al. 2013). For instance, the variable IPGE abundances and strong depletions of Pt, Pd, Re and other chalcophile elements in discordant dunite bodies in lherzolites at Balmuccia indicate that the magmas were undersaturated in sulfur, which caused the dissolution of sulfides from the lherzolitic protoliths of the dunites (Fig. 5, Wang et al. 2013).

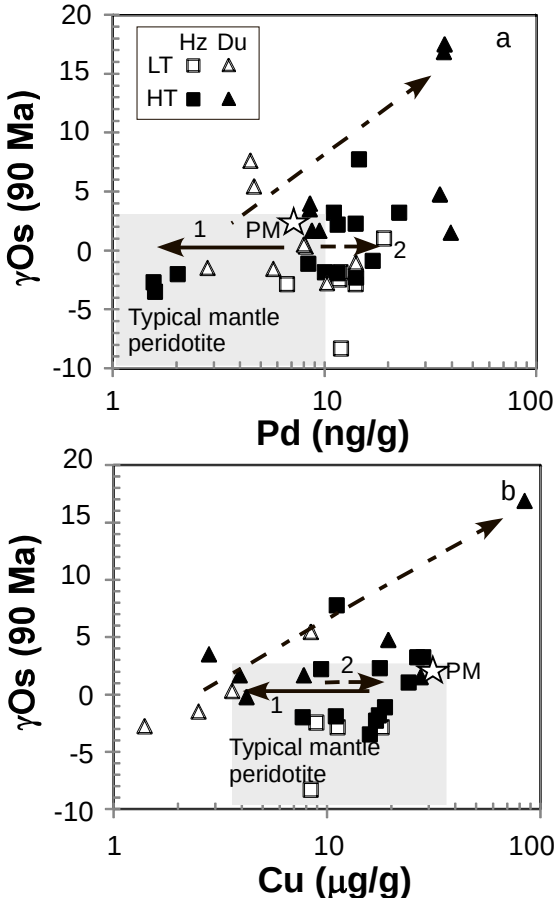

Figure 23. The enrichment of chalcophile elements in harzburgites and dunites from Wadi Tayin (Oman ophiolite, Hanghøj et al. (2010). a) γOs_i-Pd diagram shows that in most harzburgites and dunites Pd is enriched in comparison to typical mantle peridotites. b) γOs_i-Cu diagram indicates that Cu in dunites loosely correlates with γOs_i. In general, Cu is less enriched than Pd. Open symbols are low-temperature rocks, filled symbols high-temperature rocks (see Fig. 9). Arrow 1 indicates the expected depletion behavior due to melting, 2, redistribution of Pd due to dissolution and precipitation of sulfides and the dash-dotted arrow indicates correlated changes in γ_{Osi}, and Cu concentrations resulting from melts with

suprachondritic Os isotopic composition. For Pd this correlation breaks down, presumably because of local sulfide segregation from coexisting magma.

The harzburgites from Wadi Tayin (Oman ophiolite) display normal abundances of IPGE and tend to show primitive mantle-like or even slightly suprachondritic abundances of Pt, Pd and Re (Lorand et al. 2009; Hanghøj et al. 2010). Some of the harzburgites show selective enrichments of Pt that also have been noted from abyssal peridotites and other ophiolites (Fig. 10) and peridotite massifs (Fig. 5). The Pt enrichments may indicate the precipitation of Pt-enriched sulfide liquid from silicate melt that may have dissolved Pt from destabilized Pt-Ir alloys at high degrees of melting. Dunites from Wadi Tayin are similarly enriched in HSE, but show more fractionated Re/Os and PPGE/IPGE ratios. Because the dunites are thought to reflect pathways of olivine-saturated magmas, the enrichments of Pt, Pd and Re in dunites and harzburgites likely reflect sulfide segregation from magmas enriched in these elements (Fig. 23). Although this process appears to have occurred pervasively, the initial $^{187}Os/^{188}Os$ (at around 90-95 Ma) in the mantle section at Wadi Tayin were not equilibrated (Fig. 23). The high abundances of Pt, Pd and Re in otherwise incompatible element depleted mantle rocks suggest that sulfide saturation may play an important role in the uppermost mantle underneath fast-spreading ocean ridges. Dunites from the Troodos ophiolite also display 'melt-like' HSE compositions (Büchl et al. 2002). A common property of dunites is that their initial $^{187}Os/^{188}Os$ extends to suprachondritic values (γOs_i ranging from -3 to +17, e.g., Fig. 23 and Becker et al. 2001), suggesting that some of the parent magmas had suprachondritic Os isotopic compositions. However, as the case of the dunites from Balmuccia shows, not all dunites are characterized by an enrichment of Pt, Pd and Re and melt like HSE patterns.

PGE enrichments also occur in podiform chromitites, which are magmatic precipitates associated with dunites and harzburgites in ophiolites that formed in the proximity of convergent plate margins. Because chromitites may represent economically relevant sources of PGE, these high-temperature magmatic ore deposits will be discussed in Barnes and Ripley (2015, this volume).

Summary – Mantle melting and mantle-magma interaction – different sides of the same coin

Models of partial melting of mantle tectonites must consider the natural open-system behavior relevant for melting column models, diapiric upwelling of partially molten mantle or conversion of lithospheric mantle to asthenosphere by melt infiltration (as was suggested to have occurred in the magmatic history of some mantle tectonites, e.g., Müntener et al. 2005). Thus, melt infiltration and melting should occur more or less simultaneously, provided that porous flow permits melt infiltration. The composition of the residues will change with time until external processes cause upwelling and melting to stop and the mantle to cool. The HSE concentration and $^{187}Os/^{188}Os$ data on mantle tectonites with well-constrained ages (e.g., Oman ophiolite) show that the extent of sulfide-silicate equilibrium in these melting processes must be limited. Several different types of sulfide (presumably mostly liquids, but also mss and other solid phases at lower temperatures) may exist at high temperatures in peridotite (see also Lorand and Luguet 2015, this volume). Residual sulfides with subchondritic $^{187}Os/^{188}Os$ occur as inclusions in silicates and are inherited from ancient melting processes. These sulfides may represent residual sulfide liquids or mss, or both. Sulfide liquids with chondritic to suprachondritic $^{187}Os/^{188}Os$ and higher Re/Os and Pd/Ir are precipitated from infiltrating silicate melt and mostly reflect the composition of these melts with variable reaction with peridotite. Hybrid sulfide liquids may form locally where magmas and peridotite react and magmas became oversaturated in sulfur. In addition, relic PGM phases such as Pt-Ir alloys inherited from depleted protoliths may survive these magmatic

processes. An important aspect of melt infiltration in the lherzolite stability field is the co-precipitation of sulfides with pyroxene ± Al phase assemblages. Only such a process can explain correlations of Re, Re/Os and sulfur concentrations with fertility indicators such as Al_2O_3. As it is likely that the same processes were also responsible for the correlations between $^{187}Os/^{188}Os$ and Al_2O_3 in many suites of mantle peridotites, the mass balance with inherited Re-depleted sulfides suggests that the infiltrating melts had suprachondritic $^{187}Os/^{188}Os$ (the origin of such melts will be discussed later). This notion is supported by Os isotopic measurements on grain boundary sulfides in peridotites and by initial Os isotopic compositions of most mantle pyroxenites (Alard et al., 2002; Alard et al., 2005; Harvey et al., 2010, 2011; Harvey et al., 2015, this volume; Wang and Becker, 2015).

Different modeling approaches, both complicated and simple may produce appropriate HSE compositions of basalts from model mantle compositions (e.g., Rehkämper et al. 1999; Bezos et al. 2005, Harvey et al. 2011, Mungall and Brenan 2014). As discussed here and elsewhere (e.g., Lorand et al. 1999, Pearson et al. 2004, Lorand and Alard 2010, Fischer-Gödde et al. 2011, König et al. 2014, Wang and Becker 2015a), models that employ equilibrium distribution of the HSE between mantle phases have difficulties in accounting for some of the detailed compositional variations of the compatible HSE in bulk peridotites. Studies of HSE in bulk rocks of mantle peridotites and pyroxenites and their trace phases indicate that in high temperature magmatic processes in the mantle, disequilibrium between different HSE host phases and silicates may be the rule (e.g., Burton et al. 1999, Alard et al. 2000, 2002, 2005). In spite of these complexities, a useful assessment of the bulk distribution behavior of the HSE is possible and their relative behavior is consistent with abundance data in komatiites and basalts. The data on bulk rocks and sulfides of mantle pyroxenites and sulfides from grain boundaries in peridotite tectonites and in xenoliths indicate that infiltrating melts show relative fractionation of the HSE and S similar to the fractionation pattern of basalts, with mantle normalized abundances of $S \approx Re > Au > Pd > Pt \geq Rh > Ru > Ir \geq Os$. The HSE data on peridotites and pyroxenites suggest that the composition of infiltrating melts also affects the composition of peridotites (e.g., Fig. 5, 7, 20). Notably, enrichments and depletions of Re in peridotites may be caused by precipitation of sulfides with suprachondritic Re/Os. If the abundances of Re, Au, Pd, Pt and other chalcophile elements in mantle peridotites are predominantly controlled by sulfide segregation from primitive basic magma, the question arises, which partition process produced the relative fractionation among these elements in these magmas to begin with? The answer may lie in the increasing importance of alloy solubility in silicate melt during moderate to high degrees of melting in the shallow mantle, near or beyond the exhaustion of sulfide in the residues. At these conditions, the concentrations of the HSE in silicate melts may be controlled by residual PGE alloys, the different solubility of Pt, Rh, Ru, Ir and Os and possibly silicate mineral-oxide-melt partitioning (Mungall and Brenan 2014; Brenan et al. 2015, this volume). Thus, basic melt infiltrating the asthenosphere and lithosphere at greater depth likely carries the HSE and $^{187}Os/^{188}Os$ signature of oceanic crust produced in previous Wilson cycles. This conclusion is consistent with suprachondritic initial $^{187}Os/^{188}Os$ of mantle pyroxenites and some peridotites that were affected by melt infiltration and coexisting harzburgites with subchondritic $^{187}Os/^{188}Os$, which may represent ancient remnants of shallow oceanic mantle.

Os isotopic heterogeneity in the mantle

The compatibility of Os during partial mantle melting, and the existence of two radioactive decay systems producing isotopes of Os, makes it an ideal element with which to investigate mantle heterogeneity (Hart and Ravizza, 1996; Burton et al., 1999). The relative compatibility of Os and Re is primarily controlled by their differing preference for sulfide over melt (See section above: Behaviour of HSE during partial melting). This produces strong fractionation of moderately incompatible Re from compatible Os during partial melting of the

mantle, giving rise to very high Re/Os ratios in crust-forming melts (see Gannoun et al., 2015, this volume) and correspondingly low, sub-chondritic $^{187}Os/^{188}Os$ ratios in depleted mantle. In turn, crust recycled back into the mantle is potentially traceable due to its distinct Os isotope signature. Likewise, small degree melts within the mantle may also produce variations in Re/Os and thus, over time, in $^{187}Os/^{188}Os$. Due to the chalcophile affinity of Os, Re-Os isotope variations can provide different, yet complementary, information to lithophile isotope systems, and can sometimes display behavior that is decoupled from lithophiles (e.g., Class et al., 2009).

The ^{190}Pt-^{186}Os decay system, in contrast to the Re-Os system, does not typically produce resolvable differences in $^{186}Os/^{188}Os$ ratios in mantle rocks due to the much smaller decay constant compared to ^{187}Re, and due to the lower degree of fractionation between parent and daughter. Only in specific cases of high-degree melting do Pt concentrations significantly exceed those of the mantle, such as in some volcanic arc settings (Dale et al., 2012b) and in komatiites (e.g., Puchtel and Humayun, 2001; Fiorentini et al., 2011); but in the latter case Os in the melt approaches mantle concentrations and thus fractionation of Pt and Os remains limited. Recycled crust has only moderately high Pt/Os (Dale et al., 2009; Peucker-Ehrenbrink et al., 2012) which is not sufficient to produce anomalous compositions given the subsidiary Os concentrations of crust, relative to mantle. Nevertheless, ^{186}Os enrichments have been identified in some intraplate magmas (Brandon et al., 1998; 2003; Puchtel et al., 2005) and in a later section we briefly discuss whether mantle processes are a plausible mechanism by which to produce these enrichments.

In this section, we focus on broad-scale mantle heterogeneity, whereas disequilibrium on a hand specimen scale, or smaller, is covered in the previous section on 'Os isotopic disequilibrium'.

$^{187}Os/^{188}Os$ mantle composition and heterogeneity. The bulk Os isotope composition of the silicate Earth was likely set by late accretion of material with a bulk primitive composition, after core formation had ceased (Kimura et al., 1974; Chou, 1978). However, neither the $^{187}Os/^{188}Os$ composition (Meisel et al., 2001) nor the relative HSE abundances of PM estimates (Becker et al., 2006) match those of any known chondrite group. This difference has been reconciled by (i) late accretion of differentiated planetesimal core material and primitive chondritic material (Fischer-Gödde and Becker, 2012), (ii) by a hybrid model for the enrichment of Earth's HSE involving late accretion to a fractionated mantle signature (which may be a residue from metal-silicate segregation, cf. Righter et al., 2008; Walker, 2009), or (iii) by mantle processes accounting for the combination of non-chondritic ratios involving Ru and Pd and chondritic ratios of other HSE in fertile lherzolites (e.g., Lorand et al., 2010). See Day et al. (2015 this volume) for further discussion.

The processes of continental crust production and incomplete rehomogenisation of recycled oceanic crust have likely both served to reduce the $^{187}Os/^{188}Os$ of the peridotitic mantle below that of the primitive mantle. Thus, heterogeneous distribution of ^{187}Os in the mantle is due to the timing and degree of melt depletion and the presence of enriched domains, which may either be recycled surface materials or domains within the mantle fertilizes by low-degree melts.

A compilation of $^{187}Os/^{188}Os$ data for global peridotites (excluding pyroxenites), grouped according to the tectonic settings used in this chapter and in this volume, is shown in Fig 24, and a summary of the averages and ranges for each setting/sample type is shown in Table 2. Cratonic and circum-cratonic xenoliths, which won't be discussed further here, are both typically strongly unradiogenic, reflecting their severe and early melt depletion and subsequent isolation from the convecting mantle (see Aulbach et al. 2015, tbis volume, and references therein). All major tectonite and xenolith groups (continental/continent-ocean transitional tectonites, high-T convergent tectonites, ophiolites, abyssal peridotites, oceanic mantle xenoliths, sub-continental lithosphere xenoliths and sub-arc xenoliths) have a considerable 'peak' in probability of $^{187}Os/^{188}Os$ between 0.125 and 0.128, indicating a degree of effective large-scale homogenization

in the convecting mantle and younger lithosphere, albeit incomplete. Moreover, most groups have remarkably similar total ranges of $^{187}Os/^{188}Os$ (when excluding up to 3% of the most extreme data), between 0.026 and 0.029 units, with the exception of high-T convergent margin tectonites (n = 48) which have a range of 0.023, and sub-continental lithospheric mantle xenoliths, with a larger range of 0.037 (although in this latter case the primary data may be compromised by secondary processes such as weathering and reaction with host melts. Greater than 85% of samples from each tectonic setting fall within a narrower range of $^{187}Os/^{188}Os$ of around 0.015 units (the range of each group varies from 0.013 for all ophiolites, to 0.019 for continental/continent-ocean transition tectonites).

Table 2. Summary of compiled $^{187}Os/^{188}Os$ data for mantle tectonites, by setting and sample type

Sample type	Mean $^{187}Os/^{188}Os$	Mode $^{187}Os/^{188}Os$	Low	High	Main range (% included)	*n*
Abyssal peridotites	0.1243	0.1261	0.1139	0.1382	0.024 (100%)	107
Continent/cont-ocean transition	0.1255	0.1262	0.1126	0.1372	0.025 (97%)	156
High-T convergent margin	0.1259	0.1237	0.1184	0.1411	0.023 (100%)	48
Ophiolites (all*)	0.1271	0.1252	0.1162	0.1418	0.026 (97%)	142
Arc xenoliths	0.1315	0.1277	0.1206	0.1498	0.029 (97%)	37
OIB xenoliths	0.1244	0.1248	0.1138	0.1339	0.026 (99%)	134
Sub-continental xenoliths	0.1260	0.1257-67	0.1094	0.1464	0.037 (98%)	228

* 2 Ga Finland ophiolite localities omitted due to long-term isolation from convecting mantle

In detail, however, each grouping displays a variable distribution of Os isotope composition, and the positions of the modal and mean $^{187}Os/^{188}Os$ compositions differ between many of the groupings. One caveat here is that the data plotted on Fig. 24 are present-day measured $^{187}Os/^{188}Os$ ratios, to reflect the current degree of overall mantle heterogeneity, and thus do not account for any isolation of portions of lithosphere sampled in this dataset. If these portions were exposed to gradual convective stirring then some of the 'older' depletion ages may have been remixed with more radiogenic ambient mantle. Not all components of the compilation, therefore, necessarily reflect the composition of the 'convecting' mantle.

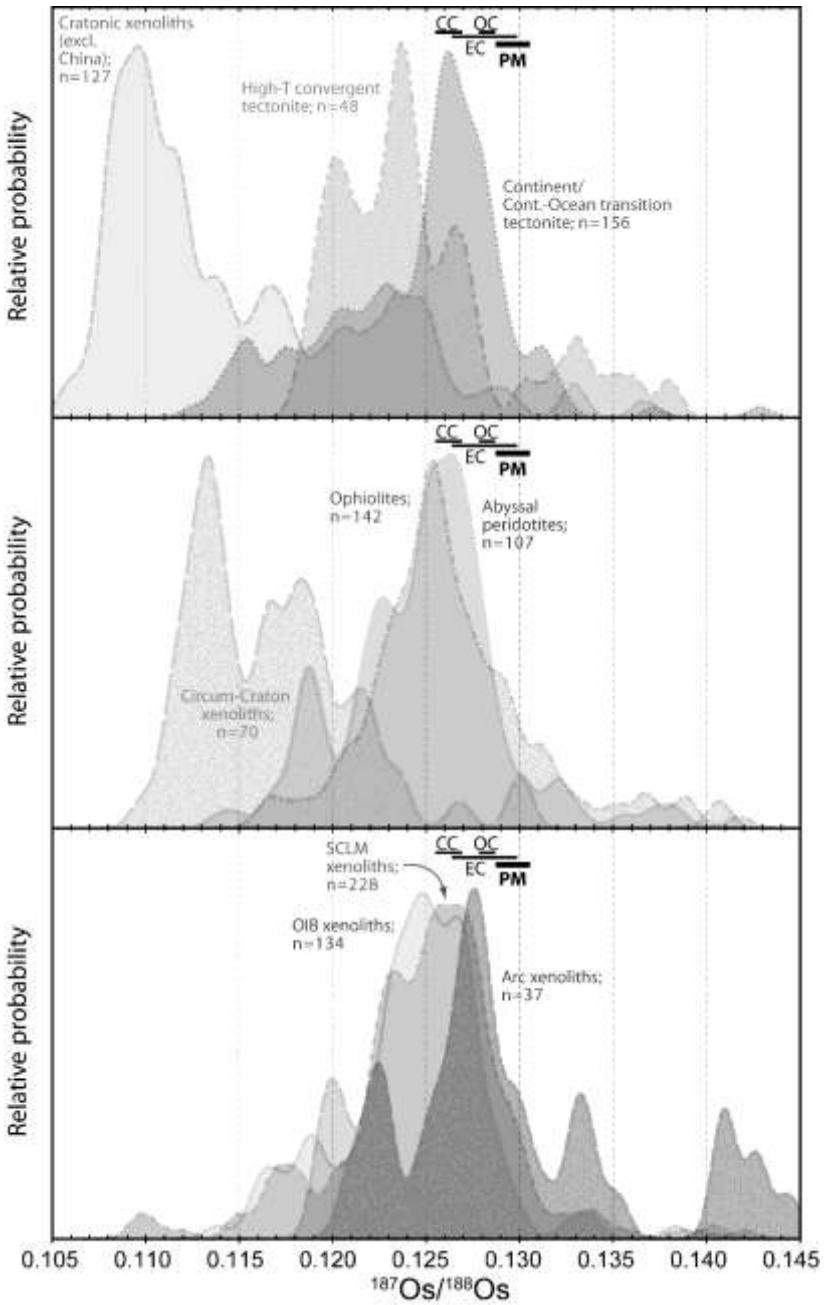

Figure 24. Probability density plots of present-day $^{187}Os/^{188}Os$ ratios in whole-rock samples grouped according to the tectonic settings discussed in this chapter: Ophiolites, abyssal peridotites, continent/continental-ocean transitional tectonite, high temperature convergent tectonite. Xenoliths from the subcontinental lithospheric mantle, oceanic lithosphere, cratonic lithosphere and circum-cratonic lithosphere are also shown (see Aulbach et al. 2015, this volume, and Luguet & Reisberg, 2015, this volume, for a discussion of HSE in these xenolith groups). Ranges for primitive mantle (Meisel et al., 2001) and major chondrite groups also shown; CC – carbonaceous, OC – ordinary, EC – enstatite (Walker et al., 2002a). A universal uncertainty of 0.00125 was applied to each datum to avoid bias towards more precise analyses and to provide sufficient smoothing for the smaller datasets, where used. For data sources see Fig. 14, except cratonic xenoliths: Walker et al. (1989); Pearson et al. (1995a); Pearson et al. (1995b); Shirey and Walker (1995); Chesley et al. (1999); Meisel et al. (2001); Pearson et al. (2004); Becker et al. (2006); Maier et al. (2012), and circum-craton xenoliths: Pearson et al. (2004); Luguet et al. (2009); Aulbach et al. (2014).

All tectonite groups have ranges that extend to sub-chondritic and supra-chondritic $^{187}Os/^{188}Os$ ratios, although some extend broadly equally in each sense, while others have a pronounced skew towards less or more radiogenic values. For instance, the ophiolite record has a modal $^{187}Os/^{188}Os$ of ~0.1255, with a broadly equal number of data extending in each sense down and up to values of 0.115 and 0.143, respectively (Fig. 24). At least half of the data fall between 0.1225 and 0.128. In contrast, the dataset for continental/continent-ocean transitional tectonites shows a modal $^{187}Os/^{188}Os$ of ~0.126, close to that of ophiolite ultramafics, but with a range extending down to 0.112 and up to 0.133, with a lower mean value than for ophiolites (Fig. 24). The abyssal peridotite samples of the convecting mantle show a remarkably similar probability profile to the continental/transitional tectonites, with a modal $^{187}Os/^{188}Os$ of ~0.126, and a range from 0.1125 to 0.140; possibly with similar subsidiary peaks at 0.1225 and perhaps even at 0.115 (although this most unradiogenic peak appears important for continental/transitional tectonites, but likely is not significant for abyssal peridotites, given the sample size).

The 'tails' to low and high $^{187}Os/^{188}Os$ reflect, respectively, ancient melt-depleted domains and enriched domains which have not fully re-homogenised with the rest of the convecting mantle through convecting stirring and potentially melt percolation and infiltration. The distribution of the data is further mentioned below in the context of platinum-group mineral studies. Qualitatively, at least, re-enrichment of ophiolitic mantle is supported by the observation that convergent margin ophiolites appear to have more radiogenic ^{187}Os than mid-ocean ridge ophiolites (Fig. 15), and by the absence of a skew to old depleted values in the overall ophiolite $^{187}Os/^{188}Os$ distribution (Fig. 24; cf. abyssal peridotite and ophiolite curves). The relatively radiogenic distribution of sub-arc xenoliths is also consistent with the process of re-enrichment in the subduction zone environment.

The chromitite and PGM record of Os isotope mantle composition and heterogeneity. Here, we focus only on the Os isotope evidence from PGM, rather than the systematics of PGM formation and composition (see O'Driscoll & Gonzáles-Jiménez 2015, this volume, for a comprehensive review). The utility of chromitites, and the PGM that they typically contain, is that they are Os-rich, Re-poor and tend to be largely robust to subsequent alteration processes caused by metamorphism and/or fluid-rock interaction. The very low Re/Os ratios mean that their $^{187}Os/^{188}Os$ isotope composition is almost 'frozen in' at the point of formation, or at worst require very small corrections for radiogenic ingrowth, even over periods of 3 Ga or greater (Malitch and Merkle, 2004). For these reasons, they have been used to estimate the Os composition of the convecting mantle, to assess mantle heterogeneity and to identify potential major mantle melting events through Earth's history. One caveat to this use, however, is that chromitite formation occurs in zones of high melt flow, and these melts may have imparted a radiogenic $^{187}Os/^{188}Os$ signature on the chromitite, thus rendering it no longer entirely representative of the 'average' upper mantle (e.g., O'Driscoll et al., 2012; see also Convergent Ophiolite section above).

A global suite of ophiolitic chromites was used to provide an estimate of the average $^{187}Os/^{188}Os$ composition of the convecting mantle (Walker et al., 2002b). Linear regression of the isotope data relative to the age of the chromite provided an evolution curve with a present-day $^{187}Os/^{188}Os$ composition of 0.1281. Although the uncertainties overlap, this best estimate equates to approximately 5% less ingrowth of ^{187}Os over the life of the Earth when compared to the PM (0.1296; Meisel et al., 2001). This is presumably due to continental crust extraction and the presence of recycled oceanic crust in the mantle, which has not (yet) been efficiently rehomogenised. A study of over 700 detrital PGM from the Josephine Ophiolite, California, found a Gaussian distribution of $^{187}Os/^{188}Os$ ratios from 0.119 to 0.130 (Meibom et al., 2002). This was interpreted to represent long-term heterogeneity (melt-enriched and -depleted endmembers) which has been partially erased and homogenised by metasomatism and melt-rock reaction processes. Further work on a range of global ophiolites, however, indicated a more

complex distribution of Os isotope ratios in Earth's mantle. Over 1000 detrital PGM from ophiolites in California, Urals, Tibet and Tasmania revealed a variety of $^{187}Os/^{188}Os$ distributions, from close to Gaussian to skewed towards old, unradiogenic values in the case of Urals, and a bimodal distribution for both Tibet and Tasmania (Pearson et al., 2007). It was proposed that the apparent 'peaks' in probability for certain $^{187}Os/^{188}Os$ ratios are consistent across different ophiolites and across other geological settings such as cratonic xenoliths, and that these peaks reflect global signatures produced by major global mantle melting episodes throughout Earth's history which match the implied crustal growth record from zircon ages. The composition of the major peak in $^{187}Os/^{188}Os$ for PGM is 0.1276 (Pearson et al., 2007; adjusted to present-day in Dale et al., 2009b), although the mean composition is likely significantly lower because of the skewed distribution to less radiogenic values. Perhaps notably, when considering representative analyses of convecting mantle composition, this upper limit of $^{187}Os/^{188}Os$ composition from PGM analysis is less radiogenic than the average of analysed chromites (0.1281; Walker et al., 2002b), even though many of the PGM are also sourced from supra-subduction zone ophiolites and therefore may be subject to the same process of radiogenic Os addition. Also of note is the fact that ultramafics from most of the tectonic settings have 'peak' values that are slightly less radiogenic than the 'peak' value from PGM (see Fig. D7; $^{187}Os/^{188}Os$ ~0.1265, compared to 0.1276).

In summary, although global compilations have inherent bias towards exposed and well-studied areas, all the larger datasets (n > 100) for mantle settings that have not been isolated for long periods (cf. cratons), have very similar modal $^{187}Os/^{188}Os$ compositions of between 0.125 and 0.127, and mean compositions between 0.1243 and 0.1271. Such values equate to around 8 to 18% less ingrowth of ^{187}Os over the life of the Earth than for PM evolution (cf. Meisel et al., 2001), presumably largely due to crustal extraction and long-term isolation – although the exact degree of mantle Re depletion is dependent on the timing of this extraction. These values are somewhat higher than the 5% estimated from chromitites (see above, cf. Walker et al. 2002b), but some of this discrepancy is due to the omission of pyroxenites and other enriched lithologies from this data compilation. The small variance in the isotopic ranges for each setting appears noteworthy in terms of gauging mantle mixing efficiency, but is beyond the scope of this review.

$^{186}Os/^{188}Os$ mantle composition and heterogeneity. Platinum-group minerals and chromitites have been used as recorders of the $^{186}Os/^{188}Os$ evolution of the mantle. Many PGM are IPGE-rich and have low Pt/Os and hence faithfully record the $^{186}Os/^{188}Os$ of the mantle at the time when those PGM formed. Brandon et al. (2006) used Os-rich PGM data, together with chondrite analyses, to constrain the terrestrial evolution of $^{186}Os/^{188}Os$ from an initial of ~0.1198269 +/- 0.0000014 (2 sigma) at 4.567 Ga to a present-day value of 0.1198382 +/- 0.0000028.

The potential for large-scale heterogeneity generated by the ^{190}Pt-^{186}Os system is far smaller than that of the ^{187}Re-^{187}Os system, and in most cases is beyond what is distinguishable given current analytical capabilities. Nevertheless, anomalously radiogenic $^{186}Os/^{188}Os$ ratios have been found in some high-degree melts in intraplate settings in Hawaii, Gorgona Island and Kostomuksha, Russia (Brandon et al., 1998; Brandon et al., 2003; Puchtel et al., 2005), coupled with only limited ^{187}Os enrichment. Possible mechanisms to generate such signatures are discussed below.

The range of Pt/Os ratios found in the supra-subduction zone environment indicates that there must be huge ^{186}Os variations on a lithological and mineral scale, if those materials were isolated. Alaskan-Uralian complexes (see Johan, 2002 for details) also display a large range of Pt/Os ratios, but these are beyond the scope of this chapter. Chromitites from ophiolites typically possess very low Pt/Os ratios (~0.1, compared with 1.95 for the PM), but can sometimes have Pt/Os of >10 (see Ophiolite sections). Platinum group minerals from within chromitites and

other PGE-saturated ores can have even more extreme Pt/Os; laurites (Ru (Os, Ir)S_2), may have ratios of <0.01 (González-Jiménez et al., 2009) while PtFe alloys can have Pt/Os of >100,000 (Walker et al., 1997). Extremely high Pt/Os ratios, such as those of the Meratus Ophiolite, Borneo (up to 2000), evolve to much higher $^{186}Os/^{188}Os$ compositions than those of the bulk mantle, and because PGM are largely robust to subsequent processes, they may show isochronous behavior and can be used to date ophiolitic complexes (Coggon et al., 2011). These PGM, after ingrowth over as little as 200 Ma, have $^{186}Os/^{188}Os$ ratios that range from a slightly sub-PM value of 0.119801 to 0.120315. As a guide to the magnitude of this difference, it is at least 30 times greater than the difference between the bulk mantle and the highest $^{186}Os/^{188}Os$ mantle melt yet discovered (0.000015; Brandon et al., 1999). These data will be discussed further in the subsequent section on the production of HSE-Os signatures in mantle melts.

A recent study of Eoarchaean chromitites from south-west Greenland found $^{186}Os/^{188}Os$ data proposed to reflect mantle melt depletion events in Earth's earliest history, during the Hadean at approximately 4.1 Ga and possibly as old as 4.36 Ga (Coggon et al., 2013). In so doing, Coggon et al. (2013) also inferred that the late veneer must have occurred prior to this time, consistent with the message of an 'early' late veneer from studies of basaltic meteorites from different parent bodies (Dale et al., 2012a).

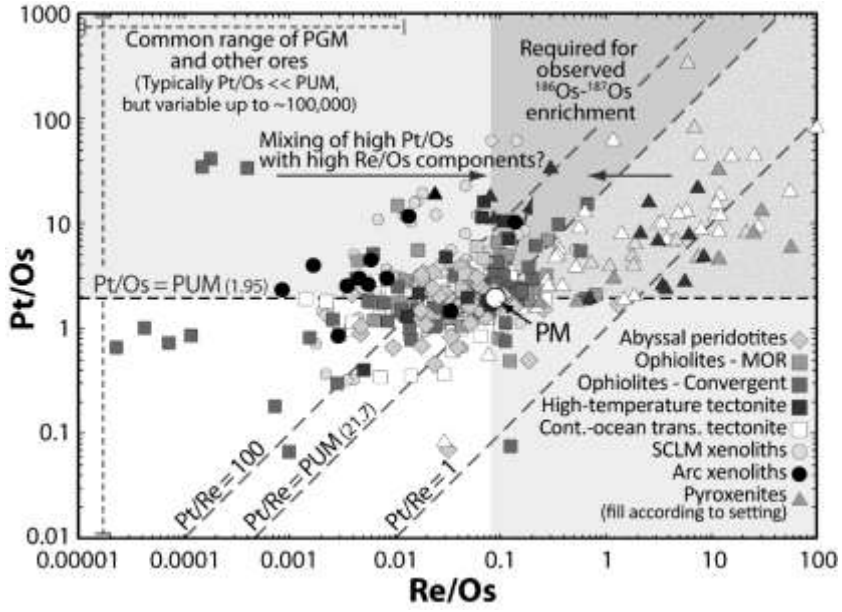

Figure 25. Pt/Os vs. Re/Os for mantle rocks and the implications for the generation of ^{186}Os-^{187}Os enrichments. The dark shaded field denotes the sense of relative fractionation of the Pt-Os and Re-Os systems. The actual required Pt/Os ratio to explain the ^{186}Os enrichment in some intraplate magmas is ~10 or greater, over an ingrowth time of 1.5 Ga. This is obviously dependent on the age and on whether the high Pt/Os component is only part of a composite source (which would require higher Pt/Os ratios or an older age). Rocks possessing the required high Pt/Os, but only mildly elevated Re/Os are only a minor component of the current mantle database. Data sources as in Fig. 14.

The role of recycled oceanic lithosphere in producing HSE and Os isotope signatures in magmas

At least part of the compositional variability observed in mantle melts at Earth's surface is derived from heterogeneity in the mantle. The biggest single process by which such heterogeneous chemistry is generated must be that of recycling of oceanic lithosphere through

subduction (e.g., Hofmann and White, 1982). In addition, there are other processes, such as melt percolation within the mantle and lithosphere (e.g., Halliday et al., 1995) that potentially play an important role in producing the variety of magma compositions that we observe at Earth's surface. Many instances of melt percolation may ultimately be sourced from enriched recycled material, but this is not a requirement in producing variations in fertility in the mantle. Here, we focus on the composition of recycled ultramafic and mafic lithosphere within the mantle, and its impact within the source regions of oceanic magmas.

Oceanic alteration. Prior to subduction, the oceanic lithosphere gains variable amounts of water and trace elements during seawater interaction or hydrothermal alteration, resulting in the formation of serpentine minerals, at the expense of olivine. This alteration can, in more extreme cases, be accompanied by elevated $^{187}Os/^{188}Os$ and the loss of Os relative to the other IPGE (see abyssal peridotite section), but typically, abyssal peridotites retain mantle-like HSE proportions and $^{187}Os/^{188}Os$ ratios. Regardless of the precise HSE signature, serpentinisation permits water transport deep into subduction zones and beyond into the deep mantle. Together with the hydrous mafic crust, this provides fluxes of fluids from the downgoing slab into the mantle wedge at a range of depths, as well as retention of water beyond the supra-subduction setting. The potential for the slab to transport water beyond the zone of sub-arc melting is likely to be important for promoting small-degree hydrous melting in the mantle, which may have an impact on HSE through refertilisation processes.

The impact of subduction zone processes on HSE in convergent margin magmas and recycled oceanic lithosphere. Fluxes into the mantle wedge produce two effects which have a bearing on HSE behavior and Os isotope composition. First, as discussed above, radiogenic Os may, in certain cases (Brandon et al., 1996; Becker et al., 2004), be transferred from the slab into the mantle wedge and then transferred by melts into arc crust and supra-subduction oceanic crust, sampled by ophiolites. Second, fluid addition will promote hydrous melting, allowing otherwise refractory mantle domains to partially melt and permitting melting of the mantle at temperatures below those of the normal geothermal regime.

The evidence for a radiogenic Os flux to arc magma sources is equivocal, due to the difficulty in knowing the precursor $^{187}Os/^{188}Os$ of the mantle source and other potential sources of radiogenic Os such as arc crust. Nevertheless, the ophiolite record provides a firmer basis for this contention. An additional HSE flux is the loss of Re from metabasic rocks during dehydration (~50-60%; Becker, 2000; Dale et al., 2007), and likely enrichment of Re in the mantle wedge (Sun et al., 2003a; Sun et al., 2003b). This flux could contribute, over time, to radiogenic ^{187}Os in the mantle wedge and also has implications for the composition of recycled crust which are outlined below. Other HSE may also be mobilised (McInnes et al., 1999; Kepezhinskas et al., 2002; Dale et al., 2009a), but whether the magnitude of flux is sufficient to produce a measureable effect in supra-subduction zone magmas is doubtful, given the relatively high concentrations of these elements in the mantle.

Melting of refractory domains increases the likelihood of sulfide exhaustion, which, under most circumstances, would reduce the compatibility of all HSE, resulting in less fractionated HSE patterns such as those seen in picrites and komatiites (e.g., Puchtel and Humayun, 2000). In the Tonga Arc, however, the relative proportions of the HSE are amongst the most fractionated for mantle melts (Dale et al., 2012b), with extreme Pt/Os approaching 15. This fractionation may be caused by increased HSE-rich phase stability during lower temperature hydrous melting (e.g., laurite stable up to 1275°C; Brenan and Andrews, 2001) and/or the promotion of chromitite formation by interaction between hydrous melts and refractory mantle (Dale et al., 2012b). Chromitite formation during melt-rock reaction in the mantle is expected to fractionate HSE significantly, sequestering IPGE in PGM and producing a melt with high (Re+Au+PPGE)/IPGE (see ophiolite sections).

The role of recycled lithosphere in producing HSE-Os signatures in convecting mantle melts. Many previous attempts have been made to model the effects of recycling oceanic lithosphere, particularly the mafic crustal portion (e.g., Roy-Barman et al., 1996; Brandon et al., 1999; Becker, 2000; Brandon et al., 2007; Dale et al., 2009b; Day et al., 2009). While we recognize the importance of quantitatively assessing whether a particular process is possible or likely, given the numerous previous attempts and the dependency on the parameters chosen, here we direct the reader to those previous studies and we instead choose to focus on the record of pyroxenites in the mantle, as direct recorders of enriched, hybridized lithologies. Of course, it is important to bear in mind that the sampled pyroxenite database is still relatively small (62 samples with HSE and/or Os isotope data collated in Fig. 25) and thus it is difficult to relate this to the mantle as a whole. That said, the processes identified are broadly applicable.

Both eclogitic and pyroxenitic enriched lithologies are present in the mantle. Eclogites represent unequivocal crustal materials, sampled as xenoliths in intraplate volcanic settings, which retain much of their crustal geochemical signature, albeit modified by subduction processing. The term 'pyroxenite' covers a complex array of lithologies and petrogenetic pathways that are beyond the scope of this chapter (see Lambart et al., 2013). In simple terms, pyroxenites are variably hybridized lithologies produced during reaction of peridotite with silica-saturated melt derived from an enriched lithology such as eclogite (or possibly also derived from small-degree melting of peridotite). Reaction with a silica-undersaturated, olivine-saturated melt would instead produce dunite, so depending on the exact mode of formation of particular dunites (some dunites might be cumulates), they may also carry an enriched Os signature, as seen in the 'convergent margin ophiolite' section. Unlike eclogites, pyroxenites form a significant part of mantle tectonites, constituting between 1 and 9% of the Beni Bousera mantle tectonite massif (Pearson and Nowell, 2004). These pyroxenites at Beni Bousera have been identified as having a recycled crust origin, on the basis of lithophile and stable isotopes. They typically have radiogenic $^{187}Os/^{188}Os$ ratios, even in samples that are Os-rich (>2 ng/g).

Pyroxenites and peridotites from the Totalp ultramafic massif, Swiss Alps, preserve a record of refertilisation of peridotites by both melt percolation from the pyroxenites and from mechanical stretching and thinning of websterite layers (van Acken et al., 2008). The pyroxenites are strongly enriched in ^{187}Os ($^{187}Os/^{188}Os$: 0.122 to 0.866; main range: 0.13-0.16) and in Re, whereas peridotites have a broadly chondritic average γOs value. It is noted, therefore, that refertilisation does not completely homogenise Os isotopes, at least not on a small scale, but isotopic differences are rapidly reduced due to assimilation of pyroxenite melt by peridotite.

A compilation of ultramafic mantle samples, in terms of Pt/Os and Re/Os ratios, is presented in Fig. 25. Pyroxenites form a distinct group at elevated Re/Os and Pt/Os ratio, relative to peridotites. The degree of this enrichment is, in itself, consistent with a partially pyroxenite source for some mantle melts with radiogenic Os over a period of ingrowth of 1 Ga or more. Actual measured $^{187}Os/^{188}Os$ for global pyroxenites, excluding the 10 highest and lowest values from a total of 94 samples, varies from 0.124 to 0.928. Obviously the ability for these pyroxenites to produce sufficiently radiogenic melts as part of a hybrid pyroxenite-peridotite mantle, depends on their Os contents. The Os concentrations also vary substantially, from 0.005 ng/g to 4.6 ng/g, and this generally co-varies negatively with $^{187}Os/^{188}Os$ ratios. Thus, at some level, the effect of the pyroxenite in the mantle is self-limiting due to reduced Os content. As well as the strongly radiogenic signatures of the pyroxenites themselves, there is also evidence for radiogenic Os addition to peridotitic rocks (Becker et al. 2001; Büchl et al. 2002; van Acken et al., 2008; Marchesi et al., 2014), and this, combined with the radiogenic pyroxenites, will more easily produce radiogenic mantle melts.

One aspect of oceanic crust recycling that has commonly been overlooked is the geochemical distinction between the gabbroic and basaltic parts of the crust. This is now generally fully recognized for HSE – with gabbroic crust being, on average, significantly more Os- and Pt-rich and slightly poorer in Re than MORB – and this has been incorporated into models for crustal recycling (Peucker-Ehrenbrink and Jahn, 2001; Dale et al., 2007; Peucker-Ehrenbrink et al., 2012)

An alternative, but related, means by which recycled lithosphere may have an impact on the HSE composition of mantle melts is through the process of sulfide metasomatism. Sulfides with radiogenic ^{187}Os have been sampled in interstitial locations within peridotites (Alard et al., 2005; Harvey et al., 2006, 2010, 2011; Warren and Shirey, 2012). The ultimate source of those sulfides is unknown, but derivation from recycled crustal material, of at least some such sulfides, is plausible. Radiogenic, interstitial sulfides can then be readily incorporated into partial melts, whereas unradiogenic residual sulfides remain shielded from melt by the silicates that enclose them. The process of sulfide addition is a similar process to other forms of refertilisation, but in this case the lithophile and chalcophile element signatures may be decoupled. However, the overall broad coupling of $^{187}Os/^{188}Os$ with Al_2O_3 contents may suggest that this process is typically not large-scale and pervasive (cf. Fig. 2).

^{186}Os-^{187}Os coupled enrichments. Over time, Pt/Os ratios greater than that of the primitive mantle (PM) will develop elevated $^{186}Os/^{188}Os$ ratios. A Pt/Os ratio of approximately greater than 8 is required, over a 1.5 Ga period, to produce the most ^{186}Os-enriched mantle melt identified to date (cf. Pt/Os PM: 1.95; Becker et al., 2006). Of the current mantle database for peridotites, dunites, and some chromitites, approximately 11% have Pt/Os ratios greater than 4, while only 4% have ratios greater than 8 (Fig. 25). Enriched pyroxenite lithologies, however, commonly have sufficiently high Pt/Os ratios; ~55% of the 62 pyroxenites compiled in Fig. 25 have Pt/Os >8. However, many rocks with elevated Pt/Os also possess elevated Re/Os which evolves to much higher $^{187}Os/^{188}Os$ ratios than observed in intraplate magmas with enriched ^{186}Os. Therefore, rocks with Pt/Os, Re/Os and Pt/Re all greater than the PM are of particular interest for the generation of coupled enrichments of ^{186}Os and ^{187}Os, but such rocks are a very minor proportion of the current mantle database (Fig. 25).

This difficulty in generating radiogenic ^{186}Os, without also producing enrichments in ^{187}Os beyond those observed, led Brandon et al. (1998), after Walker (1995), to propose a role for transfer of an outer core Os signature into the plume source of some high-degree melts in intraplate settings. Twenty years later, this remains a possible scenario, despite the alternative mechanisms proposed that are outlined here. The core-mantle interaction model does, however, require an early onset of inner core solidification (by 2.5 Ga, and earlier for 2.8 Ga Kostomuksha komatiites; Puchtel et al., 2005) in order to allow sufficient time for ingrowth to produce enrichments in ^{186}Os and ^{187}Os in the predicted high (Pt-Re)/Os outer core. A more complete discussion of the core-mantle interaction debate can be found in Brandon & Walker (2005) and Lassiter (2006).

Since the emergence of the core-mantle interaction theory, several other possible sources of radiogenic ^{186}Os have been proposed (e.g., Baker and Jensen, 2004; Luguet et al., 2008), though no proposed mechanism is completely convincing. The modification of pyroxenites, refertilisation of peridotites and accompanying sulfide removal and/or metasomatism is the most likely alternative to core-mantle interaction (Luguet et al., 2008; Marchesi et al., 2014), but suitable Pt/Os and Re/Os ratios in the current mantle database are the exception, rather than the rule (Fig. 25). One further, more complex, possibility is that signatures may be combined from separate mantle components each with either high Pt/Os or high Re/Os, but not both. As outlined in a previous section, extreme Pt/Os fractionation exists on a variety of scales in Earth's mantle, particularly during the formation of PGM. What is not yet clear is the fate of such PGM during

mantle convection and whether there is sufficient separation and sampling of particular PGM compositions to produce specific signatures in mantle melts.

In summary, processes exist in Earth's mantle that can account for the ^{186}Os-^{187}Os enrichments observed in intraplate magmas, but currently they appear to be rare.

The relationship between abyssal peridotites and MORB: an osmium isotope perspective

One major debate in the field of HSE chemistry, and a key issue for mantle geology as a whole, is the extent to which abyssal peridotites represent the mantle residues of partial melting at oceanic spreading centres. Osmium isotopes have been a key part of this debate, but the evidence is complex. Early analyses identified a large range of $^{187}Os/^{188}Os$ compositions in abyssal peridotites, ranging from sub-chondritic to significantly supra-chondritic (see Abyssal Peridotite section above). The elevated signatures were largely attributed to seawater interaction. After taking into account this process, the remaining abyssal peridotite data appeared to be far less radiogenic than data for mid-ocean ridge basalts, thus casting doubt on a genetic link between abyssal peridotites and MORB. Since that time, two important findings have been made which reduce this discrepancy.

Firstly, was the discovery of interstitial sulfides of magmatic origin possessing radiogenic, supra-chondritic $^{187}Os/^{188}Os$ ratios (Alard et al., 2005), together with non-chondritic PGE ratios (Alard et al., 2000). A preferential contribution from these interstitial sulfides to a partial melt, compared with the contribution from ancient, unradiogenic sulfides enclosed within silicates, could account for the more radiogenic signatures of MORB and other partial melts of the oceanic mantle, compared with those recorded in bulk-rock abyssal peridotites.

Secondly, but of at least equal importance, was the finding that the Os isotope compositions of MORB (see Gannoun et al., 2015, this volume) were less radiogenic than previous thought. In particular, the range of $^{187}Os/^{188}Os$ ratios in MORB glasses was found to be considerably less (0.126-0.148) than previous findings (e.g., Schiano et al., 1997), with a lower mean of 0.133 +/- 0.009, in part due to an analytical artefact in the original data (Gannoun et al., 2007). This mean value, while reduced, remains in excess of typical values for abyssal peridotites ($^{187}Os/^{188}Os$: 0.118-0.130). However, it was also found that the constituent phases of basalts had variable $^{187}Os/^{188}Os$ due to (i) ingrowth over poorly-constrained periods of time since emplacement (Gannoun et al., 2004), and (ii) the timing of crystallization of different phases with respect to the evolution of the melt and its interaction with seawater-modified crust (Gannoun et al., 2007). Most notably, the latter manifests itself in significantly less radiogenic Os isotope compositions in early-formed relatively Os-rich sulfides compared with their (Os-poor) host glasses. In some cases there is a difference of ~0.015 in the $^{187}Os/^{188}Os$ of glasses and corresponding sulfides (e.g., glasses: 0.1383 and 0.1479; sulfides: 0.1249 and 0.1308, respectively), with the sulfides falling in the range 0.1236 to 0.1310, largely equivalent to the range seen in abyssal peridotites. Moreover, a negative covariation of $^{187}Os/^{188}Os$ and Os content in MORB sulfides might indicate that sulfides are also affected by interaction with a radiogenic contaminant, casting doubt on the more radiogenic data for Os-poor sulfides.

Although sulfides included within silicates in abyssal peridotites (and other mantle tectonites) are known to possess even lower $^{187}Os/^{188}Os$ than bulk-rock samples (~0.114; Harvey et al., 2006) – and are therefore also lower than estimates of primitive MORB – such shielded sulfides likely contribute little to moderate degree partial melts relevant for MORB genesis. Therefore, in conclusion, not only has the 'gap' in composition between abyssal peridotites and MORB been largely bridged by radiogenic interstitial sulfides, but it seems likely that the gap is minor or non-existent when the most primitive parts of the MORB system are analysed.

Reinterpretation of Re-Os model ages

Model ages, whereby the isotope ratio of a sample is compared to the evolution of a reference frame such as average chondrite compositions, have been extensively used in geochemistry to give melt depletion ages in systems where recent mobility of elements has obscured any isochronous isotope systematics. The Re-Os system has been of particular use in this regard, due to the contrasting behavior of Re and Os which can result in, for high degree melts, effective Re removal from the source, while Os remains present in high enough abundances (several ng/g) to provide a degree of robustness against alteration and contamination. For Os, the measured $^{187}Os/^{188}Os$ ratio of a sample (or, for xenoliths, the ratio calculated at the time of the host eruption) is compared to the evolution curve of the mantle (commonly either a chondrite reference or the primitive mantle estimate). For Re depletion ages (T_{RD}) it is assumed that the residue is completely depleted in Re after partial melting and, thus, there is no further ingrowth of ^{187}Os. The advantage of this method is that it provides a relatively robust guide to the long-term evolution of the sample, due to the generally conservative behavior of Os, without the difficulties induced by recent Re addition or loss. In reality, however, only in high degree melting events is complete Re removal attained and in many cases the T_{RD} age merely provides a minimum age. An alternative type of model age uses the measured Re/Os ratio to calculate the time when the $^{187}Os/^{188}Os$ of the sample intersected that of the reference frame (T_{MA} or $T_{Re\text{-}Os}$). In theory, this can provide a more accurate age, but it suffers the same sensitivity to Re mobility as do attempts to identify Re-Os isochron relationships.

Numerous caveats and potential pitfalls of model age determinations have now been recognized and the reliability and interpretation of Re-Os model ages in peridotites was the subject of a comprehensive review by Rudnick and Walker (2009). Here, we summarise the main issues surrounding such model ages, in the context of the processes and tectonic settings discussed in this chapter.

Perhaps the most obvious issue encountered has already been mentioned above – that of the degree of depletion of Re. Rudnick and Walker (2009) demonstrate that mantle melting at 3.5 Ga to form a basaltic melt would result in vastly different age estimates from T_{MA} and T_{RD} methods: the T_{MA} age for the residue would be 3.5 Ga, because the Re/Os ratio of the residue is used to back-calculate the isotope evolution of the sample, whereas the assumption of complete Re depletion in the case of a T_{RD} age would produce an age of just over 1 Ga. Clearly at this level of depletion T_{RD} ages are not useful and they only become more valuable when Re removal is close to complete (probably a boninitic or komatiitic melt depletion event).

Alternatives to isochron ages and Re depletion ages have been used to gain age information for sample suites where, respectively, Re mobility is suspected or Re removal was not complete. An element of similar compatibility to Re, but less mobile, such as Al_2O_3, can be used as a proxy for Re on an isochron diagram (Reisberg and Lorand, 1995; see earlier). Although there is sometimes much scatter on such plots, they appear to be broadly robust. For large datasets of >50 samples, but preferably more, probability density function plots provide a means to identify common apparent depletion ages, which lends weight to an argument for those ages having age significance. For instance, a range of $^{187}Os/^{188}Os$ ratios could be produced by variable degrees of depletion or by the same degree of depletion at different times. The identification of peaks on probability plots might indicate discrete times of melt depletion (perhaps partially obscured by variable depletion, preservation issues and/or inheritance) rather than a more continuous spectrum of compositions which might be expected from a suite of variably depleted samples.

There is significant inherent uncertainty with any T_{RD} age, because they are based on a model evolution curve. There are two aspects to this issue: (i) it is known that Earth's mantle has broadly chondritic proportions of the HSE, but it is not known which chondrite group – if indeed

any in the global collection – supplied Earth's HSE or whether there was any fractionation of HSE during core formation. Models to account for the apparently supra-chondritic Ru/Ir and Pd/Ir ratios of the PM (Becker et al., 2006; Walker, 2009; Fischer-Gödde et al., 2011) may also have implications for the Re-Os isotope evolution of the PM. The choice of type of chondrite or PM estimate to use for the model evolution can result in an age variation of nearly 200 Ma for a $^{187}Os/^{188}Os$ of ~0.124, decreasing with increased age to an uncertainty of ~100 Ma at around 2 Ga ($^{187}Os/^{188}Os$ = 0.114). (ii) As with lithophile isotope systems (e.g., Sm-Nd) a choice has to be made whether to use a primitive or depleted mantle reference frame. This can make an even more significant difference to the age given that the estimated $^{187}Os/^{188}Os$ of the primitive mantle is 0.1296, whereas an 'average' depleted mantle composition might be somewhere between 0.1245 and 0.128, depending on whether the average for abyssal peridotites or a combination of chromitites, PGM and high-degree mantle melts is used (Walker et al., 2002b; Pearson et al., 2007; Dale et al., 2009b). This also illustrates the problem of inheritance, which relates to the large degree of Os isotope heterogeneity observed in the convecting mantle and is amongst the most important considerations. This effectively means that for small datasets without additional information there is little way of knowing whether an apparent old age reflects a significant ancient melt depletion event in the context of its tectonic setting, or whether the measured $^{187}Os/^{188}Os$ is a composite of that event superimposed on an already depleted (or enriched) Os signature. For this reason, larger datasets obviously produce more robust age estimates and plots displaying probability can be used to identify 'significant' common ages or 'peaks' (Pearson et al., 2007; Rudge, 2008).

So far, we have made no mention of potential petrological pitfalls for model ages. These encompass serpentinisation, sulfide breakdown, refertilisation and melt-rock reaction (Rudnick and Walker, 2009). Serpentinisation, as discussed in an earlier section, does not typically affect Os isotope systematics except in extreme cases, which can easily be avoided when selecting samples with which to gain age information. Sulfide breakdown is known to occur in mantle xenoliths, due to interaction with the host melt. This commonly results in Os loss which could potentially impact upon the model age if $^{187}Os/^{188}Os$ is variable between different host phases, and which also leaves the sample more susceptible to contamination and alteration.

Depending on the tectonic setting, some processes may or may not impact on model ages. For instance, melt-rock reaction in the convecting mantle is commonly associated with melting, and is therefore effectively zero age with respect to melting and won't normally affect the model age recorded for that melting event. Such melt-rock reaction also usually produces discordant samples on an $^{187}Os/^{188}Os$-Al_2O_3 diagram, and can thus be identified and avoided for the purposes of dating. Conversely, processes of melt percolation and reaction in the continental lithosphere may occur long after the melt depletion episode of interest and this has the potential to obscure the true age (Rudnick and Walker, 2009). These issues mean that samples with the lowest $^{187}Os/^{188}Os$ give the most reliable ages, but they too may still have experienced radiogenic Os input. The extent to which this process affects ages depends on the amount of addition of sulfide, and the Os isotope composition and concentrations of those sulfides. Such sulfides are typically poorer in Os than enclosed sulfides so significant additions of sulfide may be required to significantly affect the age.

Although the processes of metasomatism and refertilisation can have a significant effect on model ages, sometimes leading to recent T_{RD} ages or "future" T_{MA} ages, in some cases these processes can be traced using HSE behavior. For example, it has been recognized, in the cratonic setting, that the oldest T_{RD} ages for a suite of samples are associated with the lowest Pd/Ir ratios, reflecting the most pristine and severe melt depletion signatures (Pearson et al. 2004). Recently, the Se/Te ratio has also been combined with Pd/Ir, in order to further understand the effects of metasomatic sulfide addition on model ages and place limits on the levels of addition that can occur before the model age may no longer be reliable (Luguet et al., 2015).

In summary, there are numerous potential pitfalls and limitations for Re-Os model age determinations but, in the absence of isochron dating, the system remains amongst the most useful for providing the ages of melt depletion of the mantle.

ACKNOWLEDGMENTS

We thank Chris Ballhaus, Al Brandon, James Brenan, Kevin Burton, Rick Carlson, James Day, Mario Fischer-Gödde, Mouhcine Gannoun, Timo Gawronski, Jason Harvey, Akira Ishikawa, Yogita Kadlag, John Lassiter, Ambre Luguet, Jean-Pierre Lorand, Claudio Marchesi, Graham Pearson, Igor Puchtel, Dave Rubie, Steve Shirey, David van Acken, Richard Walker and Zaicong Wang for valuable insight and discussions over the years. Thanks to Jason Harvey, Chuan-Zhou Liu, Wendy Nelson and Jessica Warren for helpful reviews of the manuscript.

REFERENCES

Ackerman L, Pitcher L, Strnad L, Puchtel IS, Jelínek E, Walker RJ, Rohovec J (2013) Highly siderophile element geochemistry of peridotites and pyroxenites from Horní Bory, Bohemian Massif: Implications for HSE behavior in subduction-related upper mantle. Geochim Cosmochim Acta 100: 158-175.

Agranier A, Lee C-T, Li Z-XA, Leeman WP (2007) Fluid-mobile element budgets in serpentinized oceanic lithospheric mantle: Insights from B, As, Li, Pb, PGEs and Os isotopes in the Feather River Ophiolite, California. Chem Geol 245: 230-241.

Ahmed AH, Hanghøj K., Kelemen PB, Hart SR, Arai S (2006) Osmium isotope systematics of the Proterozoic and Phanerozoic ophiolitic chromitites: In situ ion probe analysis of primary Os-rich PGM. Earth Planet Sci Lett 245: 777-791.

Alard O, Griffin WL, Lorand JP, Jackson SE, O'Reilly SJ (2000) Non-chondritic distribution of the highly siderophile elements in mantle sulfides. Nature 407: 891-894.

Alard O, Griffin WL, Pearson NJ, Lorand J-P, O'Reilly SY (2002) New insights into the Re-Os systematics of sub-continental lithospheric mantle from in situ analysis of sulfides. Earth Planet Sci Lett 203: 651-663.

Alard O, Luguet A, Pearson NJ, Griffin WL, Lorand J-P, Gannoun A, Burton KW, O'Reilly SY (2005) In situ Os isotopes in abyssal peridotites bridge the isotopic gap between MORBs and their source mantle. Nature 436: 1005-1008.

Aldanmaz E, Meisel T, Celik OF, Henjes-Kunst F (2012) Osmium isotope systematics and highly siderophile element fractionation in spinel-peridotites from the Tethyan ophiolites in SW Turkey: Implications for multi-stage evolution of oceanic upper mantle. Chem Geol 294: 152-164.

Anbar AD, Creaser RA, Papanastassiou DA, Wasserburg GJ (1992) Rhenium in seawater: Confirmation of generally conservative behavior. Geochim Cosmochim Acta 56: 4099-4103.

Anders E ,Grevesse N (1989) Abundances of the elements: Meteoritic and solar. Geochim Cosmochim Acta 53: 197-214.

Aulbach S, Luchs T, Brey GP (2014) Distribution and behaviour during metasomatism of PGE-Re and Os isotopes in off-craton mantle xenoliths from Namibia. Lithos 184: 478-490.

Aulbach S, Mungall JE, Pearson DG (2015) Distribution and processing of highly siderophile elements in cratonic mantle lithosphere. Rev Mineral Geochem 81: xxx-xxx.

Bach W, Garrido CJ, Paulick H, Harvey, J, Rosner M (2004) Seawater-peridotite interactions: First insights from ODP Leg 209, MAR 15'N. Geochem Geophys Geosys 5 (9) Q09F26, doi:10.1029/2004GC000744.

Baker JA, Jensen KK. (2004) Coupled Os-186-Os-187 enrichments in the Earth's mantle - core-mantle interaction or recycling of ferromanganese crusts and nodules? Earth Planet Sci Lett 220: 277-286.

Ballhaus C (1998) Origin of podiform chromite deposits by magma mingling. Earth Planet Sci Lett 156: 185-193.

Ballhaus C, Bockrath C, Wohlgemuth-Ueberwasser C, Laurenz V, Berndt J (2006) Fractionation of the noble metals by physical processes. Contrib Mineral Petrol 152: 667-684.

Barnes S, Naldrett A, Gorton M (1985) The origin and fractionation of platinum-group elements in terrestrial magmas. Chem Geol 53: 303-323.

Barnicoat AC, Fry N (1986) High-pressure metamorphism of the Zermatt-Saas ophiolite zone, Switzerland. J Geol Soc 143: 607-618.
Becker H (1996a) Crustal trace element and isotope signatures in garnet pyroxenites and megacrysts from garnet peridotite massifs from Lower Austria. J Petrol 37: 785-810.
Becker H (1996b) Geochemistry of garnet peridotite massifs from lower Austria and the composition of deep lithosphere beneath a Paleozoic convergent plate margin. Chem Geol 134: 49-65.
Becker H (1997) Petrological constraints on the cooling history of high-temperarure garnet peridotite massifs in lower Austria. Contrib Mineral Petrol 128: 272-286.
Becker H (2000) Re-Os fractionation in eclogites and blueschists and the implications for recycling of oceanic crust into the mantle. Earth Planet Sci Lett 177: 287-300.
Becker H, Shirey SB, Carlson RW (2001) Effects of melt percolation on the Re-Os systematics from a Paleozoic convergent plate margin. Earth Planet Sci Lett 188: 107-121.
Becker H, Carlson RW, Shirey SB (2004) Slab-derived osmium and isotopic disequilibrium in garnet pyroxenites from a Paleozoic convergent plate margin (lower Austria). Chem Geol 208: 141-156.
Becker H, Horan MF, Walker RJ, Lorand JP, Gao S, Rudnick RL (2006) Highly siderophile element composition of the Earth's primitive upper mantle: Constraints from new data on peridotite massifs and xenoliths. Geochim Cosmochim Acta 70: 4528-4550.
Bezos A, Lorand J-P, Humler E, Gros M (2005) Platinum-group element systematics in Mid-Ocean Ridge basaltic glasses from the Pacific, Atlantic, and Indian Oceans. Geochim Cosmochim Acta 69: 2613-2627.
Bizimis M, Griselin M, Lassiter JC, Salters VJM, Sen G (2007) Ancient recycled mantle lithosphere in the Hawaiian plume: Osmium-Hafnium isotopic evidence from peridotite mantle xenoliths. Earth Planet Sci Lett 257: 259-273.
Blichert-Toft J, Albarede F, Kornprobst J (1999) Lu-Hf Isotope Systematics of Garnet Pyroxenites from Beni Bousera, Morocco: implications for Basalt Origin. Science 283: 1303-1306.
Bockrath C, Ballhaus C, Holzheid A (2004) Fractionation of the Platinum-Group Elements During Mantle Melting. Science 305: 1951-1953.
Bodinier JL, Guirard M, Fabries J, Dostal J, Dupuy C (1987) Petrogenesis of layered pyroxenites from the Lherz, Freychinede and Padres ultramafic bodies (Arieges, French Pyrenees). Geochim Cosmochim Acta 51: 279-290.
Bodinier J-L, Dupuy C ,Dostal J (1988) Geochemistry and petrogenesis of eastern Pyrenean peridotites. Geochim. Cosmochim. Acta, 52: 2893-2907.
Bodinier J-L, Godard M (2003) Orogenic, Ophiolitic and Abyssal Peridotites. *In*: Treatise on Geochemistry. Holland HD, Turekian KK (Eds.), Elsevier, Amsterdam.
Bodinier J-L, Garrido CJ, Chanefo I, Bruguier O, Gervilla F (2008) Origin of Pyroxenite–Peridotite Veined Mantle by Refertilization Reactions: Evidence from the Ronda Peridotite (Southern Spain). J Petrol 49: 999-1025.
Bonatti E, Ottonello G, Hamlyn PR (1986) Peridotites from the island of Zabargad (St. John), Red Sea: Petrology and goechemistry. J Geophys Res 91: 599-631.
Boudier F, Godard M, Armbruster C (2000) Significance of gabbronorite occurrence in the crustal section of the Semail ophiolite. Marine Geophys Res 21: 307-326.
Borisov A, Walker RJ (2000) Os solubility in silicate melts: New efforts and results. Am Mineral 85: 912-917.
Brandon AD, Creaser RA, Shirey SB, Carlson RW (1996) Osmium recycling in subduction zones. Science 272: 861-864.
Brandon AD, Walker RJ, Morgan JW, Norman MD, Prichard HD (1998) Coupled 186Os-187Os Evidence for Core-Mantle Interaction. Science 280: 1570-1573.
Brandon AD, Norman MD, Walker RJ, Morgan JW (1999) ^{186}Os-^{187}Os Systematics of Hawaiian Picrites. Earth Planet Sci Lett 172: 25-42.
Brandon AD, Snow JE, Walker RJ, Morgan JW (2000) ^{190}Pt-^{186}Os and ^{187}Re-^{187}Os Systematics of Abyssal Peridotites. Earth Planet Sci Lett 177: 319-335.
Brandon AD, Humayun M, Puchtel IS, Leya I, Zolensky M (2005a) Osmium Isotope Evidence for an s-Process Carrier in Primitive Chondrites. Science 309: 1233-1236.
Brandon AD, Humayun M, Puchtel IS, Zolensky ME (2005b) Re-Os isotopic systematics and platinum group element composition of the Tagish Lake carbonaceous chondrite. Geochim Cosmochim Acta 69: 1619-1631.
Brandon AD, Walker RJ (2005) The debate over core-mantle interaction. Earth Planet Sci Lett 232: 211-225.

Brandon AD, Walker RJ, Puchtel IS (2006) Platinum and osmium isotope evolution of the Earth's mantle: Constraints from chondrites and Os-rich alloys. Geochim Cosmochim Acta 70: 2093-2103.
Brandon AD, Graham DW, Waight T, Gautason B (2007) ^{186}Os and ^{187}Os enrichments and high-$^{3}He/^{4}He$ sources in the Earth's mantle: Evidence from Icelandic picrites. Geochim Cosmochim Acta 71: 4570-4591.
Brenan JM, Andrews D (2001) High-temperature stability of laurite and Ru-Os-Ir alloy and their role in PGE fractionation in mafic magmas. Can Mineral 39, 341-360.
Brenan JM (2002) Re–Os fractionation in magmatic sulfide melt by monosulfide solid solution. Earth Planet Sci Lett 199: 257-268.
Brenan JM, McDonough WF, Ash R (2005) An experimental study of the solubility and partitioning of iridium, osmium and gold between olivine and silicate melt. Earth Planet Sci Lett 237: 855-872.
Brenan JM (2008) Re-Os fractionation by sulfide melt-silicate melt partitioning: A new spin. Chem Geol 248: 140-165.
Brenan JM, Bennett N, Zajacz Z (2015) Fractionation of the highly siderophile elements (HSE) during planetary differentiation: An overview of results from experiments done at high pressure and temperature. Rev Mineral Geochem 81: xxx-xxx.
Brueckner HK, Zindler A, Seyler M, Bonatti E (1988) Zabargad and the isotopic evolution of the sub-Red Sea mantle and crust. Tectonophysics 150: 163-176.
Brueckner HK, Carswell DA, Griffin WL, Medaris Jr LG, Van Roermund HLM, Cuthbert SJ (2010) The mantle and crustal evolution of two garnet peridotite suites from the Western Gneiss Region, Norwegian Caledonides: An isotopic investigation. Lithos 117: 1-19.
Brügmann GE, Arndt NT, Hofmann AW, Tobschall HJ (1987) Noble metal abundances in komatiite suites from Alexo, Ontario, and Gorgona Island, Columbia. Geochim Cosmochim Acta 51: 2159-2169.
Büchl A, Brügmann G, Batanova VG, Münker C ,Hofmann AW (2002) Melt percolation monitored by Os isotopes and HSE abundances: a case study from the mantle section of the Troodos Ophiolite. Earth Planet Sci Lett 204: 385-402.
Büchl A, Brügmann GE, Batanova VG, Hofmann AW (2004) Os mobilization during melt percolation: The evolution of Os isotope heterogeneities in the mantle sequence of the Troodos ophiolite, Cyprus. Geochim Cosmochim Acta 68: 3397-3408.
Burnham OM, Rogers NW, Pearson DG, van Calsteren PW, Hawkesworth CJ (1998) The petrogenesis of the eastern Pyrenean peridotites: an integrated study of their whole-rock geochemistry and Re-Os isotope composition. Geochim Cosmochim Acta 62: 2293-2310.
Burton KW, Schiano P, Birck J-L, Allègre CJ (1999) Osmium isotope disequilibrium between mantle minerals in a spinel-lherzolite. Earth Planet Sci Lett 172: 311-322.
Carmichael ISE (1991) The Redox States of Basic and Silicic Magmas - A Reflection of their Source Regions. Contrib Mineral Petrol 106: 129-141.
Carswell DA, Jamtveit B (1990) Variscan Sm-Nd ages for the high-pressure metamorphism in the Moldanubian zone of the Bohemian massif, Lower Austria. Neues Jahrbuch Mineralogie Abhandlungen 162: 69-78.
Chatterjee R, Lassiter JC (2015) High precision Os isotopic measurement using N-TIMS: Quantification of various sources of error in 186Os/188Os measurements. Chem Geol 396: 112-123.
Chesley JT, Rudnick RL, Lee C-T (1999) Re-Os systematics of mantle xenoliths from the East African Rift: Age, structure, and history of the Tanzanian craton. Geochim Cosmochim Acta 63: 1203-1217.
Chou C.-L (1978) Fractionation of siderophile elements in the Earth's upper mantle. Lunar Planet Sci Conf pp. 219-230.
Class C, Goldstein SL, Shirey SB (2009) Osmium isotopes in Grande Comore lavas: A new extreme among a spectrum of EM-type mantle endmembers. Earth Planet Sci Lett 284: 219-227.
Coggon, J.A., Luguet, A., Nowell, G.M., Appel, P.W.U., 2013. Hadean mantle melting recorded by southwest Greenland chromitite Os-186 signatures. Nat Geosci 6: 871-874.
Coggon JA, Nowell GM, Pearson DG, Parman SW (2011) Application of the (190)Pt-(186)Os isotope system to dating paltinum mineralization and ophiolite formation: an example from the Meratus mountains, Borneo. Econ Geol 106: 93-117.
Dale CW, Burton KW, Greenwood RC, Gannoun A, Wade J, Wood BJ, Pearson DG (2012a) Late Accretion on the Earliest Planetesimals Revealed by the Highly Siderophile Elements. Science 336: 72-75.
Dale CW, Burton KW, Pearson DG, Gannoun A, Alard O, Argles TW, Parkinson IJ (2009a) Highly siderophile element behaviour accompanying subduction of oceanic crust: Whole rock and mineral-scale insights from a high-pressure terrain. Geochim Cosmochim Acta 73: 1394-1416.

Dale CW, Gannoun A, Burton KW, Argles TW, Parkinson IJ (2007) Rhenium–osmium isotope and elemental behaviour during subduction of oceanic crust and the implications for mantle recycling. Earth Planet Sci Lett 253: 211-225.
Dale CW, Macpherson CG, Pearson DG, Hammond SJ, Arculus RJ (2012b) Inter-element fractionation of highly siderophile elements in the Tonga Arc due to flux melting of a depleted source. Geochim Cosmochim Acta 89: 202-225.
Dale CW, Pearson DG, Starkey NA, Stuart FM, Ellam RM, Larsen LM, Fitton JG, Macpherson CG (2009b) Osmium isotopes in Baffin Island and West Greenland picrites: Implications for the Os-187/Os-188 composition of the convecting mantle and the nature of high He-3/He-4 mantle. Earth Planet Sci Lett 278: 267-277.
Day JMD, Pearson DG, Macpherson CG, Lowry D, Carracedo JC (2009) Pyroxenite-rich mantle formed by recycled oceanic lithosphere: Oxygen-osmium isotope evidence from Canary Island lavas. Geology 37: 555-558.
Day JMD, Brandon AD, Walker RJ (2015) Highly siderophile elements in Earth, Mars, the Moon and asteroids. Rev Mineral Geochem 81: xxx-xxx.
Dick, HJB, Natland JH, Alt JC, Bach W, Bideau D, Gee JS, Haggas S, Hertogen JGH, Hirth G, Holm PM Ildefonse B, Iturrino GJ, John BE, Kelley DS, Kikawa E, Kingdon A, LeRoux PJ, Maeda J, Meyer, PS, Miller DJ, Naslund HR, Niu YL, Robinson PT, Snow J, Stephen RA, Trimby PW, Worm HU, Yoshinobu A (2000) A long in situ section of the lower ocean crust: results of ODP Leg 176 drilling at the southwest Indian Ridge. Earth Planet Sci Lett 179: 31-51.
Dick HJB, Natland JH, Ildefonse B. (2006), Past and future impacts of deep drilling in the oceanic crust and mantle, Oceanography 19: 72-80.
Dijkstra AH, Sergeev DS, Spandler C, Pettke T, Meisel T, Cawood PA (2010) Highly Refractory Peridotites on Macquarie Island and the Case for Anciently Depleted Domains in the Earth's Mantle. J Petrol 51: 469-493.
Dilek Y, Moores E, Elthon D, Nicolas A (eds.) (2000). Ophiolites and Oceanic Crust: New Insights from Field Studies and the Ocean Drilling Program. Special Paper, 349. Geological Society of America, Boulder.
Dilek Y, Furnes H (eds.) (2013). Ophiolites. Elements 10.
Edwards SJ, Malpas J (1996) Melt-peridotite interactions in shallow mantle at the East Pacific Rise; evidence from ODP Site 895 (Hess Deep). Mineral Mag 60: 191-206.
Ernst WG (1978) Petrochemical Study of Lherzolitic Rocks from the Western Alps. J Petrol 19: 341-392.
Ertel W, Walter MJ, Drake MJ, Sylvester PJ (2006). Experimental study of platinum solubility in silicate melt to 14 GPa and 2273 K: Implications for accretion and core formation in Earth. Geochim Cosmochim Acta 70: 2591-2602.
Evans BW, Hattori K, Baronnet A (2013) Serpentinite: What, Why, Where. Elements 9: 99-106.
Finnigan CS, Brenan J, Mungall JE, McDonough WF (2008) Experiments and models bearing on the role of chromite as a collector of platinum group minerals by local reduction. J Petrol 49: 1647-1665.
Fiorentini ML, Barnes SJ, Maier WD, Burnham OM, Heggie G (2011) Global Variability in the Platinum-group Element Contents of Komatiites. J Petrol 52: 83-112.
Fischer-Gödde M, Becker H, Wombacher F (2010) Rhodium, gold and other highly siderophile element abundances in chondritic meteorites. Geochim Cosmochim Acta 74: 356-379.
Fischer-Gödde M, Becker H ,Wombacher F (2011) Rhodium, gold and other highly siderophile elements in orogenic peridotites and peridotite xenoliths. Chem Geol 280: 365-383.
Fonseca ROC, Mallmann G, O'Neill, HStC, Campbell IH (2007) How chalcophile is rhenium? An experimental study of the solubility of Re in sulphide mattes. Earth Planet Sci Lett 260: 537-548.
Fonseca ROC, Mallmann G, O'Neill HSC, Campbell IH, Laurenz V (2011) Solubility of Os and Ir in sulfide melt: Implications for Re/Os fractionation during mantle melting. Earth Planet Sci Lett 311: 339-350.
Fonseca ROC, Laurenz V, Mallmann G, Luguet A, Hoehne N, Jochum KP (2012) New constraints on the genesis and long-term stability of Os-rich alloys in the Earth's mantle. Geochim Cosmochim Acta 87: 227-242.
Foustoukos DI, Bizimis M, Frisby C, Shirey SB (2015) Redox controls on Ni–Fe–PGE mineralization and Re/Os fractionation during serpentinization of abyssal peridotite. Geochim Cosmochim Acta 150: 11-25.
Frey FA, Suen CJ, Stockman HW (1985) The Ronda high temperature peridotite: Geochemistry and petrogenesis. Geochim Cosmochim Acta 49: 2469-2491.

Gaetani GA, Grove TL (1999) Wetting of mantle olivine by sulfide melt: implications for Re/Os ratios in mantle peridotite and late-stage core formation. Earth Planet Sci Lett 169: 147-163.
Gannoun A, Burton KW, Alard O, Parkinson IJ, Thomas LE (2004) Assessing the scale of osmium isotope heterogeneity in Mid- Ocean Ridge Basalts. Geochim Cosmochim Acta 68: A703-A703.
Gannoun A, Burton KW, Parkinson IJ, Alard O, Schiano P, Thomas LE (2007) The scale and origin of the osmium isotope variations in mid-ocean ridge basalts. Earth Planet Sci Lett 259: 541-556.
Gannoun A, Burton KW, Schiano P, Day JMD, Harvey J (2015) Highly siderophile element and Re-Os isotope systematics of mid-ocean ridge basalt and arc volcanism. Rev Mineral Geochem 81: xxx-xxx.
Gao S, Rudnick RL, Carlson RW, McDonough WF, Liu Y-S (2002) Re-Os evidence for replacement of ancient mantle lithosphere beneath the North China craton. Earth Planet Sci Lett 198: 307-322.
González-Jiménez J-M, Gervilla F, Proenza JA, Kerestedjian T, Auge T, Bailly L (2009) Zoning of laurite (RuS2)-erlichmanite (OsS2): implications for the origin of PGM in ophiolite chromitites. Eur J MIneral 21: 419-432.
Gros M, Lorand J-P, Luguet A (2002) Analysis of platinum group elements and gold in geological materials using NiS fire assay and Te coprecipitation; the NiS dissolution step revisited. Chem Geol 185: 179-190.
Guivel C, Lagabrielle Y, Bourgois J, Maury RC, Fourcade S, Martin H, Arnaud N (1999) New geochemical constraints for the origin of ridge-subduction-related plutonic and volcanic suites from the Chile Triple Junction (Taitao Peninsula and Site 862, LEG ODP141 on the Taitao Ridge). Tectonophysics 311: 83-111.
Halliday AN, Lee D-C, Tommasini S, Davies GR, Paslick CR, Fitton JG, James DE (1995) Incompatible trace elements in OIB and MORB and source enrichment in the sub-oceanic mantle. Earth Planet Sci Lett 133: 379-395.
Handler MR, Bennett VC, Esat TM (1997) The persistence of off-cratonic lithospheric mantle: Os isotopic systematics of variably metasomatised southeast Australian xenoliths. Earth Planet Sci Lett 151: 61-75.
Hanghøj K, Kelemen PB, Hassler D, Godard M (2010) Composition and Genesis of Depleted Mantle Peridotites from the Wadi Tayin Massif, Oman Ophiolite; Major and Trace Element Geochemistry, and Os Isotope and PGE Systematics. J Petrol 51: 201-227.
Harvey J, Dale CW, Gannoun A, Burton KW (2011) Osmium mass balance in peridotite and the effects of mantle-derived sulphides on basalt petrogenesis. Geochim Cosmochim Acta 75: 5574-5596.
Harvey J, Gannoun A, Burton KW, Rogers NW, Alard O, Parkinson IJ (2006) Ancient melt extraction from the oceanic upper mantle revealed by Re-Os isotopes in abyssal peridotites from the Mid-Atlantic ridge. Earth Planet Sci Lett 244: 606-621.
Harvey J, Shirey SB,Warren JM (2015) Mantle sulfides and their role in Re-Os-Pb geochronology. Rev Mineral Geochem 81: xxx-xxx.
Hassler DR, Shimizu N (1998) Osmium isotopic evidence for ancient subcontinental lithospheric mantle beneath the Kerguelen Islands, southern Indian Ocean. Science 280: 418-421.
Hertogen J, Janssens M-J, Palme H (1980) Trace elements in oceanic ridge basalt glasses: Implications for fractionations during mantle evolution and petrogenesis. Geochim Cosmochim Acta 44: 2125-2143.
Hirth G, Guillot S (2013) Rheology and Tectonic Significance of Serpentinite. Elements 9: 107-113.
Hofmann AW, Hart SR (1978) An assessment of local and regional isotopic equilibrium in the mantle. Earth Planet Sci Lett 38: 44-62.
Hofmann AW, White WM (1982) Mantle Plumes from Ancient Oceanic-Crust. Earth Planet Sci Lett 57: 421-436.
Hofmann AW (1988) Chemical differentiation of the earth: the relationship between mantle, continental crust and oceanic crust. Earth Planet Sci Lett 90: 297-314.
Horan MF, Walker RJ, Morgan JW, Grossman JN, Rubin AE (2003) Highly siderophile elements in chondrites. Chem Geol 196: 5-20.
Ishikawa A, Pearson DG, Dale CW (2011) Ancient Os isotope signatures from the Ontong Java Plateau lithosphere: Tracing lithospheric accretion history. Earth Planet Sci Lett 301: 159-170.
Ishikawa T, Nagaishi K, Umino S (2002) Boninitic volcanism in the Oman ophiolite: Implications for thermal condition during transition from spreading ridge to arc. Geology 30: 899-902.
Ismail SA, Kettanah YA, Chalabi SN, Ahmed AH, Arai S (2014) Petrogenesis and PGE distribution in the Al- and Cr-rich chromitites of the Qalander ophiolite, northeastern Iraq: Implications for the tectonic environment of the Iraqi Zagros Suture Zone. Lithos 202: 21-36.
Jacobsen SB, Wasserburg GJ (1979) Nd and Sr isotopic study of the Bay of Island Ophiolite complex and the evolution of the source of mid-ocean ridge basalts. J Geophys Res 84: 7429-7445.

Johan Z (2002) Alaskan-type Complexes and Their Platinum-Group Element Mineralization, in: Cabri, L.J. (Ed.), The Geology, Geochemistry, Mineralogy and Mineral Beneficiation of Platinum-Group Elements. Canadian Institute of Mining, Metallurgy and Petroleum, Montréal, Canada, pp. 669-719.
Johnson KT, Dick HJ, Shimizu N (1990) Melting in the oceanic upper mantle: an ion microprobe study of diopsides in abyssal peridotites. J Geophys Res 95: 2661-2678.
Jugo PJ, Luth RW, Richards JP (2005) An Experimental Study of the Sulfur Content in Basaltic Melts Saturated with Immiscible Sulfide or Sulfate Liquids at 1300°C and 1·0 GPa. J Petrol 46: 783-798.
Jugo PJ (2009) Sulfur content at sulfide saturation in oxidized magmas. Geology 37: 415-418.
Keays RR (1995) The role of komatiitic and picritic magmatism and S-saturation in the formation of ore deposits. Lithos: 34: 1-18.
Kelemen P, Shimizu N, Salters V (1995) Extraction of MORB from the mantle by focussed flow of melt in dunite channels. Nature 375: 747-753.
Kelemen PB, Hirth G, Shimizu N, Spiegelman M, Dick HJB (1997) A review of melt migration processes in the adiabatically upwelling mantle beneath oceanic spreading ridges. Philos Trans R Soc Lond Ser. A 355: 283-318.
Kelley KA, Cottrell E (2009) Water and the Oxidation State of Subduction Zone Magmas. Science 325, 605-607.
Kepezhinskas P, Defant MJ (2001) Nonchondritic Pt/Pd ratios in arc mantle xenoliths: Evidence for platinum enrichment in depleted island-arc mantle sources. Geology 29: 851-854.
Kepezhinskas P, Defant MJ, Widom E (2002) Abundance and distribution of PGE and Au in the island-arc mantle: implications for sub-arc metasomatism. Lithos 60: 113-128.
Kimura K, Lewis RS, Anders E (1974) Distribution of gold and rhenium between nickel-iron and silicate melts - Implications for abundance of siderophile elements on Earth and Moon. Geochim Cosmochim Acta 38: 683-701.
Klein EM, Karsten JL (1995) Ocean-ridge basalts with convergent-margin geochemical affinities from the Chile Ridge. Nature 374: 52-57.
Klein F, Bach W (2009) Fe–Ni–Co–O–S Phase Relations in Peridotite–Seawater Interactions. J Petrol 50: 37-59.
Koga KT, Kelemen PB, Shimizu N (2001) Petrogenesis of the crust-mantle transition zone and the origin of lower crustal wehrlite in the Oman ophiolite. Geochem Geophys Geosys 2: 1038.
König S, Luguet A, Lorand J-P, Wombacher F, Lissner M (2012) Selenium and tellurium systematics of the Earth's mantle from high precision analyses of ultra-depleted orogenic peridotites. Geochim Cosmochim Acta 86: 354-366.
König S, Lorand J-P, Luguet A, Pearson DG (2014) A non-primitive origin of near-chondritic S–Se–Te ratios in mantle peridotites; implications for the Earth's late accretionary history. Earth Planet Sci Lett 385: 110-121.
König S, Luguet A, Lorand J-P, Lissner M, Pearson DG (2015) Reply to the comment on "A non-primitive origin of near-chondritic S–Se–Te ratios in mantle peridotites: Implications for the Earth's late accretionary history" by König S. et al. [Earth Planet. Sci. Lett. 385 (2014) 110–121]. Earth Planet Sci Lett 417: 167-169.
Kumar N, Reisberg L, Zindler L (1996) A major and trace element and strontium, neodymium, and osmium isotopic study of a thick pyroxenite layer from the Beni Bousera Ultramafic Complex of northernm Morocco. Geochim Cosmochim Acta 60: 1429-1444.
Lambart S, Laporte D, Schiano P (2013) Markers of the pyroxenite contribution in the major-element compositions of oceanic basalts: Review of the experimental constraints. Lithos 160–161: 14-36.
Langmuir CH, Klein EM, Plank T (1992) Petrological constraints on melt formation and migration beneath mid-ocean ridges. *In*: Mantle Flow and Melt Generation at Mid-Ocean Ridges. Phipps Morgan J, Blackman D, Sinton JL (Eds.), American Geophysical Union, Washington.
Lassiter JC (2006) Constraints on the coupled thermal evolution of the Earth's core and mantle, the age of the inner core, and the origin of the $^{186}Os/^{188}Os$ "core signal" in plume-derived lavas. Earth Planet Sci Lett 250: 306-317.
Lassiter JC, Byerly BL, Snow JE, Hellebrand E (2014) Constraints from Os-isotope variations on the origin of Lena Trough abyssal peridotites and implications for the composition and evolution of the depleted upper mantle. Earth Planet Sci Lett 403: 178-187.
Le Roux V, Bodinier J-L, Tommasi A, Alard O, Dautria J-M, Vauchez A, Riches AJV (2007) The Lherz spinel lherzolite: refertilized rather than pristine mantle. Earth Planet Sci Lett 259: 599-612.
Levasseur S, Birck JL, Allègre CJ (1998) Direct measurement of femtomoles of osmium and the Os-$^{187}Os/^{186}Os$ ratio in seawater. Science 282: 272-274.

Li C, Barnes SJ, Makovicky E, Rose-Hansen J, Makovicky M (1996) Partitioning of nickel, copper, iridium, rhenium, platinum, and palladium between monosulfide solid solution and sulfide liquid: Effects of composition and temperature. Geochim Cosmochim Acta 60: 1231-1238.

Li Y, Audétat A (2013) Gold solubility and partitioning between sulfide liquid, monosulfide solid solution and hydrous mantle melts: Implications for the formation of Au-rich magmas and crust–mantle differentiation. Geochim Cosmochim Acta 118: 247-262.

Liu C-Z, Snow JE, Hellebrand E, Brügmann G, von der Handt A, Buchl A, Hofmann AW (2008) Ancient, highly heterogeneous mantle beneath Gakkel ridge, Arctic Ocean. Nature 452: 311-316.

Liu C-Z, Snow JE, Brügmann G, Hellebrand E, Hofmann AW (2009) Non-chondritic HSE budget in Earth's upper mantle evidenced by abyssal peridotites from Gakkel ridge (Arctic Ocean). Earth Planet Sci Lett 283: 122-132.

Lodders K (2003) Solar System Abundances and Condensation Temperatures of the Elements. The Astrophysical Journal, 591: 1220-1247.

Lorand J-P (1988) Fe-Ni-Cu sulfides in tectonic peridotites from the Maqsad district, Sumail ophiolite, southern Oman: implications for the origin of the sulfide component in the oceanic upper mantle. Tectonophysics 151: 57-73.

Lorand J-P (1990) Are spinel lherzolite xenoliths representative of the abundance of sulfur in the upper mantle? Geochim Cosmochim Acta 54: 1487-1492.

Lorand J-P Pattou L, Gros M (1999) Fractionation of Platinum-group Elements and Gold in the Upper Mantle: a Detailed Study in Pyrenean Orogenic Lherzolites. J Petrol 40: 957-981.

Lorand J-P, Schmidt G, Palme H, Kratz K-L (2000) Highly siderophile element geochemistry of the Earth's mantle: new data for the Lanzo (Italy) and Ronda (Spain) orogenic peridotite bodies. Lithos 53: 149-164.

Lorand J-P, Luguet A, Alard O, Bezos A, Meisel T (2008) Abundance and distribution of platinum-group elements in orogenic lherzolites; a case study in a Fontete Rouge lherzolite (French Pyrénées). Chem Geol 248: 174-194.

Lorand J-P Alard O (2010) Determination of selenium and tellurium concentrations in Pyrenean peridotites (Ariege, France): New insight into S/Se/Te systematics of the upper in mantle samples. Chem Geol 278: 120-130.

Lorand J-P, Alard O, Luguet A (2010) Platinum-group element micronuggets and refertilization process in Lherz orogenic peridotite (northeastern Pyrenees, France). Earth Planet Sci Lett 289: 298-310.

Lorand J-P, Alard O, Godard M (2009) Platinum-group element signature of the primitive mantle rejuvenated by melt-rock reactions: evidence from Sumail peridotites (Oman Ophiolite). Terra Nova 21: 35-40.

Lorand J-P, Luguet A, Alard O (2013) Platinum-group element systematics and petrogenetic processing of the continental upper mantle: A review. Lithos 164–167: 2-21.

Lorand J-P, Luguet A (2015) Chalcophile/siderophile elements in mantle rocks: trace elements in trace minerals. Rev Mineral Geochem 81: xxx-xxx.

Loubet M, Allègre CJ (1982) Trace elements in orogenic lherzolites reveal the complex history of the upper mantle. Nature 298: 809-814.

Luck JM, Allègre CJ (1983) ^{187}Re-^{187}Os systematics in meteorites and cosmochemical consequences. Nature 302: 130-132.

Luguet A, Alard O, Lorand J-P, Pearson NJ, Ryan CG, O'Reilly SY (2001) Laser-ablation microprobe (LAM)-ICPMS unravels the highly siderophile element geochemistry of the oceanic mantle. Earth Planet Sci Lett 189: 285-294.

Luguet A, Lorand JP, Seyler M (2003) A coupled study of sulfide petrology and highly siderophile element geochemistry in abyssal peridotites from the Kane Fracture Zone (MARK area, Mid-Atlantic ridge. Geochim Cosmochim Acta 67: 1553-1570.

Luguet A, Lorand J-P, Alard O, Cottin J-Y (2004) A multi-technique study of platinum group element systematic in some Ligurian ophiolitic peridotites, Italy. Chem Geol 208: 175-194.

Luguet A, Shirey SB, Lorand J-P, Horan MF, Carlson RW (2007) Residual platinum-group minerals from highly depleted harzburgites of the Lherz massif (France) and their role in HSE fractionation of the mantle. Geochim Cosmochim Acta 71: 3082-3097.

Luguet A, Nowell GM, Pearson DG (2008a) ^{184}Os/^{188}Os and ^{186}Os/^{188}Os measurements by Negative Thermal Ionisation Mass Spectrometry (N-TIMS): Effects of interfering element and mass fractionation corrections on data accuracy and precision. Chem Geol 248: 342-362.

Luguet A, Pearson DG, Nowell GM, Dreher ST, Coggon JA, Spetsius ZV, Parman SW (2008b) Enriched Pt-Re-Os Isotope Systematics in Plume Lavas Explained by Metasomatic Sulfides. Science, 319: 453-456.

Luguet A, Jaques AL, Pearson DG, Smith CB, Bulanova GP, Roffey SL, Rayner MJ, Lorand JP (2009) An integrated petrological, geochemical and Re–Os isotope study of peridotite xenoliths from the Argyle lamproite, Western Australia and implications for cratonic diamond occurrences. Lithos 112: Supplement 2, 1096-1108.

Luguet A, Behrens M, Pearson DG, König S, Herwartz D (2015, in press). Significance of the whole rock Re-Os ages in cryptically and modally metasomatised cratonic peridotites: Constraints from HSE-Se-Te systematics. Geochim Cosmochim Acta. doi:10.1016/j.gca.2015.06.016

Maier WD, Peltonen P, McDonald I, Barnes SJ, Barnes SJ, Hatton C, Viljoen F (2012) The concentration of platinum-group elements and gold in southern African and Karelian kimberlite-hosted mantle xenoliths: Implications for the noble metal content of the Earth's mantle. Chem Geol 302: 119-135.

Malitch KN, Merkle RKW (2004) Ru-Os-Ir-Pt and Pt-Fe alloys from the Evander goldfield, Witwatersrand basin, South Africa: Detrital origin inferred from compositional and osmium-isotope data. Can Mineral 42: 631-650.

Malaviarachchi SPK, Makishima A, Tanimoto M, Kuritani T, Nakamura E (2008) Highly unradiogenic lead isotope ratios from the Horoman peridotite in Japan. Nature Geosci 1: 859-863.

Mallmann G, O'Neill HSC (2007) The effect of oxygen fugacity on the partitioning of Re between crystals and silicate melt during mantle melting. Geochim Cosmochim Acta 71: 2837-2857.

Marchesi C, González-Jiménez J-M, Gervilla F, Garrido CJ, Griffin WL, O'Reilly SY, Proenza JA, Pearson NJ (2011) In situ Re-Os isotopic analysis of platinum-group minerals from the Mayari-Cristal ophiolitic massif (Mayari-Baracoa Ophiolitic Belt, eastern Cuba): implications for the origin of Os-isotope heterogeneities in podiform chromitites. Contrib Mineral Petrol 161: 977-990.

Marchesi C, Garrido CJ, Harvey J, González-Jiménez J-M, Hidas K, Lorand J-P, Gervilla F (2013) Platinum-group elements, S, Se and Cu in highly depleted abyssal peridotites from the Mid-Atlantic Ocean Ridge (ODP Hole 1274A): Influence of hydrothermal and magmatic processes. Contrib Mineral Petrol 166: 1521-1538.

Marchesi C, Dale CW, Garrido CJ, Pearson DG, Bosch D, Bodinier J-L, Gervilla F, Hidas K (2014) Fractionation of highly siderophile elements in refertilized mantle: Implications for the Os isotope composition of basalts. Earth Planet Sci Lett 400: 33-44.

Martin CE (1991) Os isotopic characteristics of mantle derived rocks. Geochim Cosmochim Acta 55: 1421-1434.

Mavrogenes JA, O'Neill HSC (1999) The relative effects of pressure, temperature and oxygen fugacity on the solubility of sulfide in mafic magmas. Geochim Cosmochim Acta 63: 1173-1180.

Mazzucchelli M, Rivalenti G, Brunelli D, Zanetti A ,Boari E (2009) Formation of Highly Refractory Dunite by Focused Percolation of Pyroxenite-Derived Melt in the Balmuccia Peridotite Massif (Italy). J Petrol 50: 1205-1233.

McCulloch MT, Gregory RT, Wasserburg GJ, Taylor HPJ (1981) Sm-Nd, Rb-Sr and $^{18}O/^{16}O$ isotopic systematics in an oceanic crustal section: evidence for the Samail ophiolite. J Geophys Res 86: 2721

McDonough WF, Sun S-s (1995) The composition of the Earth. Chem Geol 120: 223-253.

McInnes BIA, McBride JS, Evans NJ, Lambert DD, Andrew AS (1999) Osmium isotope constraints on ore metal recycling in subduction zones. Science 286 512-516.

Medaris Jr G, Wang H, Jelinek E, Mihaljevic M, Jakes P (2005) Characteristics and origins of diverse Variscan peridotites in the Gfoehl Nappe, Bohemian Massif, Czech Republic. Lithos 82: 1-23.

Meibom A, Sleep NH, Chamberlain CP, Coleman RG, Frei R, Hren MT, Wooden JL (2002) Re-Os isotopic evidence for long-lived heterogeneity and equilibration processes in the Earth's upper mantle. Nature 419: 705-708.

Meisel T, Biino GG, Nagler TF (1996) Re-Os, Sm-Nd, and rare earth element evidence for Proterozoic oceanic and possible subcontinental lithosphere in tectonized ultramafic lenses from the Swiss Alps. Geochim Cosmochim Acta 60: 2583-2593.

Meisel T, Melcher F, Tomascak P, Dingeldey C, Koller F (1997) Re-Os isotopes in orogenic peridotite massifs in the Eastern Alps, Austria. Chem Geol 143: 217-229.

Meisel T, Walker RJ, Irving AJ, Lorand J-P (2001) Osmium isotopic compositions of mantle xenoliths: a global perspective. Geochim Cosmochim Acta 65: 1311-1323.

Meisel T, Moser J (2004) Reference materials for geochemical PGE analysis: new analytical data for Ru, Rh, Pd, Os, Ir, Pt and Re by isotope dilution ICP-MS in 11 geological reference materials. Chem Geol 208: 319-338.

Meisel T, Horan, MF (2015) Analytical methods in siderophile and chalcophile element geochemistry. Rev Mineral Geochem 81: xxx-xxx.
Michael PJ, Langmuir CH, Dick HJB, Snow JE, Goldstein SL, Graham DW, Lehnert K, Kurras G, Jokat W, Muhe R, Edmonds HN (2003) Magmatic and amagmatic seafloor generation at the ultraslow-spreading Gakkel ridge, Arctic Ocean. Nature 423: 956-961.
Mitchell RH, Keays RR (1981) Abundance and distribution of gold, palladium and iridium in some spinel and garnet lherzolites - implications for the nature and origin of precious metal-rich intergranular components in the upper mantle. Geochim Cosmochim Acta 45: 2425-2442.
Morgan JW (1986) Ultramafic xenoliths: clues to Earth's late accretionary history. J Geophys Res 91: 12,375-12,387.
Mukasa SB, Shervais JW (1999) Growth of subcontinental lithosphere: evidence from repeated dike injections in the Balmuccia lherzolite massif, Italian Alps. Lithos 48: 287-316.
Mungall JE, Andrews DRA, Cabri LJ, Sylvester PJ, Tubrett M (2005) Partitioning of Cu, Ni, Au, and platinum-group elements between monosulfide solid solution and sulfide melt under controlled oxygen and sulfur fugacities. Geochim Cosmochim Acta 69: 4349-4360.
Mungall JE, Brenan JM (2014) Partitioning of platinum-group elements and Au between sulfide liquid and basalt and the origins of mantle-crust fractionation of the chalcophile elements. Geochim Cosmochim Acta 125: 265-289.
Müntener O, Piccardo GB, Polino R, Zanetti A (2005) Revisiting the Lanzo peridotite (NW-Italy): 'Asthenospherization' of ancient mantle lithosphere. Ofioliti 30: 111-124.
Nimis P, Trommsdorff V (2001) Revised Thermobarometry of Alpe Arami and other Garnet Peridotites from the Central Alps. J Petrol 42: 103-115.
O'Driscoll B, Day JMD, Walker RJ, Daly JS, McDonough WF, Piccoli PM (2012) Chemical heterogeneity in the upper mantle recorded by peridotites and chromitites from the Shetland Ophiolite Complex, Scotland. Earth Planet Sci Lett 333: 226-237.
O'Driscoll B, González-Jiménez J-M (2015) An inventory and overview of natural occurrences of the platinum-group minerals (PGM) in extraterrestrial and terrestrial rocks. Rev Mineral Geochem 81: xxx-xxx.
O'Neill HStC, Dingwell DB, Borisov A, Spettel B, Palme H (1995) Experimental petrochemistry of some highly siderophile elements at high temperatures, and some implications for core formation and the mantle's early history. Chem Geol 120: 255-273.
O'Neill HSC, Mavrogenes JA (2002) The Sulfide Capacity and the Sulfur Content at Sulfide Saturation of Silicate Melts at 1400°C and 1 bar. J Petrol 43: 1049-1087.
Obata M (1980) The Ronda Peridotite: Garnet-, Spinel-, and Plagioclase-Lherzolite Facies and the P-T Trajectories of a High-Temperature Mantle Intrusion. J Petrol: 21: 533-572.
Obermiller W (1994) Chemical and isotopic variations in the Balmuccia, Baldissero and Finero peridotite massifs (Ivrea-Zone, N-Italy), Universität Mainz.
Pallister JS, Hopson CA (1981) Samail Ophiolite plutonic suite: Field relations, phase variation, cryptic variation and layering, and a model of a spreading ridge magma chamber. J Geophys Res: Solid Earth 86: 2593-2644.
Pallister JS ,Knight RJ (1981) Rare-earth element geochemistry of the Samail ophiolite near Ibra, Oman. J Geophys Res 86: 2673-2697.
Palme H, O'Neill HStC (2014) Cosmochemical Estimates of Mantle Composition. *In*: Treatise on Geochemistry 3: The mantle and core. Carlson, R.W., Holland H.D., Turekian K.K. (Eds.), Pergamon, Oxford, 1-39.
Parkinson IJ, Hawkesworth CJ, Cohen AS (1998) Ancient Mantle in a Modern Arc: Osmium Isotopes in Izu-Bonin-Mariana Forearc Peridotites. Science 281: 2011-2013.
Pattou L, Lorand JP, Gros M (1996) Non-chondritic platinum-group element ratios in the Earth's upper mantle. Nature 379: 712-715.
Pearson DG, Davies GR, Nixon PH, Greenwood PB, Mattey DP (1991a) Oxygen isotope evidence for the origin of pyroxenites in the Beni Bousera peridotite massif, North Morocco: derivation from subducted oceanic lithosphere. Earth Planet Sci Lett: 102: 289-301.
Pearson DG, Davies GR, Nixon PH, Mattey DP (1991b) A carbon isotope study of diamond facies pyroxenites from Beni Bousera, N. Morocco. Special Edition, J. Petrology: Orogenic Lherzolites and Mantle Processes: 175-189.
Pearson DG, Davies GR, Nixon PH (1993) Geochemical constraints on the petrogenesis of diamond facies pyroxenites from the Beni Bousera peridotite massif, north Morocco. J Petrol: 34: 125-172.

Pearson DG, Carlson RW, Shirey SB, Boyd FR, Nixon PH (1995a) Stabilization of Archean Lithospheric Mantle - a Re-Os Isotope Study of Peridotite Xenoliths from the Kaapvaal Craton. Earth Planet Sci Lett 134: 341-357.
Pearson DG, Shirey SB, Carlson RW, Boyd FR, Pokhilenko NP, Shimizu N (1995b) Re-Os, Sm-Nd, and Rb-Sr isotope evidence for thick Archean lithospheric mantle beneath the siberian craton modified by multistage metasomatism. Geochim Cosmochim Acta 59: 959-977.
Pearson DG, Nowell GM (2003) Re-Os and Lu-Hf isotope constraints on the origin and age of pyroxenites from the Beni Bousera peridotite massif implications for mixed peridotite-pyroxenite mantle sources, Samani, Japan, pp. 439-455.
Pearson DG, Irvine GJ, Ionov DA, Boyd FR, Dreibus GE (2004) Re-Os isotope systematics and platinum group element fractionation during mantle melt extraction: a study of massif and xenolith peridotite suites. Chem Geol: 208: 29-59.
Pearson DG, Nowell GM (2004) Re-Os and Lu-Hf isotope constraints on the origin and age of pyroxenites from the Beni Bousera peridotite massif: implications for mixed peridotite-pyroxenite melting models. J Petrol 45: 439-455.
Pearson DG, Parman SW, Nowell GM (2007) A link between large mantle melting events and continent growth seen in osmium isotopes. Nature 449: 202-205.
Pelletier L, Müntener O (2006) High-pressure metamorphism of the Lanzo peridotite and its oceanic cover, and some consequences for the Sesia–Lanzo zone (northwestern Italian Alps). Lithos 90: 111-130.
Peslier AH, Reisberg L, Ludden J, Francis D (2000) Re-Os constraints on harzburgite and lherzolite formation in the lithospheric mantle: A study of Northern Canadian Cordillera xenoliths. Geochim Cosmochim Acta 64: 3061-3071.
Peucker-Ehrenbrink B, Ravizza G (2000) The marine osmium isotope record. Terra Nova 12: 205-219.
Peucker-Ehrenbrink B, Jahn BM (2001) Rhenium-osmium isotope systematics and platinum group element concentrations: Loess and the upper continental crust. Geochem Geophys Geosyst 2: 2001GC000172.
Peucker-Ehrenbrink B, Hanghøj K, Atwood T, Kelemen PB (2012) Rhenium-osmium isotope systematics and platinum group element concentrations in oceanic crust. Geology 40: 199-202.
Piccardo G, Rampone E, Vannucci R, Shimizu N, Ottolini L, Bottazi P (1993) Mantle processes in the sub-continental lithosphere: the case study of the rifted sp-lherzolites from Zabargad (Red Sea). Eur J Mineral 5: 1039-1056.
Piccardo GB, Guarnieri L (2010) Alpine peridotites from the Ligurian Tethys: an updated critical review. Int Geology Rev 52: 1138-1159.
Pokrovski GS, Akinfiev NN, Borisova AY, Zotov AV, Kouzmanov K (2014) Gold speciation and transport in geological fluids: insights from experiments and physical-chemical modelling. Geol Soc London, Spec Pub 402.
Polvé M, Allègre CJ (1980) Orogenic lherzolite complexes studied by ^{87}Rb-^{87}Sr: a clue to understand the mantle convection processes. Earth Plan Sci Lett 51: 71-93.
Prichard HM, Lord RA (1996) A model to explain the occurrence of platinum- and palladium-rich ophiolite complexes. J Geol Soc 153: 323-328.
Puchtel I, Humayun M (2000) Platinum group elements in Kostomuksha komatiites and basalts: Implications for oceanic crust recycling and core-mantle interaction. Geochim Cosmochim Acta 64: 4227-4242.
Puchtel IS, Humayun M (2001) Platinum group element fractionation in a komatiitic basalt lava lake. Geochim Cosmochim Acta 65: 2979-2993.
Puchtel IS, Humayun M, Campbell AJ, Sproule RA, Lesher CM (2004) Platinum group element geochemistry of komatiites from the Alexo and Pyke Hill areas, Ontario, Canada. Geochim Cosmochim Acta 68: 1361-1383.
Puchtel IS, Brandon AD, Humayun M, Walker RJ (2005) Evidence for the early differentiation of the core from Pt-Re-Os isotope systematics of 2.8-Ga komatiites. Earth Planet Sci Lett 237: 118-134.
Quick JE, Sinigoi S, Peressini G, Demarchi G, Wooden JL, Sbisà A (2009) Magmatic plumbing of a large Permian caldera exposed to a depth of 25 km. Geology 37: 603-606.
Rampone E, Hofmann A, Piccardo G, Vannucci R, Bottazzi P, Ottolini L (1995) Petrology, mineral and isotope geochemistry of the External Liguride peridotites (Northern Apennines, Italy). J Petrol 36: 81-105.
Rampone E, Hofmann AW, Piccardo GB, Vannucci R, Bottazzi P, Ottolini L (1996) Trace element and isotope geochemistry of depleted peridotites from an N-MORB type ophiolite (Internal Liguride, N. Italy). Contrib Mineral Petrol 123: 61-76.

Rampone E, Hofmann AW, Raczek I (1998) Isotopic contrasts within the Internal Liguride ophiolite (N. Italy): the lack of a genetic mantle–crust link. Earth Planet Sci Lett 163: 175-189.
Rampone E, Romairone A, Hofmann AW (2004) Contrasting bulk and mineral chemistry in depleted mantle peridotites: evidence for reactive porous flow. Earth Planet Sci Lett 218: 491-506.
Rampone E, Hofmann AW (2012) A global overview of isotopic heterogeneities in the oceanic mantle. Lithos 148: 247-261.
Rehkämper M, Halliday AN, Barfod D, Fitton GJ, Dawson JB (1997) Platinum-group element abundance patterns in different mantle environments. Science 278: 1595-1598.
Rehkämper M, Halliday AN, Fitton JG, Lee DC, Wieneke M, Arndt NT (1999) Ir, Ru, Pt and Pd in basalts and komatiites: New constraints for the geochemical behavior of the platinum group elements in the mantle. Geochim Cosmochim Acta 63: 3915-3934.
Reisberg L, Zindler A (1986) Extreme isotopic variations in the upper mantle: evidence from Ronda. Earth Plan Sci Lett 81: 29-45.
Reisberg L, Zindler A, Jagoutz E (1989) Further Sr and Nd isotopic results from peridotites of the Ronda ultramafic complex. Earth Planet Sci Lett 96: 161-180.
Reisberg L, Lorand J-P (1995) Longevity of sub-continental mantle lithosphere from osmium isotope systematics in orogenic peridotite massifs. Nature 376: 159-162.
Reisberg L, Luguet A (2015) Highly Siderophile Element and $^{187}Os/^{188}Os$ signatures in non-cratonic basalt-hosted peridotite xenoliths: Unravelling the origin and evolution of the Post-Archean Lithospheric Mantle. Rev Mineral Geochem 81: xxx-xxx.
Reisberg LC, Allègre CJ, Luck J-M (1991) The Re-Os systematics of the Ronda ultramafic complex of southern Spain. Earth Planet Sci Lett 105: 196-213.
Riches AJV, Rogers NW (2011) Mineralogical and geochemical constraints on the shallow origin, ancient veining, and multi-stage modification of the Lherz peridotite. Geochim Cosmochim Acta 75: 6160-6182.
Righter K, Hauri E.H (1998) Compatibility of rhenium in garnet during mantle melting and magma genesis. Science 280: 1737-1741.
Righter K, Humayun M, Danielson L (2008) Partitioning of palladium at high pressures and temperatures during core formation. Nat Geosci 1: 321-323.
Rivalenti G, Mazzucchelli M, Vannucci R, Hofmann A, Ottolini L, Bottazzi P, Obermiller W (1995) The relationship between websterite and peridotite in the Balmuccia peridotite massif (NW Italy) as revealed by trace element variations in clinopyroxene. Contrib Mineral Petrol 121: 275-288.
Roy-Barman M, Allègre CJ (1994) $^{187}Os/^{186}Os$ ratios of mid-ocean ridge basalts and abyssal peridotites. Geochim Cosmochim Acta 58: 5043-5054.
Roy-Barman M, Luck J-M, Allègre CJ (1996) Os isotopes in orogenic lherzolite massifs and mantle heterogeneities. Chem Geol 130: 55-64.
Rudge JF (2008) Finding peaks in geochemical distributions: A re-examination of the helium-continental crust correlation. Earth Planet Sci Lett 274: 179-188.
Rudnick RL, Walker RJ (2009) Interpreting ages from Re-Os isotopes in peridotites. Lithos 112: 1083-1095.
Saal AE, Takazawa E, Frey FA, Shimizu N, Hart SR (2001) Re-Os Isotopes in the Horoman Peridotite: Evidence for Refertilization. J Petrol: 42: 25-37.
Salters VJM, Stracke A (2004) Composition of the depleted mantle. Geochem Geophys Geosyst 5: Q05004.
Schiano P, Birck JL, Allègre CJ (1997) Osmium-strontium-neodymium-lead isotopic covariations in mid-ocean ridge basalt glasses and the heterogeneity of the upper mantle. Earth Planet Sci Lett 150: 363-379.
Schmidt G, Palme H, Kratz K-L, Kurat G (2000) Are highly siderophile elements (PGE, Re and Au) fractionated in the upper mantle. New results on peridotites from Zarbargad. Chem Geol 163: 167-188.
Schulte RF, Schilling M, Anma R, Farquhar J, Horan MF, Komiya T, Piccoli PM, Pitcher L, Walker RJ (2009) Chemical and chronologic complexity in the convecting upper mantle: Evidence from the Taitao ophiolite, southern Chile. Geochim Cosmochim Acta 73: 5793-5819.
Searle M, Cox J (1999) Tectonic setting, origin, and obduction of the Oman ophiolite. Geol Soc Amer Bull 111: 104-122.
Selby D, Creaser RA, Stein HJ, Markey RJ, Hannah JL (2007) Assessment of the ^{187}Re decay constant by cross calibration of Re–Os molybdenite and U–Pb zircon chronometers in magmatic ore systems. Geochim Cosmochim Acta 71: 1999-2013.

Sergeev DS, Dijkstra AH, Meisel T, Brügmann G, Sergeev SA (2014) Traces of ancient mafic layers in the Tethys oceanic mantle. Earth Planet Sci Lett 389: 155-166.
Seyler M, Lorand J-P, Toplis MJ, Godard G (2004) Asthenospheric metasomatism beneath the mid-ocean ridge: Evidence from depleted abyssal peridotites. Geology 32: 301-304.
Sharma M, Papanastassiou DA, Wasserburg GJ (1997) The concentration and isotopic composition of osmium in the oceans. Geochim Cosmochim Acta 61: 3287-3299.
Shervais JW, Mukasa SB (1991) The Balmuccia orogenic lherzolite massif. J Petrol, Special Lherzolite Issue: 155-174.
Shi RD, Alard O, Zhi XC, O'Reilly SY, Pearson NJ, Griffin WL, Zhang M, Chen XM (2007) Multiple events in the Neo-Tethyan oceanic upper mantle: Evidence from Ru-Os-Ir alloys in the Luobusa and Dongqiao ophiolitic podiform chromitites, Tibet. Earth Planet Sci Lett 261: 33-48.
Shirey SB, Walker RJ (1998) The Re-Os isotope system in cosmochemistry and high-temperature geochemistry. Annu Rev Earth Planet Sci 26: 423-500.
Simon NSC, Neumann E-R, Bonadiman C, Coltorti M, Delpech G, Gregoire M, Widom E (2008) Ultra-refractory domains in the oceanic mantle lithosphere sampled as mantle xenoliths at ocean islands. J Petrol 49: 1223-1251.
Sinigoi S, Comin-Chiramonti P, Demarchi G, Siena F (1983) Differentiation of partial melts in the mantle: evidence from the Balmuccia peridotite, Italy. Contrib Mineral Petrol 82: 351-359.
Smoliar MI, Walker RJ, Morgan JW (1996) Re-Os ages of group IIA, IIIA, IVA, and IVB iron meteorites. Science 271: 1099-1102.
Snoke AW, Kalakay TJ, Quick JE, Sinigoi S (1999) Development of a deep-crustal shear zone in response to syntectonic intrusion of mafic magma into the lower crust, Ivrea–Verbano zone, Italy. Earth Planet Sci Lett: 166: 31-45.
Snow J, Reisberg L (1995) Os isotopic systematics of the MORB mantle: results from altered abyssal peridotites. Earth Planet Sci Lett 133: 411-421.
Snow JE, Schmidt G (1998) Constraints on Earth accretion deduced from noble metals in the oceanic mantle. Nature 391: 166-169.
Snow JE, Schmidt G, Rampone E (2000) Os isotopes and highly siderophile elements (HSE) in the Ligurian ophiolites, Italy. Earth Planet Sci Lett 175: 119-132.
Standish JJ, Hart SR, Blusztajn J, Dick HJB, Lee KL (2002) Abyssal peridotite osmium isotopic compositions from Cr-spinel. Geochem Geophys Geosys 3: 1-24.
Suen CJ, Frey FA (1987) Origins of the mafic and ultramafic rocks in the Ronda peridotite. Earth Planet Sci Lett 85: 183-202.
Sun WD, Arculus RJ, Bennett VC, Eggins SM, Binns RA (2003a) Evidence for rhenium enrichment in the mantle wedge from submarine arc-like volcanic glasses (Papua New Guinea). Geology 31: 845-848.
Sun WD, Bennett VC, Eggins SM, Kamenetsky VS, Arculus RJ (2003b) Enhanced mantle-to-crust rhenium transfer in undegassed arc magmas. Nature 422: 294-297.
Takahashi N (1992) Evidence for melt segregation towards fractures in the Horoman mantle peridotite complex. Nature 359: 52-55.
Takazawa E, Frey FA, Shimizu N, Obata M, Bodinier JL (1992) Geochemical evidence for melt migration and reaction in the upper mantle. Nature 359: 55-58.
Takazawa E, Frey F, Shimizu N, Obata M (1996) Evolution of the Horoman Peridotite (Hokkaido, Japan): Implications from pyroxene compositions. Chem Geol 134: 3-26.
Takazawa E, Frey FA, Shimizu N, Saal A, Obata M (1999) Polybaric Petrogenesis of Mafic Layers in the Horoman Peridotite Complex, Japan. J Petrol 40: 1827-1851.
Tilton GR, Hopson CA, Wright JE (1981) Uranium-lead isotopic ages of the Samail Ophiolite, Oman, with applications to Tethyan ocean ridge tectonics. J Geophys Res: Solid Earth 86: 2763-2775.
Tsuru A, Walker RJ, Kontinen A, Peltonen P, Hanski E (2000) Re-Os isotopic systematics of the 1.95 Ga Jormua Ophiolite Complex, northeastern Finland. Chem Geol 164: 123-141.
van Acken D, Becker H, Walker RJ (2008) Refertilization of Jurassic oceanic peridotites from the Tethys Ocean-Implications for the Re-Os systematics of the upper mantle. Earth Planet Sci Lett 268: 171-181.
van Acken D, Becker H, Hammerschmidt K, Walker RJ, Wombacher F (2010a) Highly siderophile elements and Sr–Nd isotopes in refertilized mantle peridotites - A case study from the Totalp ultramafic body, Swiss Alps. Chem Geol 276: 257-268.
van Acken D, Becker H, Walker RJ, McDonough WF, Wombacher F, Ash RD, Piccoli PM (2010b) Formation of pyroxenite layers in the Totalp ultramafic massif (Swiss Alps) - insights from highly siderophile elements and Os isotopes. Geochim Cosmochim Acta 74: 661-683.

Van der Wal D, Vissers RLM (1993) Uplift and emplacement of upper mantle rocks in the western Mediterranean. Geology 21: 1119-1122.
Vasseur G, Verniers J, Bodinier J-L (1991) Modelling of trace element transfer between mantle melt and heterogranular peridotite matrix. J Petrol, Lherzolite special issue: 41-54.
Vielzeuf D, Kornprobst J (1984) Crustal splitting and the emplacement of Pyrenean lherzolites and granulites. Earth Planet Sci Lett 67: 87-96.
Voshage H, Hofmann AW, Mazzucchelli M, Rivalenti G, Sinigoi S, Raczek I, Demarchi G (1990). Isotopic evidence from the Ivrea Zone for a hybrid lower crust formed by magmatic underplating. Nature 347: 731-736.
Walker RJ, Carlson RW, Shirey SB, Boyd FR (1989) Os, Sr, Nd and Pb isotope systematics of southern African peridotite xenoliths: implications for the chemical evolution of subcontinental mantle. Geochim Cosmochim Acta 53: 1583-1595.
Walker RJ, Morgan JW, Horan MF (1995) ^{187}Os Enrichment in Some Plumes - Evidence for Core-Mantle Interaction. Science 269: 819-822.
Walker RJ, Hanski E, Vuollo J, Liipo J (1996) The Os isotopic composition of Proterozoic upper mantle: Evidence for chondritic upper mantle from the Outokumpu ophiolite, Finland. Earth Planet Sci Lett 141: 161-173.
Walker RJ, Morgan JW, Smoliar MI, Beary E, Czamanske GK, Horan MF (1997) Applications of the ^{190}Pt-^{186}Os isotope system to geochemistry and cosmochemistry. Geochim Cosmochim Acta 61: 4799-4808.
Walker RJ, Horan MF, Morgan JW, Becker H, Grossman JN (2002a) Comparative ^{187}Re-^{187}Os systematics of chondrites: Implications regarding early solar system processes. Geochim Cosmochim Acta 66: 4187-4201.
Walker RJ, Prichard HM, Ishiwatari A, Pimentel M (2002b) The osmium isotopic composition of convecting upper mantle deduced from ophiolite chromites. Geochim Cosmochim Acta 66: 329-345.
Walker RJ (2009) Highly siderophile elements in the Earth, Moon and Mars: Update and implications for planetary accretion and differentiation. Chemie Der Erde-Geochemistry 69: 101-125.
Wang Z, Becker H (2013) Ratios of S, Se and Te in the silicate Earth require a volatile-rich late veneer. Nature 499: 328-331.
Wang Z, Becker H, Gawronski T (2013) Partial re-equilibration of highly siderophile elements and the chalcogens in the mantle: A case study on the Baldissero and Balmuccia peridotite massifs (Ivrea Zone, Italian Alps). Geochim Cosmochim Acta 108: 21-44.
Wang Z, Becker H (2015a) Comment on "A non-primitive origin of near-chondritic S-Se-Te ratios in mantle peridotites: implications for the Earth's late accretionary history" by König S. et al. [Earth Planet Sci Lett 385 (2014) 110-121]. Earth Planet Sci Lett 417: 164-166.
Wang Z, Becker H (2015b) Abundances of Ag and Cu in mantle peridotites and the implications for the behavior of chalcophile elements in mantle processes. Geochim Cosmochim Acta 160: 209-226.
Wang Z, Becker H (2015c) Fractionation of highly siderophile and chalcogen elements during magma transport in the mantle: constraints from pyroxenites of the Balmuccia peridotite massif. Geochim Cosmochim Acta 159: 254-263.
Warren JM, Shirey SB (2012) Lead and osmium isotopic constraints on the oceanic mantle from single abyssal peridotite sulfides. Earth Planet Sci Lett 359–360: 279-293.
Widom E, Hoernle KA, Shirey SB, Schmincke HU (1999) Os isotope systematics in the Canary Islands and Madeira: Lithospheric contamination and mantle plume signatures. J Petrol 40: 279-296.
Widom E, Kepezhinskas P, Defant M (2003) The nature of metasomatism in the sub-arc mantle wedge: evidence from Re-Os isotopes in Kamchatka peridotite xenoliths. Chem Geol 196: 283-306.
Xiong Y, Wood SA (1999) Experimental determination of the solubility of ReO_2 and the dominant oxidation state of rhenium in hydrothermal solutions. Chem Geol 158: 245-256.
Zhou M-F, Robinson PT, Su B-X, Gao J-F, Li J-W, Yang J-S, Malpas J (2014) Compositions of chromite, associated minerals, and parental magmas of podiform chromite deposits: The role of slab contamination of asthenospheric melts in suprasubduction zone environments. Gondwana Res 26, 262-283.
Zhou MF, Robinson PT, Malpas J, Li ZJ (1996) Podiform chromitites in the Luobusa ophiolite (southern Tibet): Implications for melt-rock interaction and chromite segregation in the upper mantle. J Petrol 37: 3-21.
Zhou MF, Sun M, Keays RR, Kerrich RW (1998) Controls on platinum-group elemental distributions of podiform chromitites: A case study of high-Cr and high-Al chromitites from Chinese orogenic belts. Geochim Cosmochim Acta 62: 677-688.

Zhou MF, Yumul GP, Malpas J, Sun M (2000) Comparative study of platinum-group elements in the Coto and Acoje blocks of the Zambales Ophiolite Complex, Philippines. Isl Arc 9: 556-564.